Aus dem Institut für Physiologie
der Universität Tübingen

SPAK and OSR1 kinases role in the regulation of ion transport in Kir2.1 (KCNJ2), CreaT (SLC6A8) and NaPi-IIb (SLC34A2)

Inaugural-Dissertation
zur Erlangung des Doktorgrades
der Humanwissenschaften

der Medizinischen Fakultät
der Eberhard Karls Universität
zu Tübingen

vorgelegt von

Fezai, Myriam

2018

Dekan :	Professor Dr. I. B. Autenrieth
1. Berichterstatter :	Professor Dr. F. Lang
2. Berichterstatter :	Professor Dr. P. Ruth

Tag der Disputation: 16.03.2018

Dedicated to
My parents, for believing in me…
Rached Fezai and Katinka Buhk for giving me wings…
Rocco, “Yes, we’ve created a way…”
Emna Fezai, “the Nobel prize, we will win it together!”

Table of contents

Abbreviation list:

AMPK:	Adenosine monophosphate-activated protein kinase
ATP:	Adenosine triphosphate
ATS:	Anderson Tawil syndrome
BK:	Large conductance Ca^{2+} activated K^+ channel
BSA:	Bovin serum albumin
Ca^{2+}:	Calcium
Cl^-:	Chloride
CreaT:	Creatine transporter
cRNA:	copped Ribonucleotide acid
Cys^{144}:	Cysteine residue 144
DNA:	Deoxyribonucleic acid
FASD:	Fetal alcohol spectrum disorder
GABA:	Gamma aminobutyric acid
HRD:	Horseradish peroxidase enzyme
Hz:	Hertz
JAK2:	Janus kinase 2
JAK3:	Janus kinase 3
K^+:	Potassium
Kir2.1:	The inwardly rectifying K^+ channel
Kir2.1-HA:	The inwardly rectifying K^+ channel Kir2.1 with an external HA-tag
K_m:	Affinity constant of a transporter
MAPK-like kinase:	Mitogen-activated protein kinases
mTOR:	mammalian target of rapamycin
n:	number of oocytes measured
Na^+:	Sodium
NaPi-IIa:	Na+ coupled phosphate transporter type II a, SLC34A1
NaPi-IIb:	Na+ coupled phosphate transporter type II b, SLC34A2
NCC:	Na^+/Cl^- co-transporter
NKCC:	$Na^+/K^+/2Cl^-$ co-transporter
OSR1:	Oxidative stress-responsive kinase 1
PGC-1α:	Peroxisome proliferator- activated receptor-δ co-activator-1alpha
PGC-1β:	Peroxisome proliferator-activated receptor-δ co-activator-1beta
P_i:	inorganic phosphate
PIKfyve:	Phosphoinositide kinase FYVE
RNA:	Ribonucleic acid
ROS:	Reactive oxygen species
SEM:	Standard error mean
SGK1:	Serum and glucocorticoid inducible kinase 1
SGK3:	Serum and glucocorticoid inducible kinase 3
SLC family:	Solute carrier family
SPAK:	STE20 (sterile 20) / SPS1-related Proline/Alanine rich Kinase
V_m:	Vitesse maximal, maximal transport rate of a transporter
WNK:	With-no- lysine kinase K[lys]

List of figures

List of tables

1. INTRODUCTION

1.1 The inwardly rectifying K^+ channel Kir2.1

The inwardly rectifying potassium channel Kir2.1 belongs to the Kir2.X family of inward rectifier K^+ channels encoded by the genes KCNJ/IRK (1-3) and was the first time cloned from mouse macrophages (4). The flow of positive charged cations from the extracellular to the intracellular domain defines the inward current (5). Kir channels allow preferentially K^+ to pass through their pores (1, 5, 6).

The rectification function of Kir channels results from the "nonlinear change in the ion current through the ion channel" as a function of the electrochemical driving force (5). Thus, Kir channels have a determinant contribution to repolarization of the action potential and to maintain the resting membrane potential in excitable cells such as neurons, skeletal muscle and cardiac myocytes (1, 2). Therefore, many research studies focus on their potential as therapy targets for different disorders as cardiac arrhythmias, hypertension, learning and memory, epithelial transport and pain modulation (5).

1.1.1 Kir2.1 structure

Kir channels share the same structure composed of a pore forming loop and a single transmembrane domain (7). The tetramer structure is composed of four either homo-tetrameric or hetero-tetrameric transmembrane subunits bordering a water filled pore delimiting the passage of K^+ ions down their electrochemical gradient. Each inward K^+ channel subunit displays two α- helices crossing the plasma membrane with an extracellular K^+ selective site loop separating them (5) (Figure 1). Kir2.1 channel structure presents two main distinct parts namely: the transmembrane pore and the cytoplasmic pore (1, 8). The inward rectification function is ensured by the presence of magnesium ions (9, 10) or polyamines (11-13).

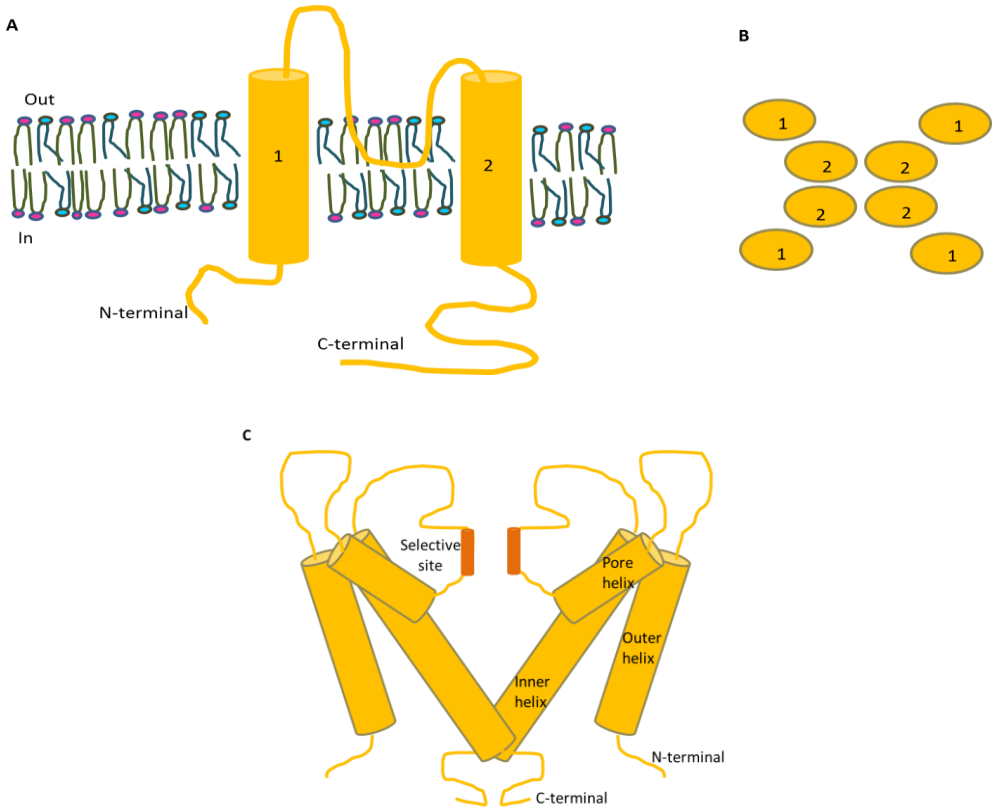

Figure 1: Kir channels general structure: A: Topology of an inward rectifying K^+ channel subunit model. B: Illustration of Kir tetramers organization. C: Schematic representation of KcsA K+ channel showing two subunits of the homo-tetramer, each subunit is composed of: an outer helix, inner helix, pore helix and a K^+ selective site. Adapted from Sepúlveda 2015 (14).

1.1.2 Kir2.1 expression and physiological function

Kir2.1 is expressed in several tissues namely: brain, heart, smooth and skeletal muscle, retina, kidney and placenta (15, 16).

1.1.2.1. Kir2.1 in Brain

In the brain, the inward rectifying K^+ channel Kir2.1 is expressed in excitable and non-excitable cells, and plays a major role in maintaining the hyperpolarized membrane potential (1, 17). Inward rectifying K^+ currents of Kir2.1 were detected in rodent microglia (18-20) in both resting and activated states (21-24), as well as in brain slices (25-27). It was

proven that Kir2.1 channel is needed for Ca^{2+} signaling in microglia and for migration in normal and anti-inflammatory conditions, whereas it has little inhibitory effect of proliferation (28). Kir current was also recorded in hippocampal neurons (29) and neonatal spinal motor neurons in rats (30). Further studies show the expression of Kir in the Schwann cells of the nodes of Ranvier, where it controls extracellular K^+, necessary for nerve fibers activity (31).

1.1.2.2. Kir2.1 in Heart and blood vessels

Kir channels are highly represented in cardiomyocytes including atrial, ventricular cells and Purkinje fibers (32-35). Kir contributes to the action potential and the resting membrane potential in cardiac cells, and is responsible for the plateau and the repolarization phase (1). Moreover, Kir channels are expressed in the endothelial as well as the smooth muscle cells (36, 37), they ensure the driving force for $Ca2^+$ flow through $Ca2^+$-permeable channels by keeping a negative potential in endothelial cells (38).

1.1.2.3. Kir2.1 in skeletal muscle

Kir channels activity in skeletal muscles is necessary to hyperpolarize the membrane potential and activation of Na^+ channels to allow the propagation of the action potential (39). The expression of Kir2.1 was also shown to be involved in the maintain of the membrane potential so that Ca^{2+} flows through the Ca^{2+}-permeable channels enhancing the differentiation of myoblasts (40).

1.1.2.4. Kir2.1 in kidney

The inwardly rectifying K^+ channel is expressed in the kidney and exactly in the juxtaglomerular cells (41), where it is involved in maintaining the membrane potential. In proximal renal tubules, Kir2.1 stimulates the cellular acidification, resulting in stimulation of Na^+ entry, thus activating Na/K-pump (42).

1.1.3 Kir2.1 modulation

The inward rectifier Kir2.1 plays a major role in cell excitability, thus the alteration of Kir2.1 activity suggests either a pro-excitotoxic or a pro-arrhythmic effect (43). Studies on mitochondrial dysfunction revealed a relation with cell membrane excitability and more precisely, Kir channels are regulated by mitochondrial function inhibitors (43-45). Kir2.1 among other Kir2.X inward rectifiers, is an heteromultimer (7, 46, 47) sensitive to mitochondrial dysfunction (43). In addition, Kir2.1 channels contribute to the ischemic pre-conditioning protection (48), which is a mechanism delaying and limiting cell death occurring following myocardium ischemia (49). During ischemia, K^+ flows out of cardiomyocytes through different K^+ channels, thus the concentration of the extracellular K^+ increases (50). Consequently, myocardium approaches the resting membrane potential, a state called electrical quiescence, and hence the activation of voltage gated K^+ channels is reduced drastically (48). Inward rectifier K^+ currents are activated because of the high extracellular K^+ concentrations (48).

Moreover, Kir2.1 channels are regulated by further factors such as the TNF-alpha (51) during neurological systemic inflammation in brain, which downregulates Kir2.1 expression (51). As well, PSD-93/chapsyn 110 binds to Kir2.1 channel and modifies the protein channel spatial and temporal distribution by enhancing the channels assembly and inhibition of protein internalization in neurons (52). Studies showed that filamin A increases Kir2.1 channel protein expression and insertion in the plasma membrane of the vascular smooth muscle (53). Cholesterol was proved to regulate the channel transition from active to inactive state (54). Kir2.1 is further regulated by PKC (55, 56), tyrosine kinase (57), kinase anchoring protein AKAP79 (58), SAP97, CASK, Veli and Mint1 (59), GTPase Rho (60) and the parvovirus B19 capsid protein VP1 (61).

1.1.4 Kir2.1 physiopathology

Mutations of KCNJ2, the gene encoding for the inwardly rectifying K^+ channel Kir2.1, induce severe channalopathies. The most known is caused by the loss of function mutations that results in Andersen Tawil syndrome (ATS). ATS is characterized by periodic paralysis, cardiac ventricular arrhythmia and developmental abnormalities (3, 39, 62-64). Also an

associated rare syndrome of a monogenic disease occurs with developmental defects of bone structures, periodic paralysis and cardiac arrhythmia alluding to (long Q-T) LQT syndrome (3, 65-67). The mutations affect negatively the potassium currents in Kir2.1 (68, 69) by blocking the protein channel migration to the cell surface (68) or by alteration of the interaction of the channel protein with the phosphatidylinositol4,5-bisphosphate (PIP2) (70). The loss of function mutation of KCNJ2 induces a prolonged plateau phase in the action potential and depolarization of the resting membrane potential (1).

The gain of function mutation of KCNJ2 gene encoding for Kir2.1 defines the short Q-T syndrome, which is characterized by sudden death following cardiac defect, syncope and/or atrial fibrillation (71). Moreover, Kir2.1 mutations is associated to phenocopies traits of the fetal alcohol spectrum disorder (FASD) which is characterized by several birth defects affecting cognition and structure like clef lip/palate, dental anomalies, digits anomalies and small jaws, head and stature. Kir2.1 channel turns out to be the molecular target of alcohol which modulates the channel activity by direct binding (72).

1.2 The creatine transporter CreaT

The Creatine transporter CreaT is encoded by the gene SLC6A8 and belongs to the solute carrier superfamily (i.e. SLC6) (73-75) which is the class of carriers that insure solute flow through the cellular plasma membrane down their electrochemical gradient. This transport is possible by coupling the transport of the solute to sodium Na^+ and chloride Cl^- (76). The co-transported solute can be a neurotransmitter such as the gamma aminobutyric acid GABA, glycine, norepinephrine, serotonin and dopamine (73, 76, 77) or an organic osmolyte i.e. betaine, taurine, the amino acid proline (76, 78, 79) and the metabolic compound creatine (76).

1.2.1. Creatine substrate

Creatine is a metabolic compound (figure 2) synthetized endogenously from the three following amino-acids: arginine, glycine and methionine, but can be provided from food

(meat and fish) (80). Creatine transport in a muscle cell is limited to 160mmol/kg (81).

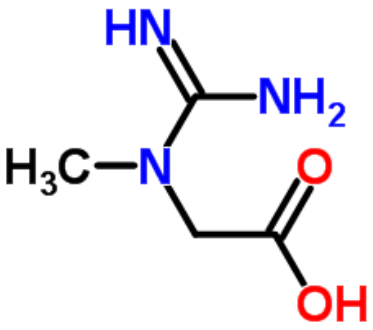

Figure 2: Creatine chemical structure. Molecular formula: $C_4H_9N_3O_2$, Mass 131.133 Da. (ChemSpider website, ID566)

Creatine is stored in the skeletal muscles (95%), the rest 5% resides in the brain, liver, testis and kidneys (80, 82), therefore, creatine supplementation is preconized for athletes' diet to enhance the muscular mass (80). Creatine main and well-known physiological role is the energy production, since it maintains the concentration of ATP (adenosine triphosphate) in muscles. ATP is the result of an oxidative phosphorylation mediated by mitochondria (80, 83).

1.2.2. Creatine transporter Structure

Transporters of SLC6 family present 12 transmembrane domains among which homo-oligomers. The C-terminal and the N-terminal tails are located in the intracellular space (76). Creatine transporter has a cysteine residue (Cys^{144}) unlike the rest of Na/Cl-coupled neurotransmitters carriers. Investigations on the role of Cys^{144} using site directed mutagenesis and methane thiosulfonate reaction, showed that replacing cysteine by serine did not change neither the kinetics nor the activity of CreaT, while alanine and leucine both increased the K_m (74). Nevertheless, the replacement of creatine by structural analogues like GABA, choline, glycine, beta alanine, taurine and betaine did not activate the intestinal creatine transporter demonstrating the high affinity of CreaT (84) and dependence to Na^+

(75). The creatine transporter CreaT is a 70kDa glycoprotein. It was isolated from HEK293 cells and displays a structure of alpha helices with 12 transmembrane domains (73).

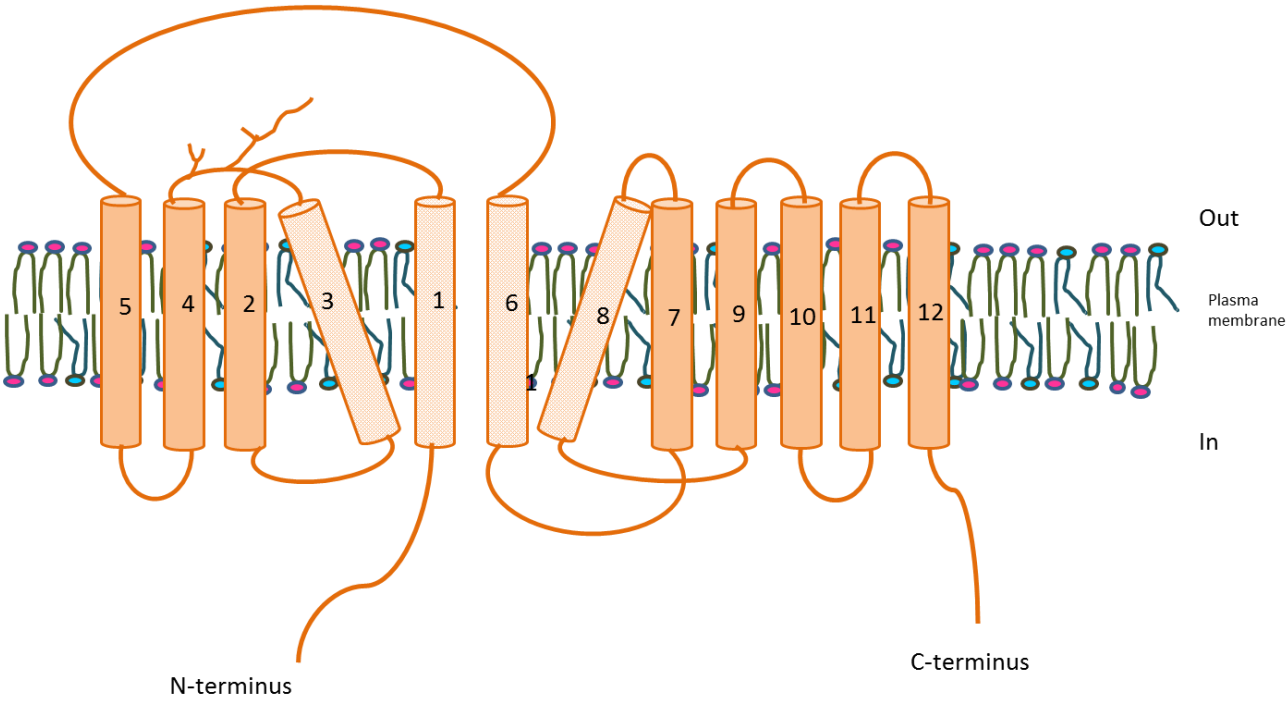

Figure 3: **Schematic structure of Creatine transporter CreaT SLC6A8**: showing 12 transmembrane domains with the transmembrane domains 1,6,3 and 8 contributing to creatine permeation and kinetics. Model adapted from the proposed models by Dodd and Christie 2007 (74) and Santacruz 2016 (85).

1.2.3. Creatine transporter expression and physiology function

SLC6 carriers are activated in order to regulate the extracellular concentration of a given solute and they modulate neuron signaling (76). The cloning and hybridization of the creaT isolated from human brain stem cells and spinal cord revealed that the creatine transporter is expressed in skeletal muscle, heart and kidney (75, 86). CreaT is also expressed in the intestinal villus where it ensures Na^+ and Cl^- coupled creatine transport with high affinity

(84). Moreover, the development of CreaT antibody allowed researchers to localize the creatine carrier expression in the brain, skeletal muscle and retina (77, 87, 88).

The creatine transporter is needed to supply creatine to cells with high energy demand (73, 77). Creatine is necessary to produce a high-energy phosphate buffering system in order to ensure the required ATP level in these tissues (77). For brain function, creatine provides the needed ATP concentrations; therefore the creatine transporter is specifically expressed in neurons of the olfactory bulb, granule cells of the dentate gyrus in hippocampus, pyramidal neurons of the cerebral cortex, Purkinje cells of cerebellum, motor and sensory cranial nerves nuclei of brainstem cells as well as dorsal and ventral horn in spinal cord. On the whole, CreaT is preferentially expressed in the forebrain, brainstem and the spinal cord, tissues responsible for learning process, memory modulation and function of the limbs (88). In addition, creatine in the brain shows an antioxidant effect, diminishes mental fatigue and prevents neurotoxicity. It is also known to improve neurological disorders especially depression and bipolarity (80).

1.2.4. Creatine transporter physiophathology

Mutations in the transporters of the solute carrier superfamily SLC6 are subject of several neurological disorders (76). CreaT is necessary for brain activity since mutations in the SLC6A8 gene leads to X-linked mental retardation, which is due to a severe lack of creatine in the brain. It engenders autistic behavior, epilepsy, speech and language delay (77) and also unusual alteration of language function and mental retardation (89, 90). Creatine deficiency syndrome results in major part from a lack of creatine transporter SLC6A8 expression, which explains the absence or the severe decreased creatine concentrations in brain (87, 91). Mutations in SLC6A8 have negative effect on the metabolism of stress, where intracellular creatine impacts directly on energy depletion which leads to the activation of metabolic stress hallmarks namely: reactive oxygen species (ROS), p38MAPK activation, uncontrolled proliferation and apoptosis (92-94). Moreover, the low expression of SLC6A8 in astrocyte in the blood-brain barrier influences creatine uptake from periphery (87).

1.3 The phosphate transporter NaPi-IIb

The phosphate transporter NaPi-IIb belongs to SLC34 family of Na^+ dependent phosphate carriers. Their role is to transport the inorganic phosphate (HPO_4^{2-}) coupled to sodium Na^+ (95). Phosphate homeostasis depends on three things: the first is phosphate uptake in intestines, the second is phosphate re-absorption and excretion in kidneys and the last is phosphate exchange between the extracellular and the stored P_i in bones (96). Intestinal phosphate absorption involves the Na^+ coupled phosphate transporter type II NaPi-IIb which is encoded by the gene SLC34a2 (97)

1.3.1. NaPi-IIb structure

The structure of the Na^+-coupled phosphate transporter NaPi-IIb analyzed via bioinformatics represents eight transmembrane domains, with five cytoplasmic and four extracellular loops, the N-terminal as well as the C- terminal are intracellular (98, 99). Figure 4.

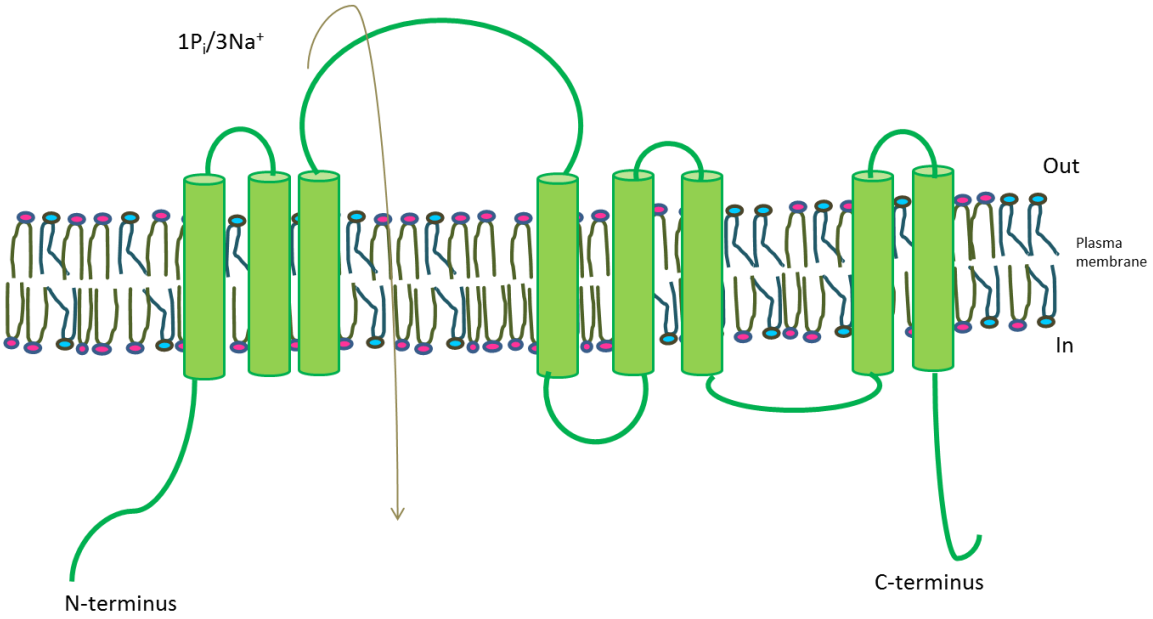

Figure 4: Phosphate transporter type II NaPi-IIb (SLC34A2) structure. Schematic structure of NaPi-IIb showing the 8 transmembrane domains and kinetics of inorganic phosphate and sodium. Adapted from Cerri et al. 2010 **(103).**

1.3.2. NaPi-IIb expression and physiology function

Inorganic phosphate (P_i) is important for several biological processes, for instance: bioenergetics, metabolic modulation needed for intracellular signaling (glycolysis, oxidative phosphorylation), cell proliferation (DNA and RNA composition), bone and membrane structure (100, 101). Phosphate participates in the balance acid-base in blood and urine. 85% of the total phosphate is accumulated in bones and teeth, the rest is located in erythrocytes and muscles (102).

The phosphate Na^+-dependent transporter NaPi-IIb is expressed in different tissues, namely: the small intestine brush border membrane, lung, liver, testis, salivary glands, thyroid, mammary glands and uterus (95, 104). The Na^+-coupled phosphate carrier NaPi-IIb determines the compensatory mechanism to phosphate homeostasis in kidney (97). NaPi-IIb has a major role in the phosphate absorption with more than 90% of the total absorbed phosphate in intestine (97).

SLC34A2 gene encoding for the phosphate transporter type II, is in addition expressed in the epididymis (105) and some types of cancer such as: ovarian (106), papillary thyroid (107) and breast cancer (108).

1.3.3. NaPi-IIb physiophathology

Hypophosphatemia caused by inherited disorder and resulting in renal phosphate reabsorption include hypophosphatemic rickets, X-linked hypophosphatemia and tumor induced osteomalacia (96, 109, 110).

Long term phosphate deficiency induces bone demineralization and thus leads to skeletal disorder like rickets in young individuals and osteomalacia in adults (111, 112) and enhances nephrolithiasis (113). Other disorders observed in hypophosphatemia such as the rhabdomyolisis, hemolysis, respiratory failure due to weak muscles and low myocardial contractility (114-116). On the other hand, hyper-phosphatmia is a severe chronic renal failure (117), involved in hyper-parathyroid activity, and also participates in the cardiovascular morbidity and mortality cases (118). Moreover, mutations in NaPi-IIb gene

induce pulmonary alveolar microlithiasis, a disorder due to calcification in alveoli induced by accumulation of phosphate in lungs (119). Phosphate imbalance presenting excessive phosphate exposure is cytotoxic and leads to cardiovascular disorders, which is consequent to P_i and Ca^{2+} deposition in vessels (120).

1.4. SPAK and OSR1 kinases

The mammalian kinases SPAK (STE20 (sterile 20) /SPS1-related proline/alanine rich kinase) and OSR1 (oxidative stress-responsive kinase 1) belong to the STE20 superfamily of the MAPK-like protein kinases (mitogen-activated protein kinases) (121-124). SPAK and OSR1 are homologous, sharing 96% of their N-terminal catalytic domain and 67% of their C- terminal regulator domain sequences (121).

1.4.1. SPAK tissues expression

SPAK was first identified in β-cells of pancreas (122, 123). Later it was shown to be ubiquitously expressed, since it was detected via Northern blot in brain, salivary gland, thymus, cardiac cells, lungs, spleen, stomach, intestines, adrenal glands, kidneys, testis, epididymis, ovaries and uterus (122, 125, 126). As well, SPAK was localized in rat embryos in the choroid plexus, myocardium, mesonephron and dorsal root ganglia (122, 127). SPAK kinase is expressed the most in the apical membrane of epithelium choroid plexus and in the cranial nerve nucleus of brain stem cells (126, 128).

1.4.2. OSR1 tissues expression

OSR1 gene was isolated and identified from chromosome 3 (124). OSR1 kinase is expressed in brain, heart, lung, kidney, colon and small intestine, thymus, liver, spleen, pancreas, skeletal muscles, ovaries, testis, prostate and placenta (122, 124). It was shown to be further expressed in the nuclear fractions of stomach among the rest of pre-cited tissues (129). OSR1 kinase shows a lower expression in brain stem cells than SPAK (128).

1.4.3. Physiological role of SPAK and OSR1

SPAK and OSR1 share important homology in the catalytic and regulator domain in addition to the several same tissues expression (121). They are both the downstream kinases of WNK1 and WNK4 and the upstream modulators of Na/K/Cl (NKCC1 and 2) and Na/Cl cotransporters (NCC) (130-132). SPAK and OSR1 are powerful modulators of ion transport in epithelial cells. Both kinases are co-localized with the $Na^+/K^+/2Cl^-$ cotransporter (NKCC2) in the thick ascending limb of Henle loop in kidney and also with the Na^+/Cl^- cotransporter (NCC) in the distal convoluted tubule (122, 133-135). Moreover, SPAK kinase is highly expressed in tissues secreting Cl^-, such as the gastric, sublingual and salivary glands (122, 126, 130). The kinases upregulate the Na^+ and Cl^- (NCC) cotransporter, as well, they enhance the activity of the $Na^+/K^+/2Cl^-$ (NKCC) cotransporters (122, 131-133, 136-138). In addition, SPAK/OSR1contribute to the regulation of blood pressure (122) through interaction with WNK to modulate the NCC and NKCC in kidney and blood vessels (135). In brain, and specifically in olfactory sensory cilia, SPAK and OSR1 expression is directly correlated with Cl^- accumulation due to NKCC1 activity and GABA depolarizing effect (122).

1.4.4. SPAK and OSR1 modulation

SPAK and OSR1 kinases are modulated mainly by With-no-lys kinases WNK phosphorylation (131, 132, 139, 140). This effect participates in the regulation of ion transport and blood pressure (132, 140-142). The kinases are present in the downstream pathway of WNK1 and WNK4 kinases (130-132). SPAK and OSR1 are phosphorylated and activated by WNK kinases consequently both SPAK and OSR1 activate NCC and NKCC1 by phosphorylation (143). Research on WNK kinases showed that only a subset of these kinases contributes to the activation of SPAK/OSR1 signaling (122). In the intestines, SPAK and OSR1 are regulated by forskolin, the adenylate cyclase stimulator (144). SPAK transcription is enhanced by the transcription factor NF-kappaB and SP1 (145). Further, SPAK activity is stimulated by angiotensin II (146, 147). Other modulators of SPAK and

OSR1 such as: glycoprotein CD46, TNF-α receptor, heat shock protein 105 (Hsp105) and calcium binding protein 39 (Cab39) (122).

1.4.5. Physiopathology of SPAK and OSR1

Genetic defects impairing the activity of the WNK kinases induce Gordon's syndrome, a monogenic disease presenting hyperkalemia and hypertension as well (142), which makes this syndrome different from the other forms of hypertension disorders that are inducing hypokalemia (148). Mutations in WNK and their downstream kinases SPAK and OSR1 are involved in Gordon's syndrome, by phosphorylation and activation of the Na/Cl and the Na/K/Cl cotransporters (148). SPAK deficiency leads to the decrease in the permeability in the para-cellular space and also induces resistance to inflammatory bowel disease (149). SPAK gene defects induce disturbed NCC activity in kidney and disturbed NKCC1 in blood vessels, which results in renal salt wasting followed by vasodilation, and causes a hypotension, these observations suggest SPAK to be a potential drug target (135).

OSR1 is a hypertension drug target (136). SPAK and OSR1 demonstrated a further role in cancer cells proliferation and migration (122). Furthermore, investigation of SPAK knock-out mice revealed that SPAK deficiency induces, through NKCC1 decaying function, mice latency in responding to noxious heat stimuli, together with balance and locomotion difficulty (122, 150).

Note: This introduction may lack some explanatory figures, avoiding any conflict and considering plagiarism rules.

Aim of the study

The regulation of ion transport involves several kinases including SPAK (SPS1-related proline/alanine-rich kinase) and OSR1 (oxidative stress-responsive kinase 1) which are the downstream of WNK (with-no-K[Lys]) kinases. SPAK and OSR1 are expressed in many tissues where they contribute to a variety of functions, among the most known the modulation of blood pressure and neuroexcitability (122, 151). Since the discovery of SPAK and OSR1 kinases, research studies focus rather on their tissues expression, interaction with WNK kinases or their role in the modulation of Na/K/Cl and Na/Cl cotransporters (122, 131-133, 136-138). Nevertheless, so far very few information is known about the role of SPAK and OSR1 in the regulation of further channels and transporters.

The present study sheds the light on the effect of both kinases SPAK and OSR1 on the following channels and transporters: the first channel is the inwardly rectifying K^+ channel Kir2.1 (KCNJ2), which is expressed in brain, heart and skeletal muscle, it is important to maintain the resting membrane potential and is determinant for cell volume regulation, preventing cell shrinkage and thus apoptosis (152). The second transporter is the creatine transporter CreaT (SLC6A8), a Na^+ and Cl^- coupled creatine carrier expressed in cells with high energy demand such as brain, heart, retina and skeletal muscle, where it provides creatine needed for energy. CreaT defects leads to mental retardation, seizure and intellectual disability (122). The third is the Na^+ coupled phosphate transporter NaPi-IIb, which mediates phosphate up-take in the intestine needed for bioenergetics and cell proliferation (100).

The aim of this study is to investigate whether the co-expression of the kinases SPAK and OSR1 influences the ion transport of Kir2.1, CreaT and NaPi-IIb and if it is related to WNK signaling. Moreover, this work investigates the effect on the channel conductance, and the kinetics of the transporters. Further, this study explores the effect of the kinases on the protein expression of the channel and the protein trafficking.

2. MATERIALS and METHODS

2.1. Materials:

2.1.1. Equipment:

Equipment Name	Manufacturer
Autoclave	HICLAVE-50 HMC Labor systemtechnik, Germany.
Digitizer digidata 1322A	Axon Instruments, Union City, CA, USA.
DMZ universal puller	Zeitz-instruments, Martinsried. Germany.
Eppendorf centrifuge 5415R	Hinz GmbH. Hamburg. Germany.
Gene Clamp 500 amplifier	Axon Instruments, Union City, USA.
HS-2A Headstage	Axon Instruments, Union City, USA.
Luminometer Wallac Victor	Perkin Elmer, Juegesheim, Germany.
(1420 multilabel counter plate reader)	
Maclab D/A converter AD	Instruments, Castle Hill, Australia.
Microscope Leica MS5	Leica microsystems, Germany.
Magnetic stirrer Combimag RCT	IKA-Werke GmbH & Co. KG, Germany.
Nanoliter injector 2000	World precision instruments, Germany
pH meter 646	Carl Zeiss, Oberkochen. Germany
Spectrophotometer: Biophotometer	Eppendorf, Hamburg, Germany.
Tube roller	Scilogex MX-T6-S, Michigan, USA.
Vortex Mixer VX-100	Labned, Langenfeld, Germany

2.1.2. Instruments:

Instrument Name	Manufacturer
Dissecting scissors	Fine Science Tools, Dumont, Switzerland.
Eppendorf pipettes 0.1-1000ul	Eppendorf. Hamburg. Germany.
Eppendorf pipettes 10-100ul	Eppendorf. Hamburg. Germany.
Eppendorf pipettes 0.5-10ul	Eppendorf. Hamburg. Germany.
Kelly forceps	Fine Science Tools, Dumont, Swizerland.
Thumb forceps	Fine Science Tools, Dumont, Swizerland.
Toothed forceps	Fine Science Tools, Dumont, Swizerland.

2.1.3. Consumable materials:

Material Name	Manufacturer
Borosilicate glass capillaries (OD: 1.14mm,ID: 0.5mm)	Harvard apparatus, USA.
Borosilicate glass capillaries (OD: 1.5mm,ID: 1.17mm)	Harvard apparatus, USA.
Bottle-top filters (0.5 l)	Carl Roth, Karlsruhe, Germany.
Cell Culture dishes PS (627 160 & 628 160)	Greiner bio-one, Frickenhausen, Germany.
Eppendorf tubes	Eppendorf, Hamburg, Germany.
Falcon tubes (15, 50ml)	Greiner bio-one, Frickenhausen, Germany.
Filter tips 10µl (SurPhob)	Biozym, Gemrany.
Hardshell 96 well plates	Biozym Biotech trading GmBH Vienna, Austria.
SteriCup-GP (0,22µm) Millipore	Merck Millipore, Germany.
Vicryl: Suture filament, polyglactin 910: (45cm) needle: 13mm 3/8c	Johnson & Jonhson, Medical GmbH, Ethicon Deutschland, Norderstedt, Germany

2.1.4. Chemicals:

Reagent Name	Manufacturer
CaCl2 x 2H2O	Sigma-Aldrich, Steinheim, Germany.
Ciprofloxacin	Fresenius Kabi Austria GmdH, Austria.
Collagenase Type II	Worthington Biochemical Corp., NJ, USA.
Creatine hydrate	Sigma-Aldrich, Steinheim, Germany.
HEPES	Carl Roth GmbH, Karlsruhe, Germany.
Gentamycinsultaf (Refobacin c)	Merck Serono, Dramstadt, Germany.
KCl	Carl Roth GmbH, Karlsruhe, Germany.
MgCl2 x 6H2O	Sigma-Aldrich, Steinheim, Germany.
NaCl	Sigma-Aldrich, Steinheim, Germany.
NaOH	Applichem GmbH O, Darmstadt, Germany.
Paraffin Oil	Merck, Darmstadt, Germany.
Di-NatriumhydrogenPhosphate di-hydrate (Na2HPO4*2H2O)	Sigma-Aldrich, Steinheim, Germany.
Sodium pyruvate	Sigma-Aldrich, Steinheim, Germany.
SuperSignal ELISA Femto Substrate	Thermo Fisher Scientific, Germany.
Tetracycline	Sigma-Aldrich, Steinheim, Germany.
Theophyline (Euphylon c)	Nycomed GmbH, Konstanz, Germany.
Tricaine methanesulfonate	Sigma-Aldrich, Steinheim, Germany.

2.1.5. Solutions:

2.1.5.1. ND96+ antibiotics solution for oocytes culture:

Reagent	Concentration
NaCl	88.5 mM
KCl	2 mM
CaCl*2H2O	1.8 mM
MgCl2*6H2O	1 mM
Hepes	5 mM
NaOH	2.5 mM
Sodium Pyruvate	5 mM
Gentamycin	100mg/L
Tetracyclin	50mg/L
Ciprofloxacin	1.6mg/L
Theophylin	90mg/L

*The pH is adjusted to 7.4 and this solution is filtred maintained at 4°C.

2.1.5.2. ND96 superfusate solution for measurement:

Reagent	Concentration
NaCl	93.5 mM
KCl	2 mM
CaCl*2H2O	1.8 mM
MgCl2*6H2O	1 mM
Hepes	5 mM
NaOH	2.5 mM

*The pH is adjusted to 7.4 and this solution is maintained at room temperature.

2.1.5.3. OR2 Solution:

Reagent	Concentration
NaCl	82.5 mM
KCl	2 mM
MgCl2*6H2O	1 mM
Hepes	5 mM
NaOH	2.5 mM

*The pH is adjusted to 7.4 and this solution is filtered and maintained at 4°C.

2.1.5.4. OR2 solution for oocytes defolliculation:

Reagent	Concentration
NaCl	82.5 mM
KCl	2 mM
MgCl2*6H2O	1 mM
Hepes	5 mM
NaOH	2.5 mM
Collagenase II	1 mg/ml

*The pH is adjusted to 7.4, freshly prepared.

2.1.5.5. Anesthesia Solution for frog:

Reagent	Concentration
Tricaine	1mg/ml

*This solution should be mixed very well with fresh water.

2.1.6. Animal material: *Xenopus laevis*

Xenopus Laevis female specimens were provided from NASCO, Fort Atkinson, USA, and maintained in the animal facility of the Physiology Institute of Tübingen University.
Frogs were kept humanely in accordance with the German law for the welfare of animals and were approved by local authorities.

2.1.7. Software:

Software Name	Company
GraphPad InStat v3.05	GraphPad Software Inc., La Jolla, CA, USA.
GraphPad Prism 5.0	GraphPad Software Inc., La Jolla, CA, USA.
Microcal Origin 6.0G	Microcal software, Northampton, MA, USA.
pClamp 9.2 software package: - Clampex 9.2 Data acquisition - Clampfit 9.2 Data analysis	Axon Instruments, Union City, CA, USA. Axon Instruments, Union City, CA, USA. Axon Instruments, Union City, CA, USA.
Wallac 1420 manager prog.	Wallac Victor, Perkin Elmer, Germany.

2.2. Methods:

2.2.1. cRNA preparation:

The cRNA needed to be injected in the Xenopus oocytes to express the corresponding protein, are synthesized from the corresponding DNA each. These constructs encode for the following wild-type kinases: human Kir 2.1(153), Kir 2.1-HA having an extracellular hemagglutinin epitope (154), bovine creatine transporter (CreaT) (88), human NaPi-IIb (155), human SPAK (131), human OSR1 (156) and the following mutant human kinases ^{T233E}SPAK, ^{T233A}SPAK, ^{D212A}SPAK (131), ^{T185E}OSR1, ^{T185A}OSR1 and ^{D164A}OSR1 (156).

The production of the cRNA is the result of two main following steps:

2.2.1.1. Plasmid DNA linearization:

Specific restriction endonucleases were used to cut at 3' end of every insert.

Table 1: Plasmids containing the gene encoding the specific protein and restriction Endonucleases and polymerases.

Plasmid	Vector	Restriction enzyme	Polymerase
Kir2.1 (KCNJ2)	pGHJ	Mlu I	SP6
Kir2.1-HA	pGHJ	Mlu I	SP6
CreaT (SLC6A8)	pGHJ	Not I / Spe I	T7
NaPi-IIb (SLC34A2)	Psport1	Sal l	SP6
SPAK	pGHJ	Sal I/Sph I	T7
^{T233E}SPAK	pGHJ	Sal I/Sph I	T7
^{T233A}SPAK	pGHJ	Sal I/Sph I	T7
^{D212A}SPAK	pGHJ	Sal I/Sph I	T7
OSR1	pGHJ	Spe I	T7
^{T185E}OSR1	pGHJ	Spe I	T7
^{T185A}OSR1	pGHJ	Spe I	T7
^{D164A}OSR1	pGHJ	Spe I	T7

The following reaction mixture is used to linearize the DNA plasmid: (see Table 2)

Table 2: Mixture of reagents for DNA linearization

Mixture	Volume/Concentration
10X Buffer	5µl
DNA plasmid (10µg)	Depends on DNA concentration
Restriction enzyme (20U)	2µl

Deionized water (nucleases free) DEPC	The needed to reach the total volume of 25µl

This mixture was incubated overnight at 37°C. Then, a careful purification of the DNA using a NucleoSpin® Gel and PCR celan-up: 250µl of NTI Buffer was added to the mixture and loaded in NucleoSpin® Gel. PCR clean up column is centrifuged at 11000rpm/30 seconds. The column was then washed twice with 700µl NT3 Buffer and centrifuged again at 11000/1minute. The DNA was then eluted with 20µl NE Buffer. Later, cRNA concentration was measured via the Bio-photometer (Eppendorf, Hamburg, Germany), using a spectrophotometer cuvette (1µl cRNA + 69µl water).

2.2.1.2. cRNA synthesis:

The DNA linearized was used as a template to synthesize the cRNA. For this purpose we do need the following mixture: (see table 3)

Table 3: Mixture of reagents for cRNA synthesis

Mixture	**Volume/Concentration**
Linearized DNA (1µg)	Depends on the DNA concentration
10X Buffer	2.5µl
rNTPs	1µl
Cap analog	2.5µl
RNAse inhibitor	1µl
Deionized water	The needed volume to reach 25µl

All the reagents were mixed together by a gentle vortexing. The specific RNA polymerase was then added to the mixture, prior to an incubation of 2 full hours at 37°C. Afterwards, 5µl of DNAase was added to avoid any possible DNA contamination, and the whole mixture was then incubated at 37°C for 15 minutes on a shaker.
The corresponding polymerases were added following the Table 1.

The following step consists on the purification of the new synthesized RNA. For this purpose, 129µl of phenol chloroform was mixed to 100µl of DEPC water and centrifuged at 11000 rpm/5minutes. The result of the centrifugation shows two different phases, the inorganic phase (the upper phase) was thoroughly separated in a new Eppendorf tube. Later, 375µl of 100% Ethanol and 12.5µl of 3M Sodium acetate (pH=5.2) were added and all was mixed together to be incubated at -70°C for 30 minutes. At the end of the incubation time, a centrifugation at 20000 rpm/15minutes/4°C was performed. Only the pellet was kept for a wash with 500µl Ethanol 70%. Then, the tube was placed in the Speedvac for 5 minutes in order to dry. Then after, 40µl of DEPC water was added to dilute the pellet. The cRNA concentration was measured via an Eppendorf Biophotometer (Hamburg, Germany) using 1µl of the new synthesized cRNA and 69µl of water mixed in a cuvette. Finally, the cRNA was run on a gel electrophoresis to confirm its quality. Good cRNA was kept in -80°C for a later use.

2.2.2. Frog Operation:

- **Pre-operative considerations**:

Frog needs to fast 12hours prior to surgery. The surgical area must be clean with a disinfectant (Descosept AF alcoholic rapid, Dr. Schumacher, Value-Rx, Inc.).

- **Instruments sterilization**:

Instruments must be sterilized in the sterilization center of the UniversitätsKlinikum Tübingen, before the surgery and placed on a sterile wrap during surgery.

- **Anesthesia**:

To anesthetize the frog, a fresh solution of 1mg/ml Tricaine methane sulfonate (ethyl 3-aminobenzoate methanesulfonate salt) mixed very well in fresh water is prepared. The *Xenopus laevis* is placed in the anesthesia solution for 15 to 30 minutes (depending on the frog). To check whether the frog is well anesthetized, a mechanical stimulus is used by pressing the hind paw with fingers, when the leg drawing-back reflex is lost, the frog is enough unconscious. The animal is removed from the solution and placed on the clean wet pad, to keep the frog's skin moist.

- **Surgical procedure**:

Skin preparation is not always necessary, but when needed, cotton stick is used. An incision of 0.5 to 2 cm is operated through the skin first and then incision through the muscle layer. This should be done on either the left or the right side. A portion of oocytes are exteriorized with forceps and placed in OR2 solution. Then, both tissue layers are closed back separately with a monofilament suture (Vicryl).

- **Post-surgical care**:

The frog must be placed in dechlorinated water in a shallow recovery container. Water should not cover the nostrils of the frog. Once frog is active again, it can be placed in a tank and labelled with date and operation side. The animal should be checked every day after the operation.

2.2.3. Oocytes treatment, injection and culture:

- **Defolliculation**:

The oocytes extracted from the *Xenopus* ovary, are placed immediately in OR2 solution. Later, these cells are immerged in the defolliculation solution (OR2+collagenase type II) to undergo collagenase digestion for 3hours, under a slow rotation on a tube roller, considering the obscurity condition. The oocytes are then washed with OR2 and checked under microscope, if the follicular layer is ruptured, a second wash with ND96 enriched solution with anti-biotics to stop the collagenase effect as well as cell division. (Figure 5).

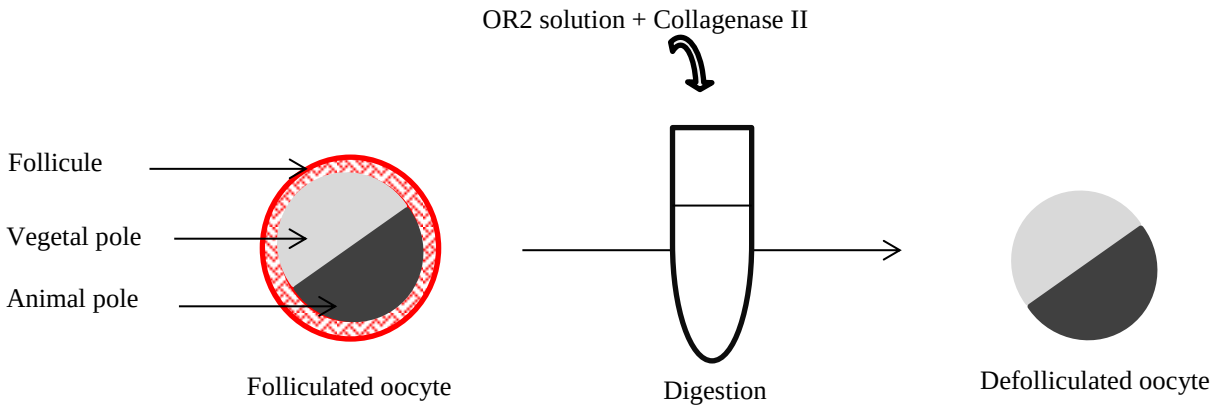

Figure 5: Defolliculation process.

- **Oocytes selection**:

A meticulous selection of mature oocytes (at stage V and VI) presenting a clear differentiation between the two poles of the oocyte, namely: the vegetal pole and the animal pole, sign of healthy and adequate oocyte for injection is needed.

- **Oocytes injection**:

Oocytes treated beforehand, take a rest of 1 to 2 hours prior to injection. They were divided into groups corresponding to the needed experiment and then placed on a netted petri dish being ready for manual injection, using a Nano-liter injector. Borosilicate (or Glass) capillaries used in injection are prepared using the Pullar, beforehand. The capillary tip should be cut to open a diameter of 20µm allowing the flow of RNA afterwards. An injection of Paraffin oil in the capillary is needed prior to RNA suction. (Figure 6 and Table 4).

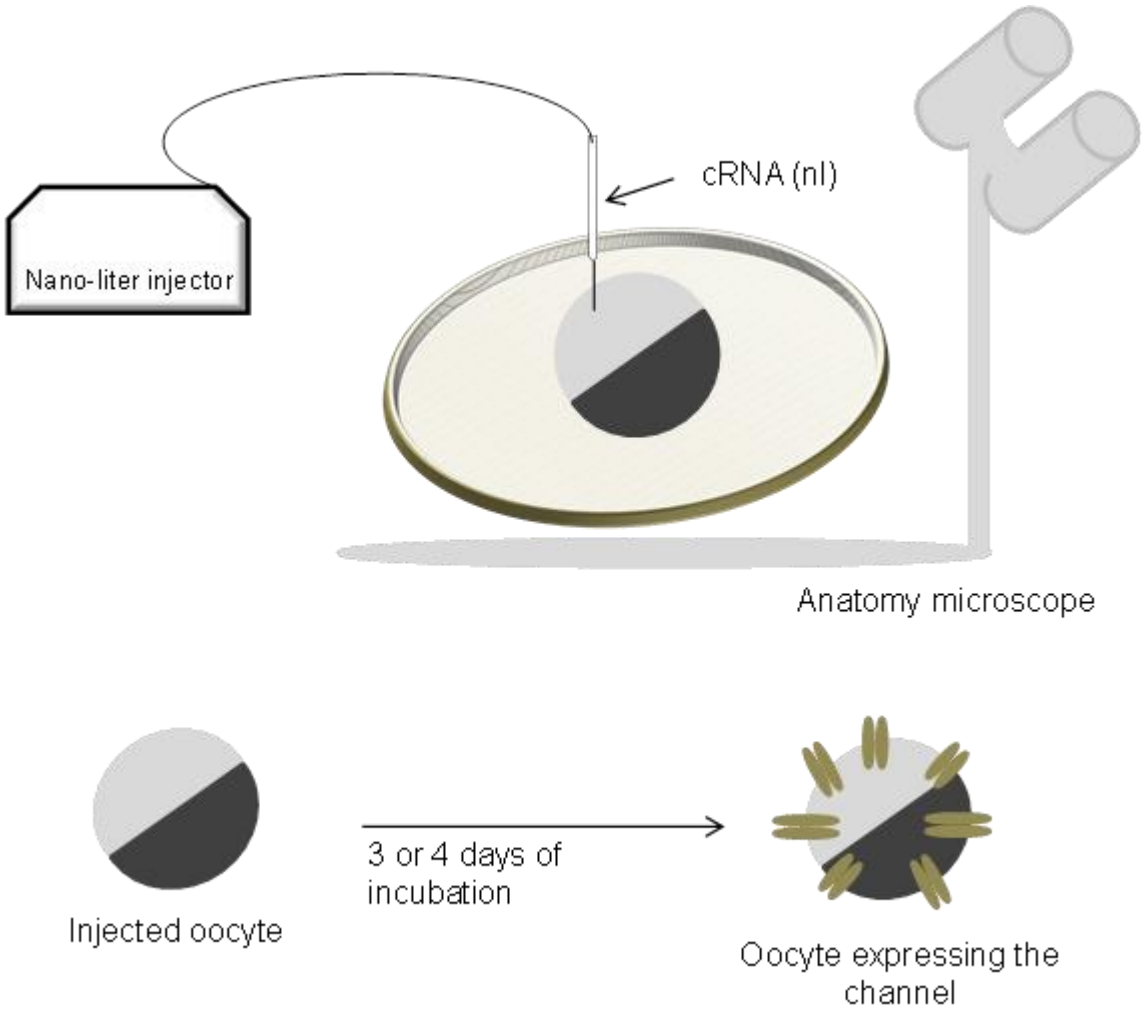

Figure 6: Oocytes manual injection

- **Culture**:

Oocytes are kept in petri dishes filled with ND96 solution for culture, at 17°C temperature, for later use. Medium is changed daily, and dead oocytes are removed from the medium. The expression of a given protein (transporter, channel) on the cell membrane takes in general from 3 to 10 days depending on the molecule complexity. Here, we explain in the following Table 4.

Table 4: Days required for protein expression and cRNA concentrations.

Protein	[cRNA] (ng) / oocyte	Days of incubation
Kir2.1	10ng	3 days
Kir2.1-HA	10ng	3 days
CreaT	15ng	4 days
NaPi-IIb	15ng	4 days
SPAK	10ng	3 days
^{T233E}SPAK	10ng	3 days
^{T233A}SPAK	10ng	3 days
^{D212A}SPAK	10ng	3 days
OSR1	10ng	3 days
^{T185E}OSR1	10ng	3 days
^{T185A}OSR1	10ng	3 days
^{D164A}OSR1	10ng	3 days

2.2.4. Dual Electrode Voltage Clamp measurement:

The dual electrode voltage clamp technique was used to measure in a real time the activity of ion channel and transporters in this study. This is the conventional technique of electrophysiology used to control artificially the membrane potential of the macroscopic single cell, namely the *Xenopus laevis* oocyte. (See figure 7). All the electrophysiological measurements were performed at room temperature after the corresponding incubation days.

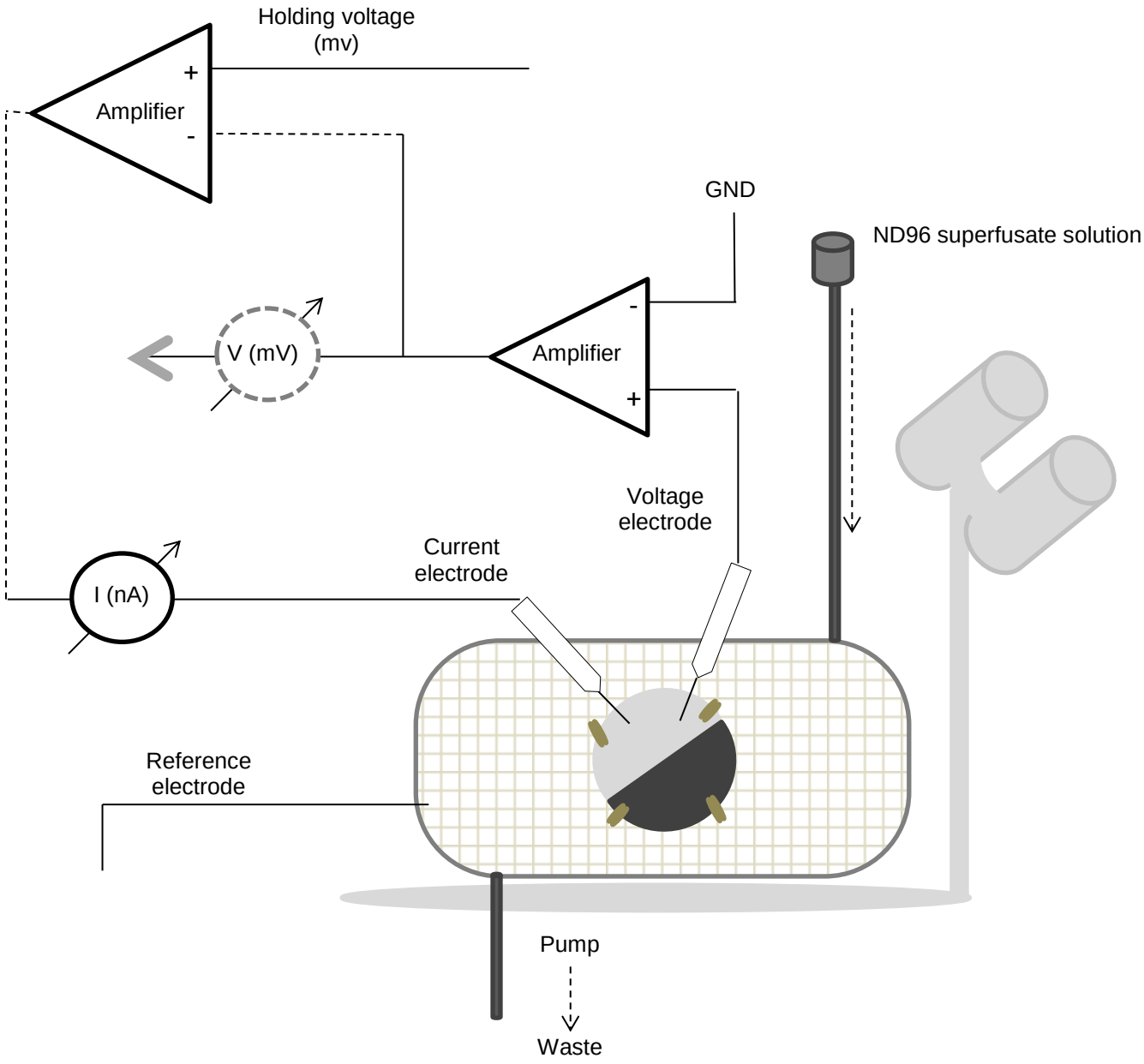

Figure 7: Dual Electrode Voltage Clamp Principle

2.2.4.1. Inwardly rectifying K^+ current in real-time recording of Kir2.1, KCNJ2

The recording of the inwardly rectifying potassium currents through Kir2.1 channels via voltage clamp needed a concentration of 5mM KCl in the ND96 superfusate solution. The flow rate of the superfusion was about 20ml/min.

Measurement was done at a holding potential of -60mV. The inwardly rectifying K^+ currents were obtained every 20 seconds with 1 second pulses, from -150 mV to +30 mV, 10mV increment (figure 8). Data were filtred at 2 kHz and recorded with digita A/D-D/A converter 1322A Axon instruments. pClamp 9.2 software package from Axon Insruments, Union City, CA, USA was used as corresponding: Clampex 9.2 software for data acquisition and Clampfit 9.2 software for Data analysis, respectively.

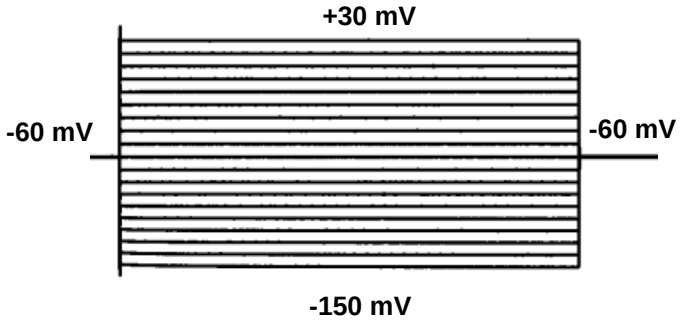

Figure 8: Voltage Clamp recording protocol of the inwardly rectifying K^+ channel Kir2.1

2.2.4.2: Ion Transporter real-time recording:

The recording of ion transport through carriers necessitates the addition of the specific substrate to the ND96 superfusate solution. The superfusate flows at 20ml/min. The data were filtred at 10Hz and recorded with digita A/D-D/A converter 1322A Axon instruments.

pClamp 9.2 softwares package (Axon Insruments, Union City, CA, USA): Clampex 9.2 and Clampfit 9.2 were used for data acquisition and Data analysis, respectively.

2.2.4.2.1. Creatine transporter: CreaT, SLC6A8

For CreaT (SLC6A8) activity assessment, 1Mm creatine hydrate was added to the ND96 superfusate in all experiments, expect the measurement of carrier kinetics, where increasing concentrations of creatine were used as following in mM: 0.003, 0.03, 0.1, 0.3, 1 and 3. Current recording used CreaT protocol with -60mV pre-set holding potential.

2.2.4.2.2. Phosphate transporter: NaPi-IIb, SLC34A2

The phosphate transport was possible by addition of 1Mm phosphate di-hydrate to the ND96 superfusate in all experiments. The transporter kinetics assessment needed the use of different concentrations of phosphate as following in mM: 0.1, 0.2, 0.4, 0.8, 1, 2 and 4. Current recording used CreaT protocol with -60mV pre-set holding potential.

2.2.5. Quantification of Protein cell surface abundance via Chemiluminescence:

- **Principle**:

The chemiluminescence is the technique that allows the assessment of the abundance of a given protein expressed on cell surface through light. Chemiluminescence (or chemoluminescence) is defined as the emission of light (luminescence) following a chemical reaction without heat. The 'Horseradish Peroxidase' (HRD) enzyme catalyzes the substrate, resulting in a luminescent product, which quantification is possible via a luminometer machine. (Figure 9)

- **Cell surface proteins expression**:

For the purpose, the inwardly rectifying K^+ channel Kir2.1 with an external HA-tag was expressed in *Xenopus* defolliculated oocytes with or without co-expression of the kinase SPAK or OSR1, compared to oocytes injected with water as a negative control.

- **Monoclonal anti-body treatment**:

After 3 days of culture, oocytes were incubated in a blocking solution composed of 1ml ND96 (see subheading 2.1.5.2) with 1% BSA for 20 minutes placed in a crushed ice box on a plate shaker. The blocking solution was then removed and replaced by 1:500 monoclonal anti-HA antibody conjugated to Horseradish Peroxidase (Miltenyi Biotech, Germany) diluted in 1% BSA/ND96. Oocytes were incubated for 1 hour on the plate shaker at 4°C. The oocytes were first washed with 1ml of 1% BSA in ND96 for 5 minutes under shaking condition at 4°C. This first wash step was repeated 3 times. The second wash step was done with ND96 solution only, again for 5 minutes at 4°C under shaking condition and repeated 3 times. Immediately afterwards, each oocyte was placed in an individual well of a hardshell 96 well plate, appropriate to avoid any possible light crossing, along with 100µl ND96 + 20µl of SuperSignal (Elisa Femto Substrate) under protection from light.

- **Quantification and Analysis**:

Chemiluminescence of every oocyte was measured by a Wallac Victor2 plate reader, by integrating the signal over 1 second-period. The results are given as normalized relative light units and assessed visually to prevent any unspecific cytosolic light. The analysis was possible through Wallac 1420 manager programme.

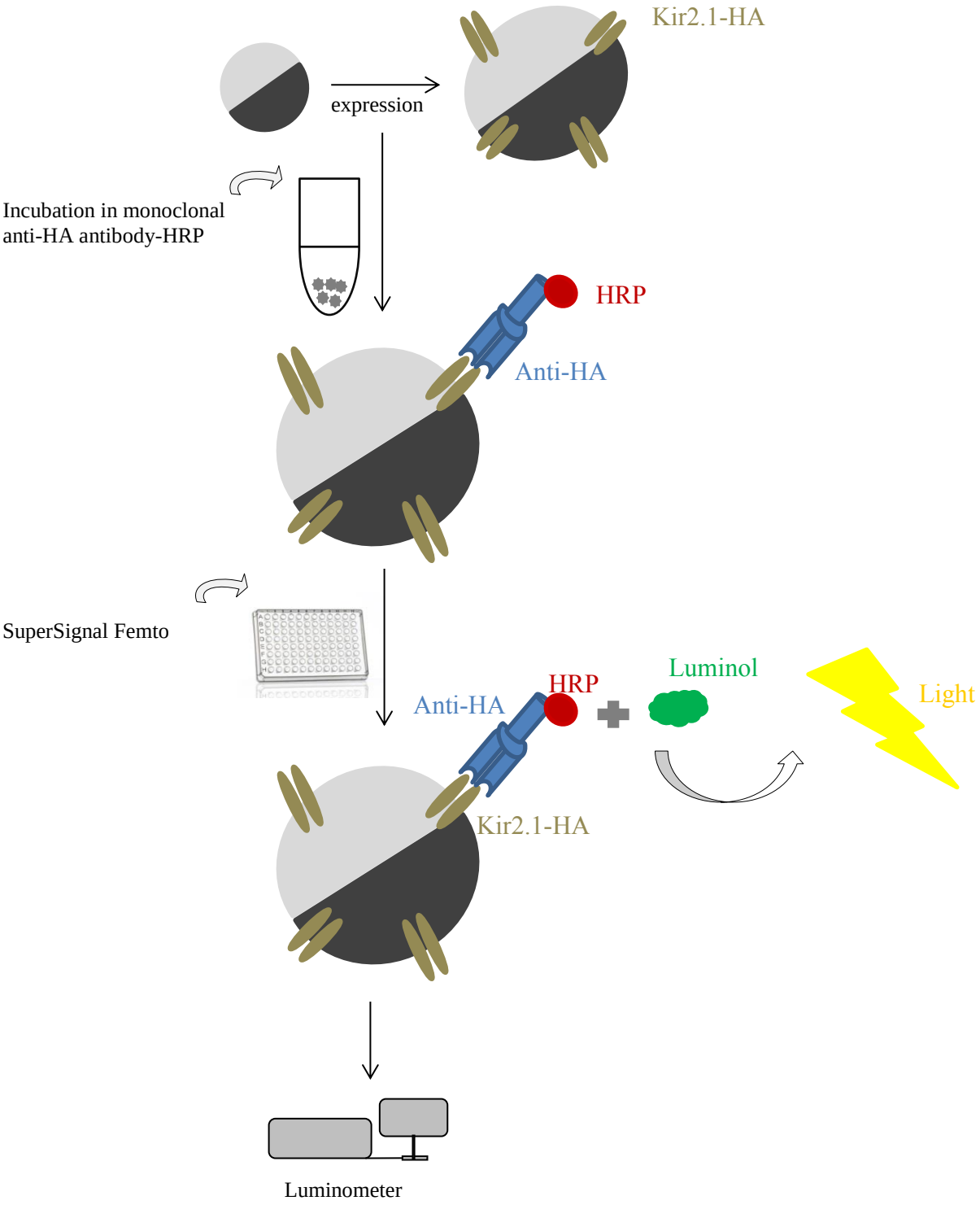

Figure 9: Chemiluminescence principle

2.2.6. Brefeldin A treatment

Brefeldin A is a natural fungal macrocyclic lactone extracted from *Eupenicillium brefeldianum*. It is shown to inhibit protein trafficking by a rapid accumulation of proteins in the endoplasmic reticulum and by blocking the secretion and redistribution of vesicles leading to the collapse of Golgi apparatus. For such property, brefeldin A had been widely used as a biological tool in the study of protein transport (157-159) (Figure 17).

After oocytes injection with the KCNJ2 cRNA encoding for Kir2.1channel, oocytes were incubated in ND96 culture solution for 3 days. The treated groups were supplemented with 5 µM of Brefeldin A in their culture media 24 hours prior to the dual voltage clamp measurement.

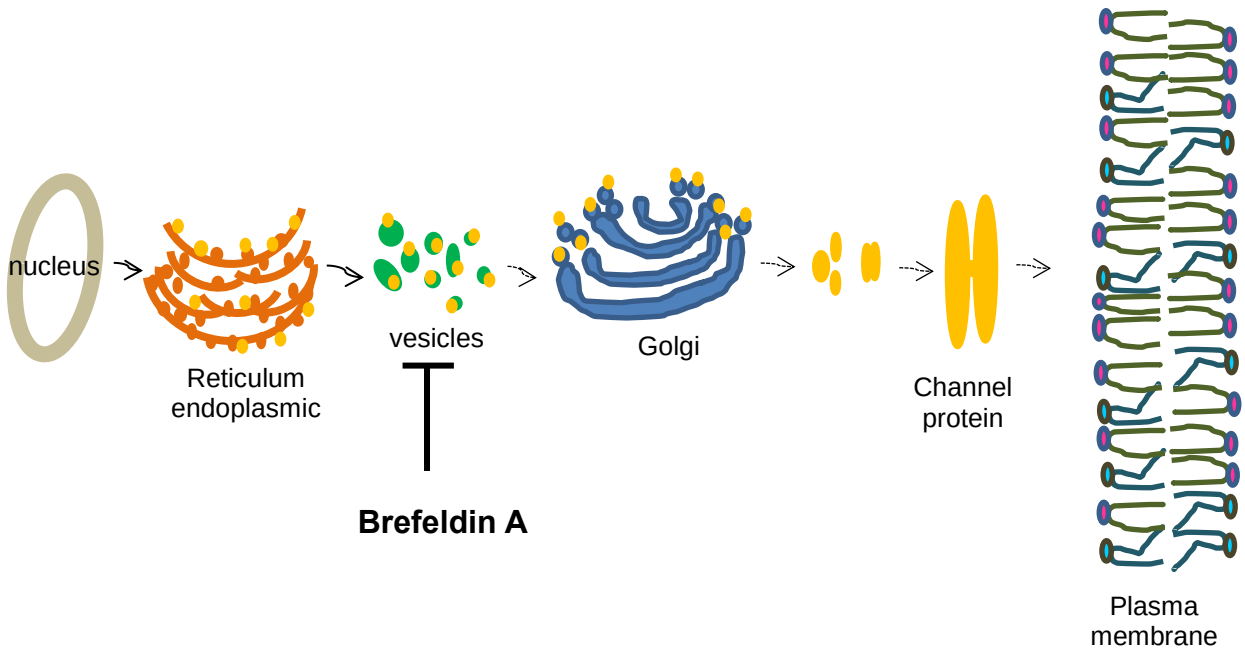

Figure 10: **Brefeldin A inhibiting protein channel migration to the membrane principle**

2.2.7. Ethical Statement:

All experiments were conform to the 'European Convention for the Protection of Vertebrate Animals used for Experimental and other Scientific Purposes' (Council of Europe No 123, Strasbourg 1985) and were conducted according to the German law for the welfare of animals. Surgical procedures on the adult *Xenopus laevis* were reviewed and approved by the respective government authority of the state Baden-Württemberg (Regierungspräsidium) prior to the start of the study (Anzeige für Organentnahme nach 36).

2.2.8. Statistics:

The Data are expressed as arithmetic means ± standard error mean (SEM), where (n) represents the number of oocytes measured. All voltage-clamp and chemiluminescence experiments were repeated at least 3 batches of oocytes; in all repetitions qualitatively similar data were obtained. Statistical analysis used either the Student t-test or ANOVA (analysis of variance), as appropriate. Values of $P < 0.05$ were considered statistically significant.

3. RESULTS

The results are composed of three main parts.

Part of the results presented here is published in the following papers:

Fezai M, Ahmed M, Hosseinzadeh Z, Elvira B, Lang F. SPAK and OSR1 sensitive Kir2.1 K^+ Channels. Neurosignals. 2015 Dec 17; 23(1):20-33.

Fezai M, Elvira B, Borras J, Ben-Attia M, Hoseinzadeh Z, Lang F. Negative regulation of the creatine transporter SLC6A8 by SPAK and OSR1. Kidney Blood Press Res. 2014 Dec 8;39(6):546-54.

Fezai M, Elvira B, Warsi J, Ben-Attia M, Hosseinzadeh Z, Lang F. Up-Regulation of Intestinal Phosphate Transporter NaPi-IIb (SLC34A2) by the Kinases SPAK and OSR1. Kidney Blood Press Res. 2015Oct 28; 40(6):555-64.

3.1. Kir2.1 sensitive to SPAK and OSR1

3.1.1. SPAK up-regulated Kir2.1

3.1.1.1. Wild-type SPAK increased the inwardly rectifying K^+ current in KCNJ2-expressing *Xenopus laevis* oocytes

3.1.1.1.1. The inward rectifying K^+ currents enhanced by SPAK co-expression

In order to investigate the effect of SPAK on Kir2.1 channel, the inwardly rectifying K^+ currents were measured in *Xenopus laevis* oocytes by two electrode voltage clamp technique. *Xenopus* oocytes were divided in 4 different groups: oocytes expressing either Kir2.1 (KCNJ2) channels alone, or the kinase SPAK only, or co-expressing both the channel and the kinase Kir2.1+SPAK and a negative control group was injected with water. Oocytes membrane current was recorded at a holding potential of -60mV. The inwardly rectifying K^+ currents were obtained every 20s with 1s pulses, from -150 mV to +30 mV, 10mV increment.

Negative control as well as SPAK-injected oocytes did not show any appreciable inward K^+ current, on one hand, which confirms that the oocytes expressed negligible inwardly rectifying K^+ currents. On the other hand, Kir2.1-expressing oocytes showed large measurable inward rectifying K^+ currents. This current was significantly increased in the presence of the wild-type SPAK. As illustrated in figure 11 (A) the original tracings along with the recording protocol and figure 11 (B) showing the histogram of the arithmetic means of maximal inward K^+ currents of the different groups (160).

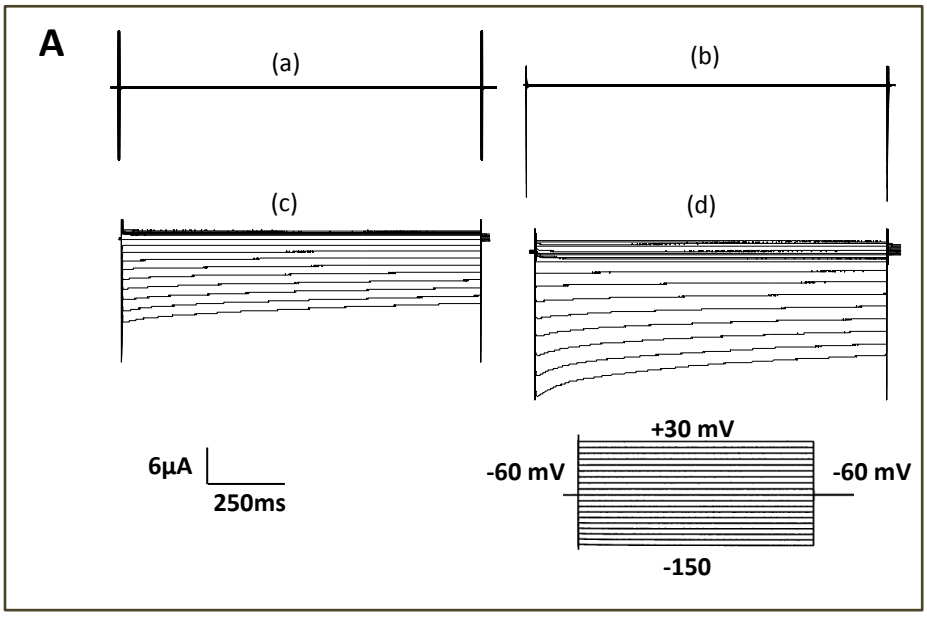

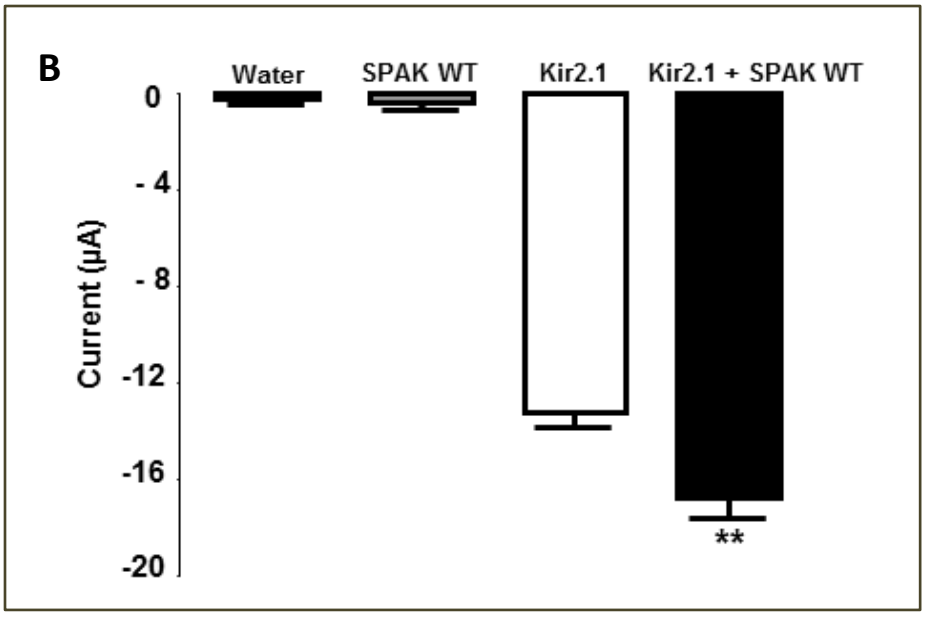

Figure 11: The inward rectifying K^+ current in Kir2.1 is up-regulated by wild-type SPAK additional expression. (**A)**: Original tracings of currents measured in *Xenopus laevis* oocytes expressing water (a), SPAK alone (b), Kir2.1 (KCNJ2) alone (c) and Kir2.1 + wild-type SPAK (d). The recording protocol is not to scale. (**B)**: Histogram of means of the maximal inward K^+ current I (µA) recorded at -150mV (±SEM), respectively in negative control water (dotted bar), SPAK WT only (grey bar), Kir2.1 (white bar) and Kir2.1 co-injected with SPAK WT (black bar). (n = 9-37), 3 different batches of oocytes. **(p<0.01) express the statistical significant difference between Kir2.1 and kir2.1+ SPAK WT (160).

3.1.1.1.2. The Current-Voltage (I/V) curve characteristic assessment with wild-type SPAK

The current-voltage curve (I/V curve) characteristic refers to the current and voltage relationship of K^+ channel activation and voltage dependent inactivation. I/V refers to the current amplitude recorded during the test pulse after conditioning the pre-pulse (amplitude V) and I is the maximum current during the test pulse (161).

For Kir2.1 (I/V) curve, the holding potential is preset to -60mV. Applying the pulses from -150mV to +30mV induces channels opening and thus inward current could be measured. The current through Kir2.1 channel at each precise potential is then proportional to the driving force and the opening probability.

Current amplitudes serve to plot the (I/V) curve as illustrated in figure 12 showing current carried by K^+ with negative reversal potential and a characteristic shape of the inwardly rectifying K^+ currents. The I/V curves show a clear up-regulation of the K^+ currents between Kir2.1-expressing oocytes and Kir2.1+SPAK co-expressing oocytes, while both water injected oocytes and SPAK expressing oocytes did not show any curve (160).

.

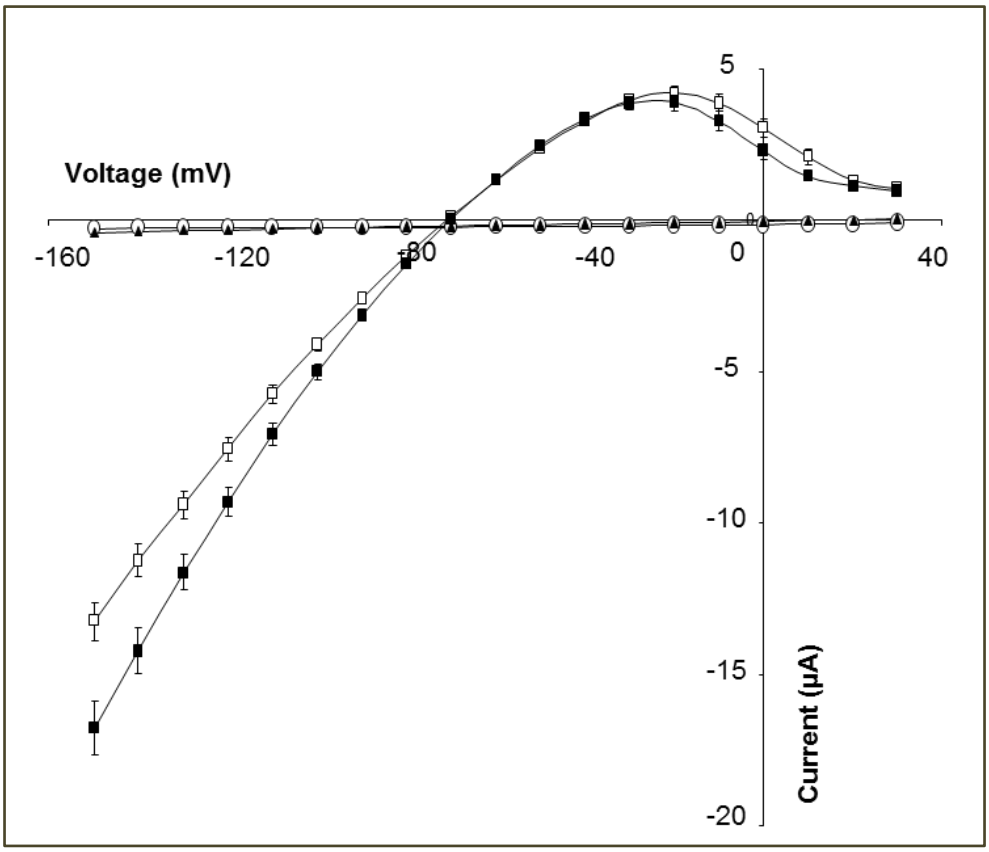

Figure 12: Current-Voltage (I/V) curve: current as function of potential difference across the cell membrane demonstrated a stimulation effect of SPAK on Kir2.1 currents. Curves plotted by means of the current I (µA) (±SEM) as a function of the voltage steps applied on the oocyte membrane V(mV) from -150mV to +30mV. (I/V)-curves correspond respectively to water injected oocytes (white circles), SPAK alone (black triangles), Kir2.1 alone (white squares) and kir2.1 + SPAK wt (black squares). (n=9-37), 3 different batches of oocytes. (160)

3.1.1.1.3. The wild-type SPAK up-regulated the Kir2.1 channel Conductance

The conductance is one of the measurable properties of ion channels. It defines the rate of ions flowing through the channel, which electrophysiological analysis applies Ohm's low (the current through a conductor between two points is proportional to the voltage: I=V/R). The conductance is calculated as the ratio of ion current to the applied voltage. $g_i = I_i/(V_m-E_i)$ with (g_i = conductance , I_i = the flowing ions, (V_m-E_i) = the driving force).

The comparison of the conductance between Kir2.1-expressing oocytes and Kir2.1co-expressing SPAK wild-type, considered the linear fit of I/V-curves between the amplitudes -150mV and -120mV. The conductance was significantly increased in the presence of wild-type SPAK kinase as shown in the figure 13 (160).

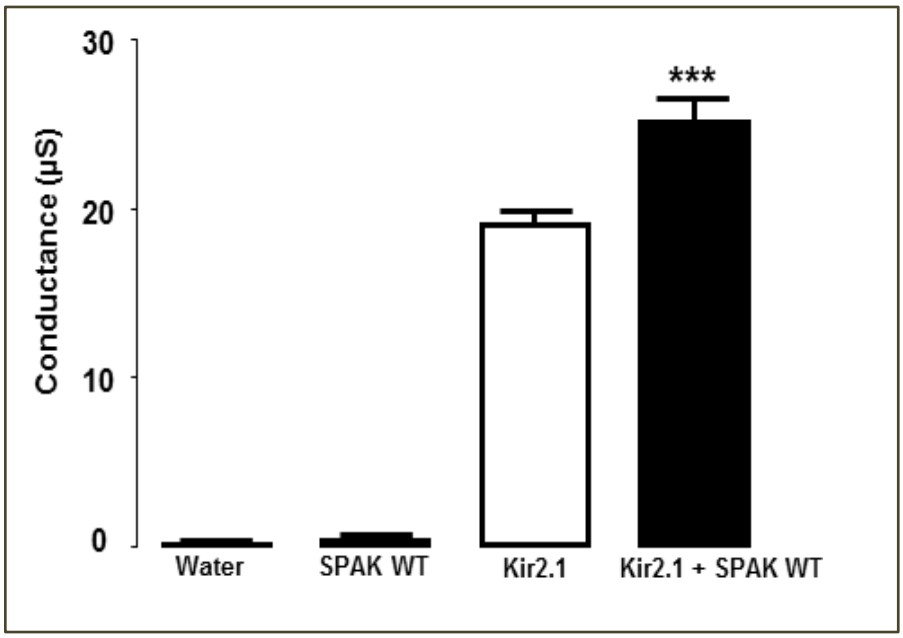

Figure 13: The Kir2.1 conductance (µS) is increased in the presence of the co-expressed wild type SPAK. Conductance calculated between -150mV to -120mV from the (I/V) curves (±SEM), of respectively water oocytes (dotted bar), SPAKWT (grey bar), Kir2.1 (white bar) and Kir2.1 + SPAK WT (black bar). (n=9-37), 3 different batches of oocytes. ***(p<0.001) shows the statistical significant difference from Kir2.1 oocytes (160).

3.1.1.2. SPAK mutants effect on the inward K^+ current in Kir2.1-expressing *Xenopus laevis* oocytes

3.1.1.2.1. The inward rectifying K^+ currents enhanced by constitutively active ^{T233E}SPAK but not by WNK insensitive ^{T233A}SPAK or the catalytically inactive ^{D212A}SPAK co-expression

Kir2.1 (KCNJ2) was co-expressed with the different SPAK mutants to evaluate the effect of each mutation on the channel activity. The constitutively active ^{T233E}SPAK demonstrated a similar effect as the wild-type SPAK by stimulating the inwardly rectifying K^+ currents in Kir2.1 expressing oocytes. In contrast, the WNK insensitive ^{T233A}SPAK as well as the catalytically inactive ^{D212A}SPAK did not exert any observable effect on Kir2.1 currents. Figure 14 illustrates the original tracings (A), translated in histograms (B) showing the arithmetic means of the maximal currents of the different groups (160).

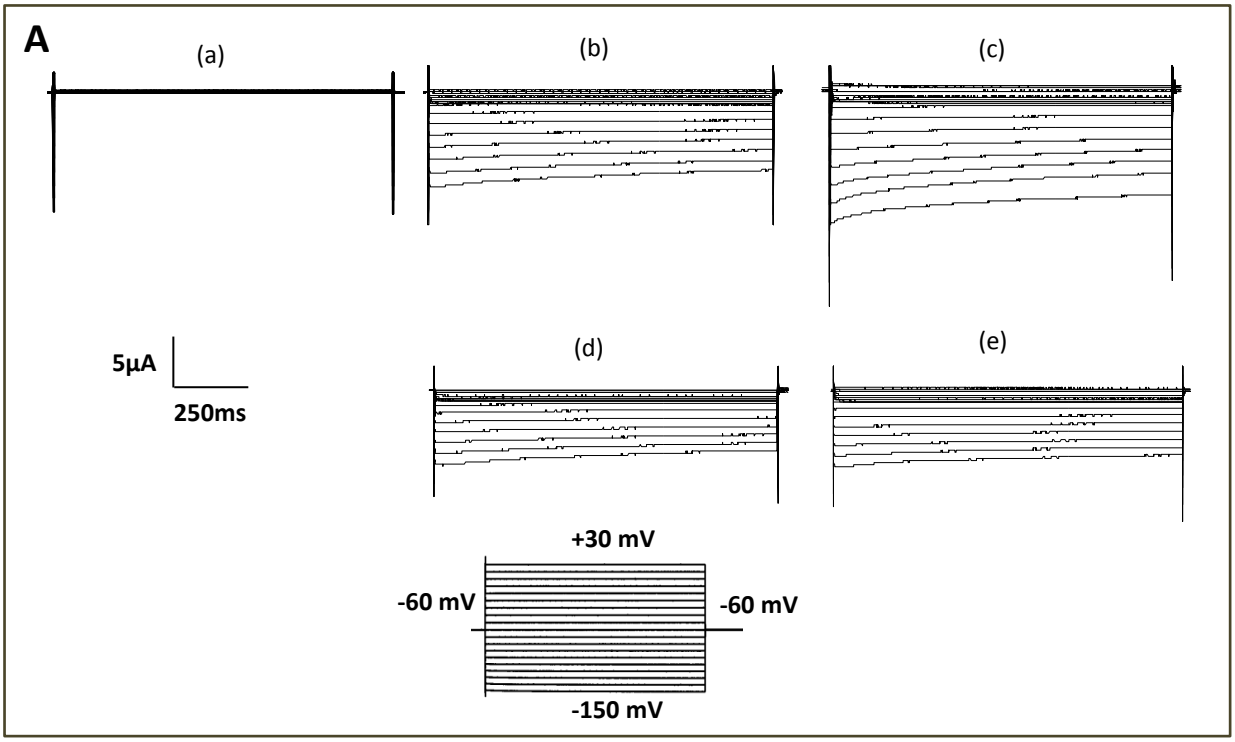

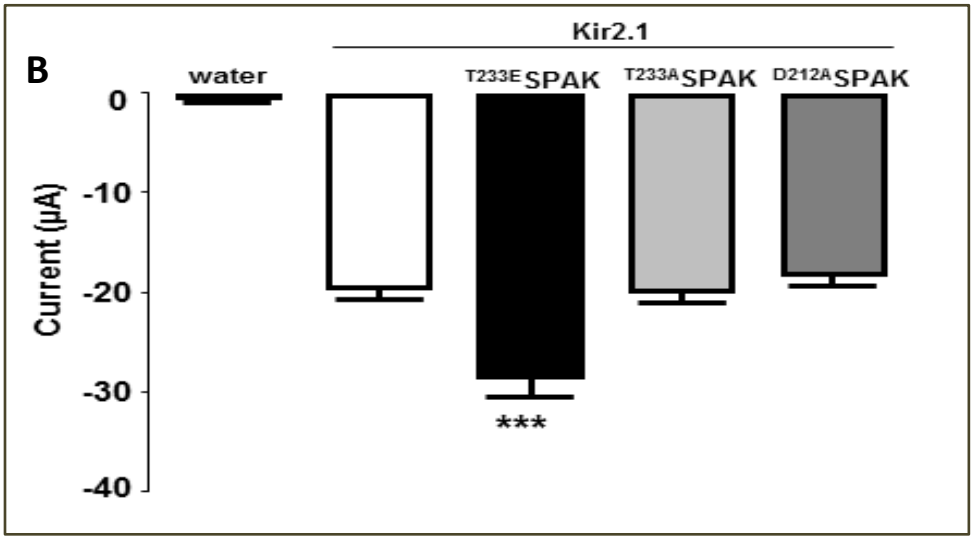

Figure 14: Kir2.1 inward current enhanced by the co-expression of the constitutively active mutant ^{T233E}SPAK but not by the co-expression of the WNK insensitive ^{T233A}SPAK or the catalytically inactive ^{D212A}SPAK. (A): original tracings of current in oocytes injected respectively with water (a), kir2.1 (b), Kir2.1+ ^{T233E}SPAK (c), Kir2.1+ ^{T233A}SPAK (d) and Kir2.1+ ^{D212A}SPAK (e). The recording protocol is shown, not to scale. **(B)**: Histogram showing means of the maximal inward K^+ currents I (µA) recorded at -150mV (±SEM), respectively in negative control water (dotted bar), Kir2.1 (white bar), Kir2.1 co-injected with ^{T233E}SPAK (black bar), Kir2.1 co-injected with ^{T233A}SPAK (light grey bar) and Kir2.1 co-injected with ^{D212A}SPAK (dark grey bar). (n = 13-33), 3 different batches of oocytes. ***(p<0.001) express the statistical significant difference from Kir2.1 alone (160).

3.1.1.2.2. The Current-Voltage (I/V) curve characteristic assessment with SPAK mutants

The illustration of the I-V curves in the figure 15 displays the stimulation effect of the constitutively active mutant ^{T233E}SPAK on the inwardly rectifying K^+ currents of Kir2.1 expressed in *Xenopus* oocytes at the different applied voltages of the curve. The WNK insensitive ^{T233A}SPAK and the catalytically inactive ^{D212A}SPAK, both did not show a significant change on the (I/V) curve of Kir2.1 channel (160).

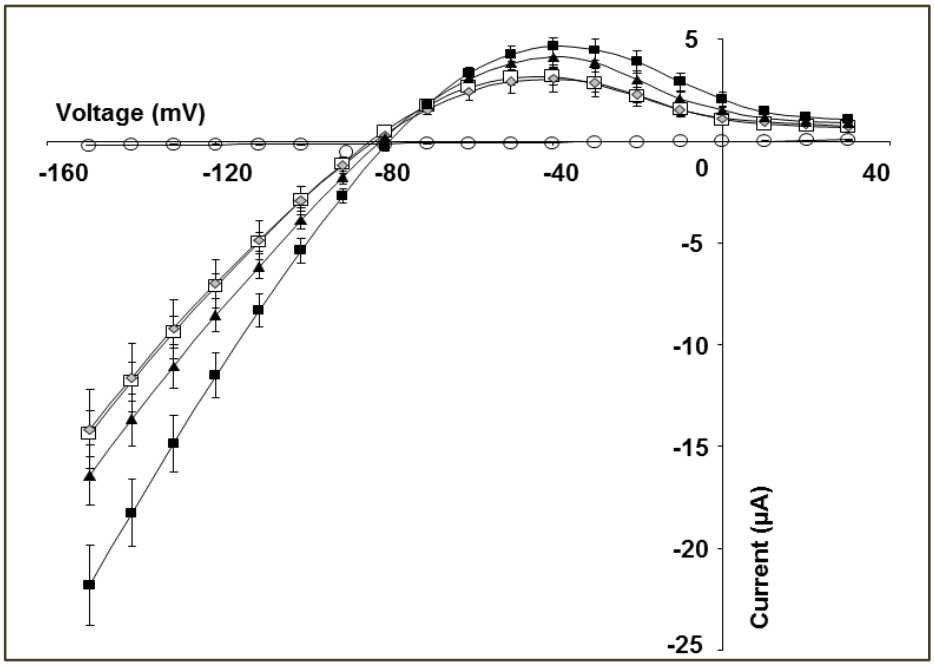

Figure 15: Current-Voltage (I/V) curve: current as function of potential difference across the

cell membrane demonstrates a stimulation effect of the constitutively active ^{T233E}SPAK on Kir2.1 currents. Curves plotted by means of the current I (µA) (±SEM) as a function of the voltage steps applied on the oocyte membrane V(mV) from -150mV to +30mV. (I/V)-curves correspond respectively to water injected oocytes (white circles), Kir2.1 alone (white squares), Kir2.1+ ^{T233E}SPAK (black squares), Kir2.1 + ^{T233A}SPAK (grey diamonds), Kir2.1 + ^{D212A}SPAK (black triangles). (n=13-33), 3 different batches of oocytes. ***(p<0.001) express the statistical significant difference from Kir2.1 alone (160).

3.1.1.2.3. The constitutively active ^{T233E}SPAK up-regulated the Kir2.1 channel Conductance, but not WNK insensitive ^{T233A}SPAK or the catalytically inactive ^{D212A}SPAK

The figure 16 is in perfect concord with the previous results, demonstrating the enhanced conductance of Kir2.1 by the co-expression of the constitutively active ^{T233E}SPAK, but not by the co-expression of the WNK insensitive ^{T233A}SPAK or the catalytically inactive ^{D212A}SPAK (160).

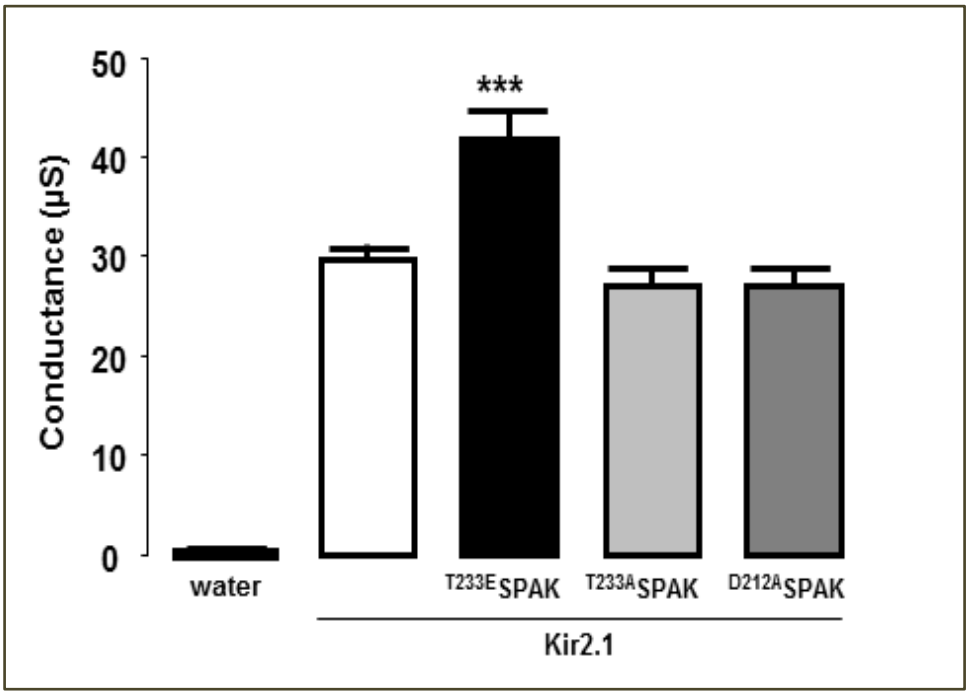

Figure 16: The Kir2.1 conductance (µS) is increased in the presence of the constitutively active ^{T233E}SPAK. Conductance calculated between -150mV to -120mV from the (I/V) curves

(±SEM), of respectively water oocytes (dotted bar), Kir2.1 (white bar) and Kir2.1 + ^{T233E}SPAK (black bar), Kir2.1 +^{T233A}SPAK (light grey bar), Kir2.1+^{D212A}SPAK (dark grey bar). (n=13-33), 3 different batches of oocytes. ***(p<0.001) shows the statistical significant difference from Kir2.1 oocytes (160).

3.1.1.3. Wild-type SPAK increased Kir2.1 protein abundance in the cell membrane

Previous results from dual electrode voltage clamp technique showed that SPAK could increase the K^+ currents through the inwardly rectifying K^+ channel Kir2.1. In order to check whether this stimulation of the currents is the result of an increase in the protein abundance on the cell membrane, chemiluminescence was used to highlight the increased insertion of the protein channel on the oocytes surface.

Three groups of oocytes injected respectively with water, Kir2.1-HA alone and Kir2.1-HA with additional wild-type SPAK cRNA. Oocytes were incubated in HA-specific antibody (AB) and washed to eliminate excess and/or unspecific epitope binding. The quantification of Kir2.1-HA-specific binding by the luminometer was possible due to the Horseradish Peroxidase HRP-conjugated to the AB reaction with the substrate (SuperSignal).

The results displayed in the figure 17 show a statistically significant increase (p<0.001) of the chemiluminescence of cell membrane of the oocytes expressing Kir2.1-HA+SPAK wt comparing to oocytes expressing Kir2.1-HA alone (160).

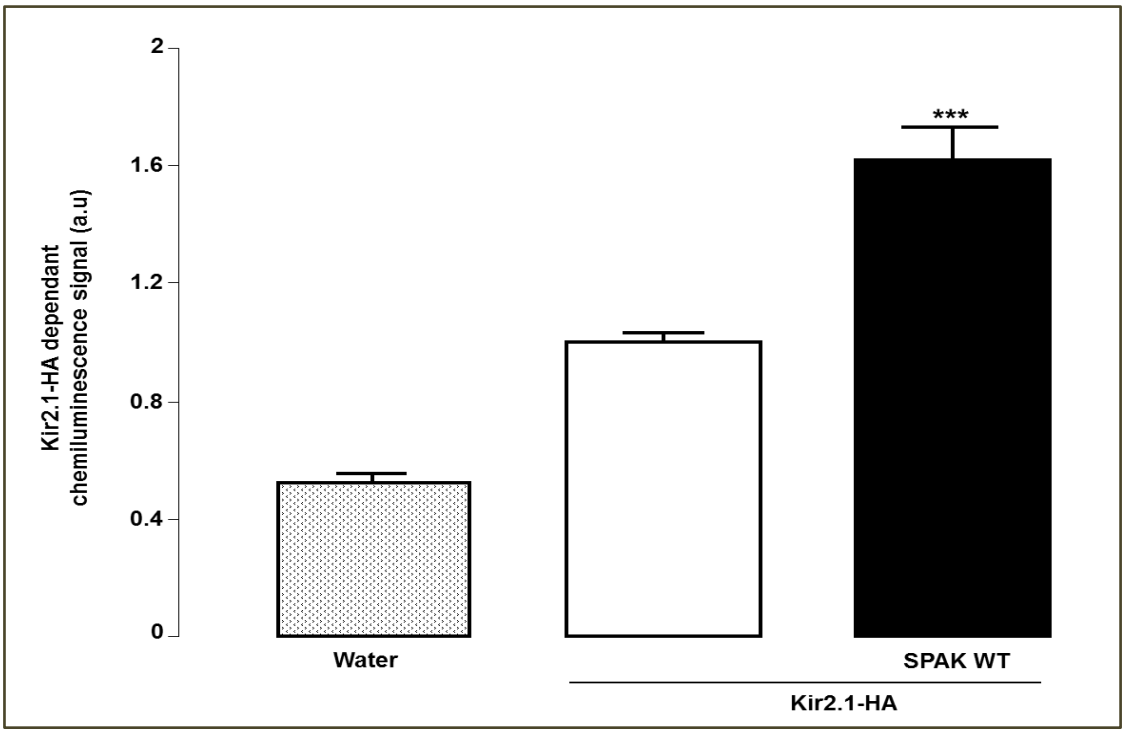

Figure 17: SPAK Wild-type increased Kir2.1-HA protein abundance in cell surface. Normalized means of chemiluminescence signal of Kir2.1-HA protein abundance from *Xenopus laevis* oocytes injected with water (dotted bar), Kir2.1-HA (white bar) and Kir2.1-HA+SPAKwt (black bar). (n=84-88), 4 different batches of oocytes. (p<0.001) statistical significance difference from kir2.1-HA group (160).

3.1.1.4. Wild-type SPAK role in Kir2.1 current stimulation is abolished by Brefeldin A

Previous results demonstrated that SPAK up-regulated Kir2.1 channel by increasing the K^+ inward rectifying current flowing through the channel and thus increasing the conductance, which is paralleled to an increase in the Kir2.1-HA protein abundance on the cell surface. In order to check if this effect is due to enhancement of the protein channel insertion in the cell membrane, or rather to a delay of the protein retrieval from the plasma membrane; Brefeldin A was used.

Oocytes were injected respectively with Kir2.1 alone and Kir2.1+SPAK, and then divided in two groups control and treated group. The control oocytes were maintained in the ND96

solution for culture; whereas for the treated group, oocytes were treated 24 hours prior to recording with additional 5µM Brefeldin A in the normal culture media.

As illustrated in the figure 18, the incubation in Brefeldin A, resulted in a significant decrease of the inwardly rectifying K^+ currents in Kir2.1 expressing oocytes indicating retrieval of channel protein from the plasma membrane. As well, following 24 hours of Brefeldin A treatment, the stimulating effect of the kinase on the K^+ channel was abolished completely, and the currents showed a significant decrease in both Kir2.1 alone or Kir2.1 and SPAK co-expressing oocytes. Therefore, the presence of SPAK did not retard retrieval of the protein channel from the plasma membrane (160).

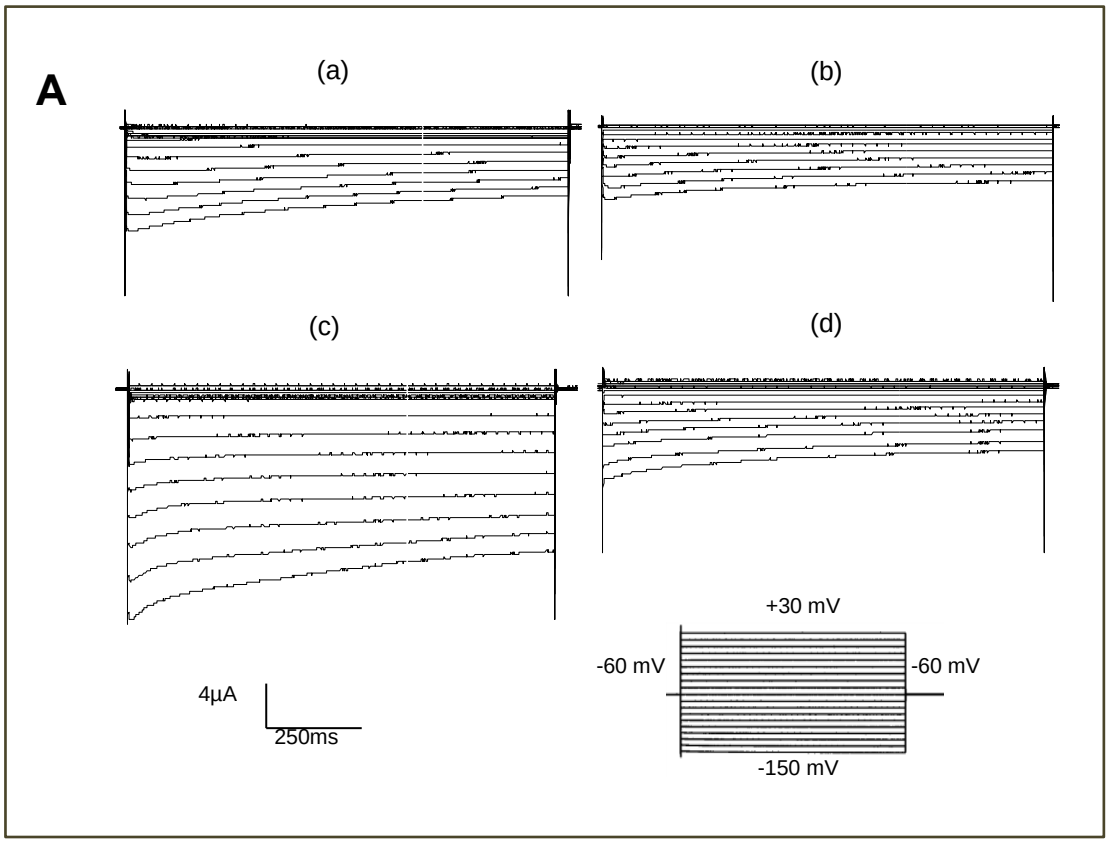

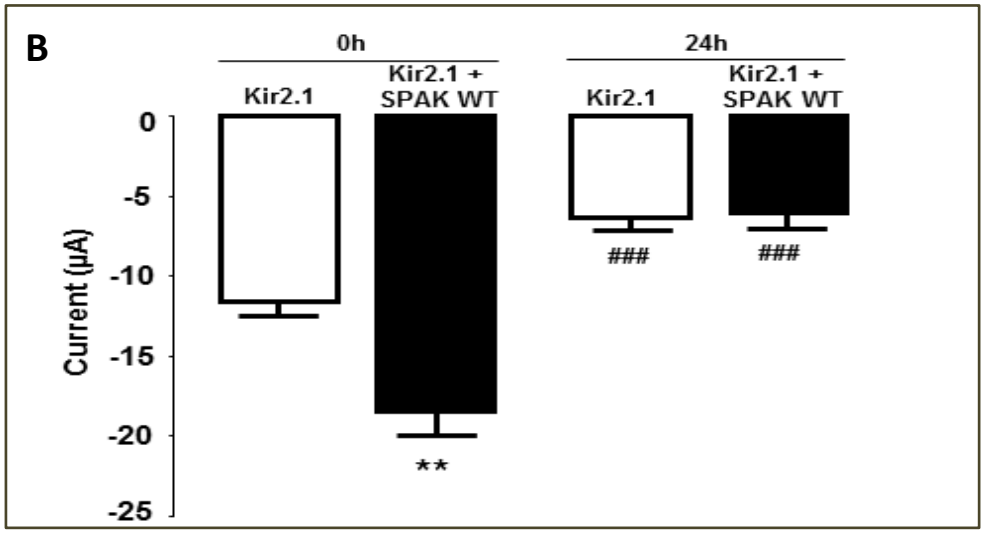
B
0h
24h
Kir2.1
Kir2.1 +
SPAK WT
Kir2.1
Kir2.1 +
SPAK WT
0
-5
-10
-15
-20
-25
Current (µA)
**
###
###

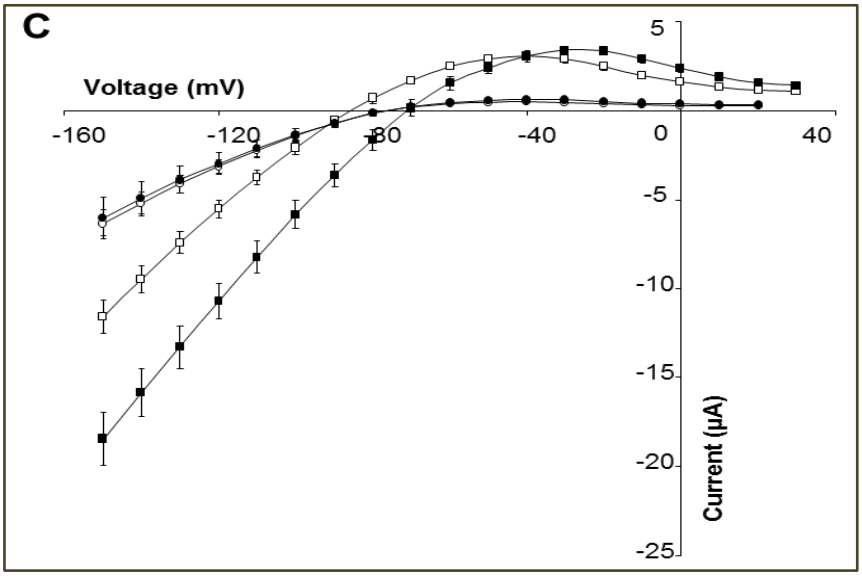
C
Voltage (mV)
-160
-120
-80
-40
0
40
5
-5
-10
-15
-20
-25
Current (µA)

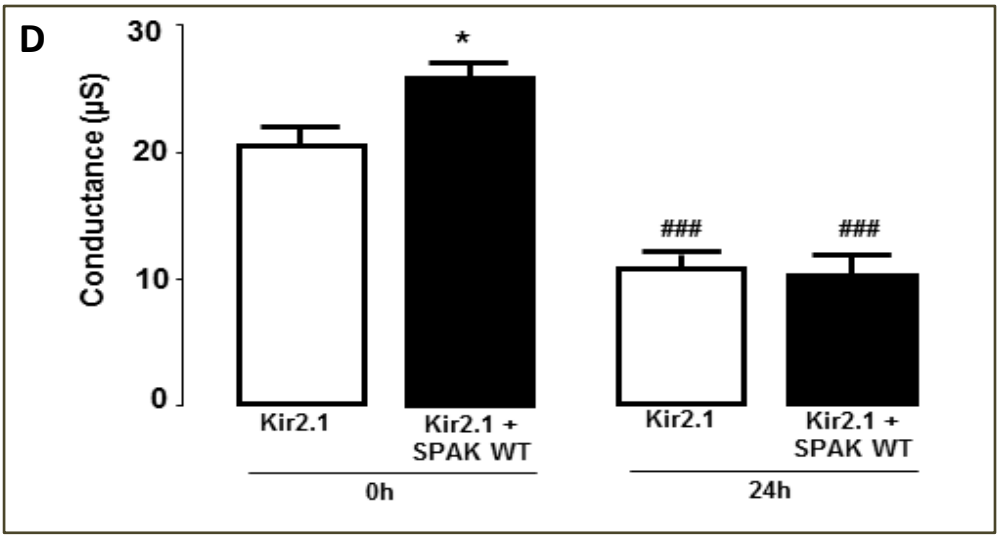
D
30
20
10
0
Conductance (µS)
*
###
###
Kir2.1
Kir2.1 +
SPAK WT
Kir2.1
Kir2.1 +
SPAK WT
0h
24h

Figure 18: Brefeldin A abolished the stimulating effect of the wild-type SPAK on Kir2.1 currents. (A): Original tracings of K^+ inwardly rectifying currents in oocytes injected with Kir2.1 alone (a,b) and kir2.1+SPAK (c,d), without (a,c) or with (b,d) 24h treatment with 24h Brefeldin A (5µM). **(B)**: Means of the maximal currents (±SEM) at -150mV in oocytes injected with Kir2.1 only (white bars) or kir2.1+SPAK (black bars) without (left bars) or with (right bars) 24h Brefeldin A treatment. **(C)**: Means of the current as a function of the potential difference (I/Vcurves) through oocytes membrane expressing Kir2.1 alone (white), kir2.1+SPAK (black) without (squares) or with (circles) 24h Brefeldin A treatment. **(D)**: Arithmetic means of the conductance (from -150mV to -120mV) (±SEM) in oocytes injected with kir2.1 alone (white bars) or kir2.1+SPAK (black bars) without (left bars) or with (right bars) 24h of Brefeldin A incubation. (n=14-21), 3 different batches of oocytes. *(p<0.05) and **(p<0.01) show the statistical significance from Kir2.1, ###(p<0.001) shows the statistical significance from respective group without Brefeldin A incubation (160).

3.1.2. OSR1 up-regulated Kir2.1

3.1.2.1. Wild-type OSR1 increased the inwardly rectifying K^+ current in KCNJ2-expressing *Xenopus laevis* oocytes

To explore the effect of OSR1 on the inwardly rectifying K^+ channel Kir2.1, K^+ current was recorded in *Xenopus laevis* oocytes via two dual voltage clamp technique. *Xenopus laevis* oocytes were divided in 4 groups: oocytes expressing either Kir2.1 channel alone, or OSR1 the kinase only, or co-expressing both the channel and the kinase Kir2.1+OSR1 and water was injected in the negative control group. Negative control as well as OSR1-injected oocytes did not demonstrate any appreciable inward K^+ current, confirming that *Xenopus* oocytes expressed negligible inwardly rectifying K^+ currents. In contrast, Kir2.1-expressing oocytes showed large measurable inward rectifying K^+ currents which increased significantly in the presence of wild-type OSR1. As illustrated in figure 19 (A) the original tracings and (B) the histogram of the arithmetic means of maximal inward K^+ currents demonstrate the increasing effect of OSR1 on the maximal current of Kir2.1.

Figure 19 (C) shows the current carried by K^+ with negative reversal potential and the characteristic curve shape of the inwardly rectifying K^+ currents of Kir2.1. The I/V curves show an up-regulation of the K^+ currents between Kir2.1-expressing oocytes and Kir2.1+OSR1 co-expressing oocytes, while both water injected oocytes and OSR1

expressing oocytes did not demonstrate a characteristic shaped (I/V) curve. Figure 19 (D) displays the conductance of Kir2.1-expressing oocytes and Kir2.1co-expressing OSR1 wild-type, considering the linear fit of I/V-curves between the amplitudes -150mV and -120mV. The conductance was significantly enhanced in the presence of wild-type OSR1 (160).

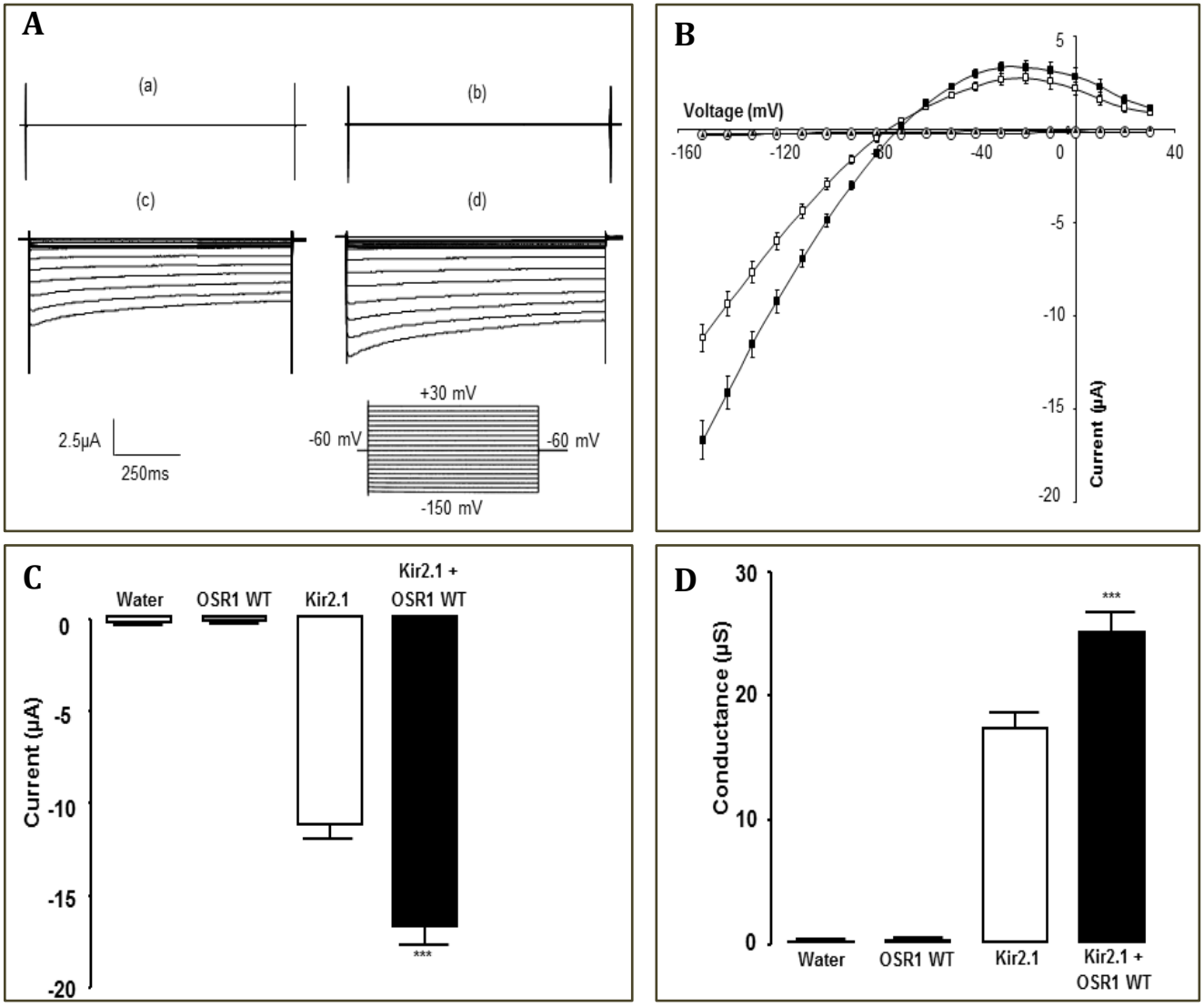

Figure 19: Wild type OSR1 enhanced the inwardly rectifying K^+ currents through Kir2.1 channel in Xenopus oocytes. **(A)**: Representative tracings of original currents in Xenopus oocytes

injected respectively with water (a), OSR1 wild type (b), Kir2.1 (c) and Kir2.1+OSR wild type. The represented protocol is not to scale. **(B)**: Means (±SEM) of the maximal inward currents at -150mV of water (dotted bar), OSR1 (grey bar), Kir2.1 (white bar) and Kir2.1+OSR1wild type (black bar) expressing oocytes. **(C)**: Current-voltage I/V curves at the different potentials applied to the cell membrane, of oocytes expressing respectively: water (white circles), OSR1 (black triangles), Kir2.1 alone (white squares) and Kir2.1+OSR1 wild type (black squares). **(D)**: Arithmetic means of the channel conductance (±SEM) calculated from -150mV to -120mV. (n=9-35), 3 different batches of oocytes. ***(p<0.001) shows statistical significant difference between Kir2.1 and Kir2.1+OSR1 (160).

3.1.2.2 OSR1 mutants effect on the inward K^+ current in Kir2.1-expressing *Xenopus laevis* oocytes

Similarly to SPAK, OSR1 mutants were tested for their effect on Kir2.1 activity. The channel was co-expressed with the different OSR1 mutants.

The constitutively active ^{T185E}OSR1 demonstrated a similar effect as the wild-type OSR1 by stimulating the inwardly rectifying K^+ currents in Kir2.1 expressing oocytes. In contrast, the WNK insensitive ^{T185A}OSR1 as well as the catalytically inactive ^{D164A}OSR1 did not show any observable stimulation of Kir2.1.

Figure 20 shows a significant up-regulation of Kir2.1 conductance by the wild type OSR1 between -150mV and -120mV (160).

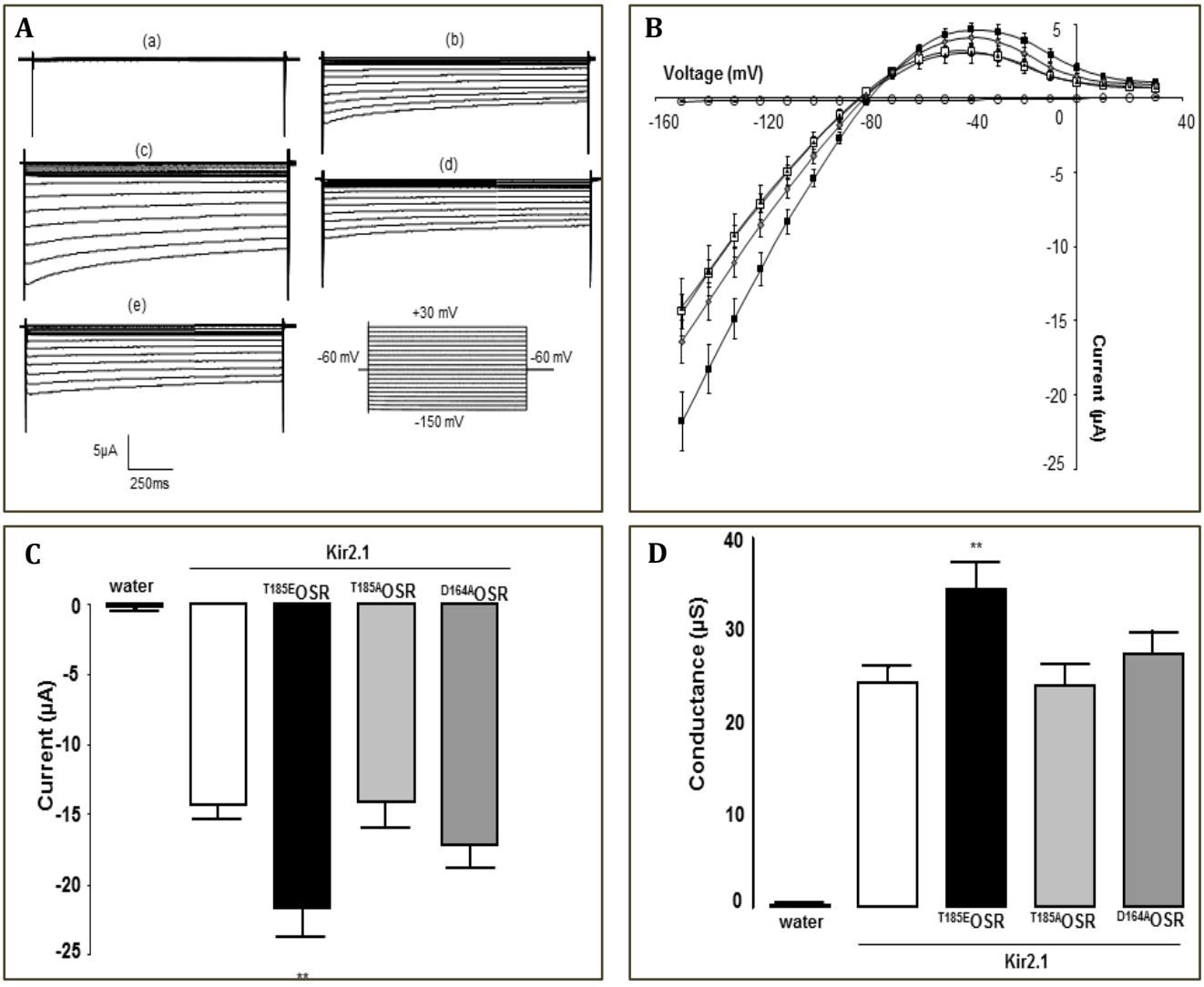

Figure 20: Kir2.1 inward current increased by the co-expression of the constitutively active mutant ^{T185E}OSR1 but not by the co-expression of the WNK insensitive ^{T185A}OSR1 and the catalytically inactive ^{D164A}OSR1. **(A)**: Original tracings of current in oocytes injected respectively with water (a), kir2.1 (b), Kir2.1+ ^{T185E}OSR1(c), Kir2.1+ ^{T185A}OSR1 (d) and Kir2.1+ ^{D164A}OSR1 (e). The recording protocol shown is not to scale. **(B)**: Histogram showing means of the maximal inward K^+ currents I (µA) recorded at -150mV (±SEM), respectively in negative control water (dotted bar), Kir2.1 (white bar), Kir2.1 co-injected with ^{T185E}OSR1 (black bar), Kir2.1 co-injected with

^{T185A}OSR1 (light grey bar) and Kir2.1 co-injected with ^{D164A}OSR1 (dark grey bar). **(C)**: Curves plotted by means of the current I (µA) (±SEM) as a function of the voltage steps applied on the oocyte membrane V(mV) from -150mV to +30mV of respectively: water injected oocytes (white circles), Kir2.1 alone (white squares), Kir2.1+ ^{T185E}OSR1 (black squares), Kir2.1 + ^{T185A}OSR1 (grey diamonds), Kir2.1 + ^{D164A}OSR1 (black triangles). **(D)**: Conductance (µS) calculated between -150mV to -120mV from the (I/V) curves (±SEM), of respectively water oocytes (dotted bar), Kir2.1 (white bar) and Kir2.1 + ^{T185E}OSR1 (black bar), Kir2.1 + ^{T185A}OSR1 (light grey bar), Kir2.1+ ^{D164A}OSR1 (dark grey bar). (n = 17-35), 3 different batches of oocytes. **(p<0.01) expresses the statistical significant difference from Kir2.1 alone.(160).

3.1.2.3. Wild-type OSR1 enhanced Kir2.1 protein abundance in the cell membrane

Currents recording via dual electrode voltage clamp technique demonstrated that OSR1 could enhance the inwardly rectifying K^+ currents in Kir2.1 channel. In order to check whether this currents stimulation results from an increase in the protein abundance on the cell surface, chemiluminescence was the technique used to quantify the protein channel insertion in the oocytes plasma membrane.

Xenopus oocytes were divided into three groups, injected respectively with water, Kir2.1-HA and Kir2.1-HA with additional injection of wild-type OSR1 cRNA. Oocytes were treated with HA-specific antibody (AB) and washed 3 times in order to eliminate unspecific and excess of epitope binding. Quantification of Kir2.1-HA-specific binding via luminometer was possible by the presence of the Horseradish Peroxidase HRP-conjugated to the AB, which binds to SuperSignal substrate. Results analysis shows a significant increase in the quantified chemiluminescence dependent- HA in oocytes expressing Kir2.1-HA+OSR1 wild type comparing to oocytes expressing Kir2.1-HA alone.

See figure 21.

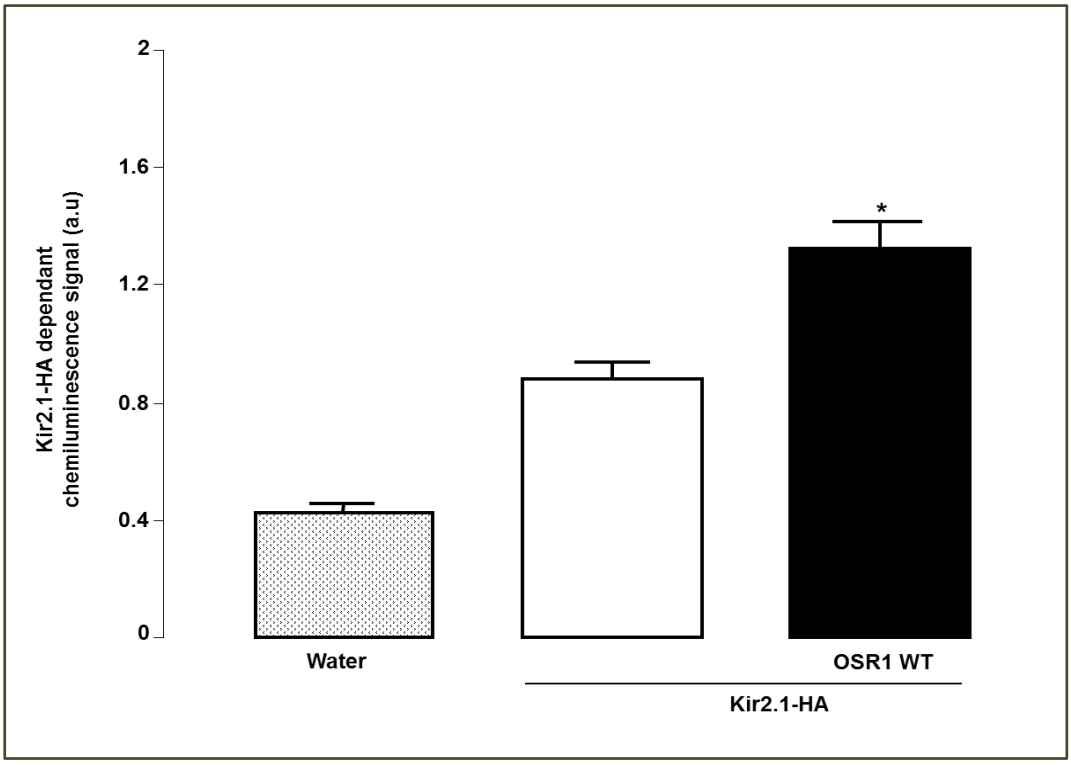

Figure 21: OSR1 Wild-type enhanced Kir2.1-HA protein abundance in Xenopus oocytes surface. Normalized means of chemiluminescence signal of Kir2.1-HA protein abundance from oocytes injected with water (dotted bar), Kir2.1-HA (white bar) and Kir2.1-HA+OSR1 WT (black bar). (n=78-84), 4 different batches of oocytes. (*p<0.01) statistical significant difference from kir2.1-HA group.

3.1.2.4. Wild-type OSR1 role in Kir2.1 current stimulation is abolished by Brefeldin A

Similar to SPAK, OSR1 currents recording via two electrode voltage clamp showed that OSR1 enhanced Kir2.1 activity with an increase in the K^+ inward rectifying flow and consequently increasing the conductance of the channel, which is simultaneous to an increase in the Kir2.1-HA protein abundance on the cell membrane. Brefeldin A was used in order to check if this effect is due to increase of the channel insertion in the cell surface, or rather due to a protein retrieval delay.

Xenopus oocytes expressed respectively Kir2.1 only and Kir2.1+OSR1 shared in control and treated groups. The control oocytes were cultured in the ND96 solution; for the treated

group, oocytes were incubated 24 hours prior to measurement with additional 5µM Brefeldin A to the ND96 media. As shown in the figure 22, incubation in Brefeldin A was followed by a significant decrease of the inwardly rectifying K^+ currents in Kir2.1 expressing oocytes indicating channel protein retrieval from the plasma membrane of *Xenopus* oocytes. Hence, OSR1 did not delay protein channel retrieval from the membrane (160).

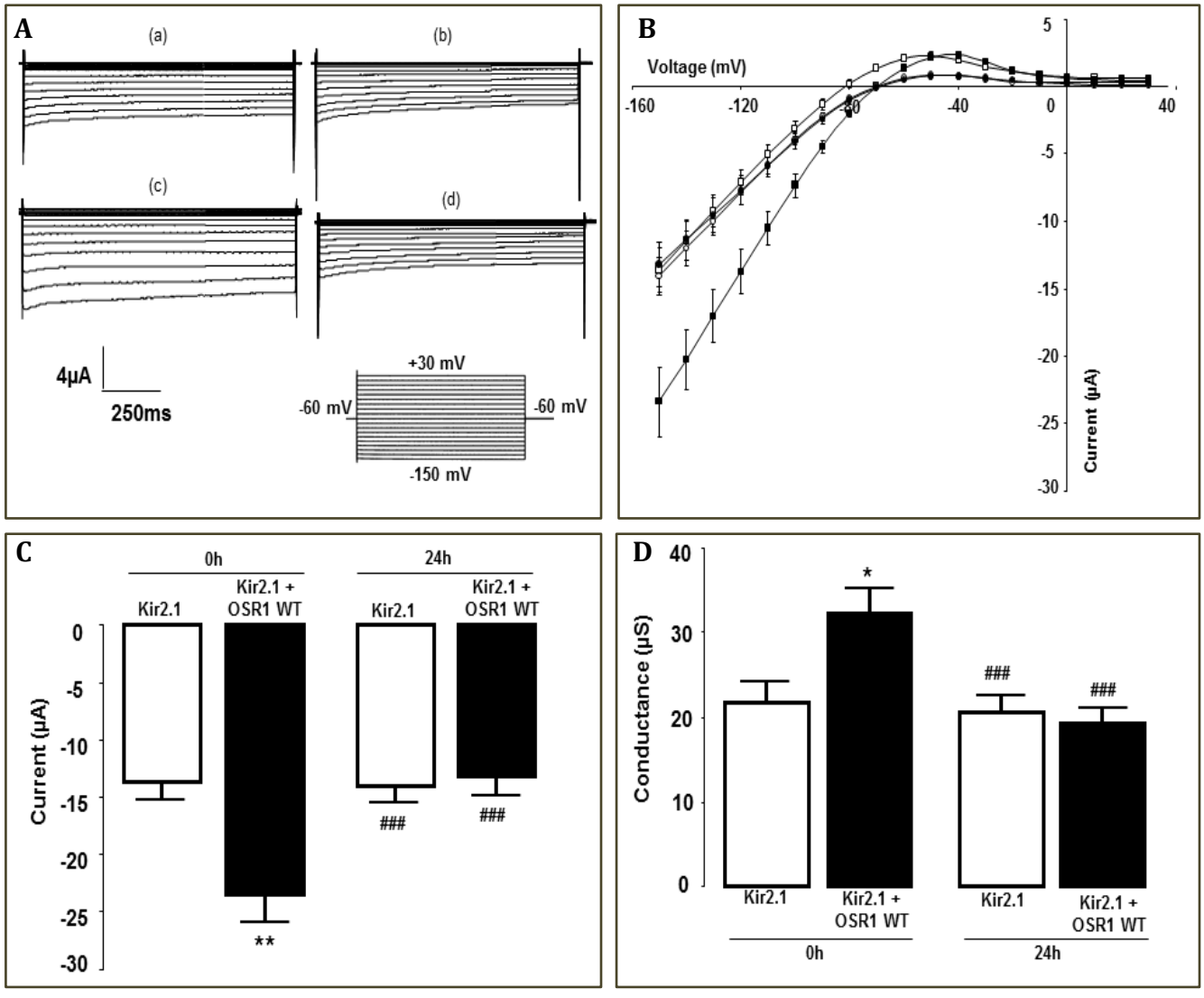

Figure 22: Brefeldin A abolished the stimulating effect of the wild-type OSR1 on Kir2.1 currents. (A): Original tracings of K^+ inwardly rectifying currents in oocytes injected with Kir2.1

alone (a,b) and kir2.1+OSR1 (c,d), without (a,c) or with (b,d) 24h treatment with Brefeldin A (5µM). **(B)**: Means of the maximal currents (±SEM) at -150mV in oocytes injected with Kir2.1 only (white bars) or kir2.1+ OSR1 (black bars) without (left bars) or with (right bars) 24h Brefeldin A treatment. **(C)**: Means of the current as a function of the potential difference (I/Vcurves) through oocytes membrane expressing Kir2.1 alone (white), kir2.1+ OSR1 (black) without (squares) or with (circles) 24h Brefeldin A treatment. **(D)**: Arithmetic means of the conductance (from -150mV to -120mV) (±SEM) in oocytes injected with kir2.1 alone (white bars) or kir2.1+ OSR1 (black bars) without (left bars) or with (right bars) 24h of Brefeldin A incubation. (n=14-20), 3 different batches of oocytes. *(p<0.05) and **(p<0.01) show the statistical significance from Kir2.1, ###(p<0.001) shows the statistical significance from Brefeldin A incubation (160).

3.2. Creatine transporter CreaT (SLC6A8) negative regulation by SPAK and OSR1

3.2.1. SPAK down-regulated CreaT (SLC6A8)

3.2.1. 1. SPAK down-regulated the electrogenic creatine transport in CreaT

In order to explore the potential effect of SPAK on the creatine carrier CreaT (SLC6A8), the creatine induced-current was recorded in different conditions by the technique of dual electrode voltage clamp. To this end, *Xenopus laevis* oocytes were injected after defolliculation with cRNA encoding for the transporter and/or the kinase. Three groups representing: oocytes expressing CreaT (SLC6A8), CreaT (SLC6A8) with co-expressing of SPAK wild type and the negative control oocytes group injected with water.

Creatine-induced currents were recorded with dual electrode voltage clamp, at a holding potential of -60mV, according to the specified CreaT protocol by addition of 1mM creatine as substrate to the ND96 superfusate solution. The superfusate flows at 20ml/min.

In the control group, oocytes did not show observable current, meaning that *Xenopus* oocytes did not express electrogenic creatine transport. For oocytes expressing SLC6A8, the supplementation of the superfusate media ND96 with 1mM creatine substrate, resulted in a large appreciable inward creatine induced current, while in oocytes co-expressing both CreaT and SPAK wild type, the creatine induced current was significantly lowered. The

figure 23 shows in **A** the comparative original tracings translated in histogram of the respectively maximal creatine induced currents in **B** (162).

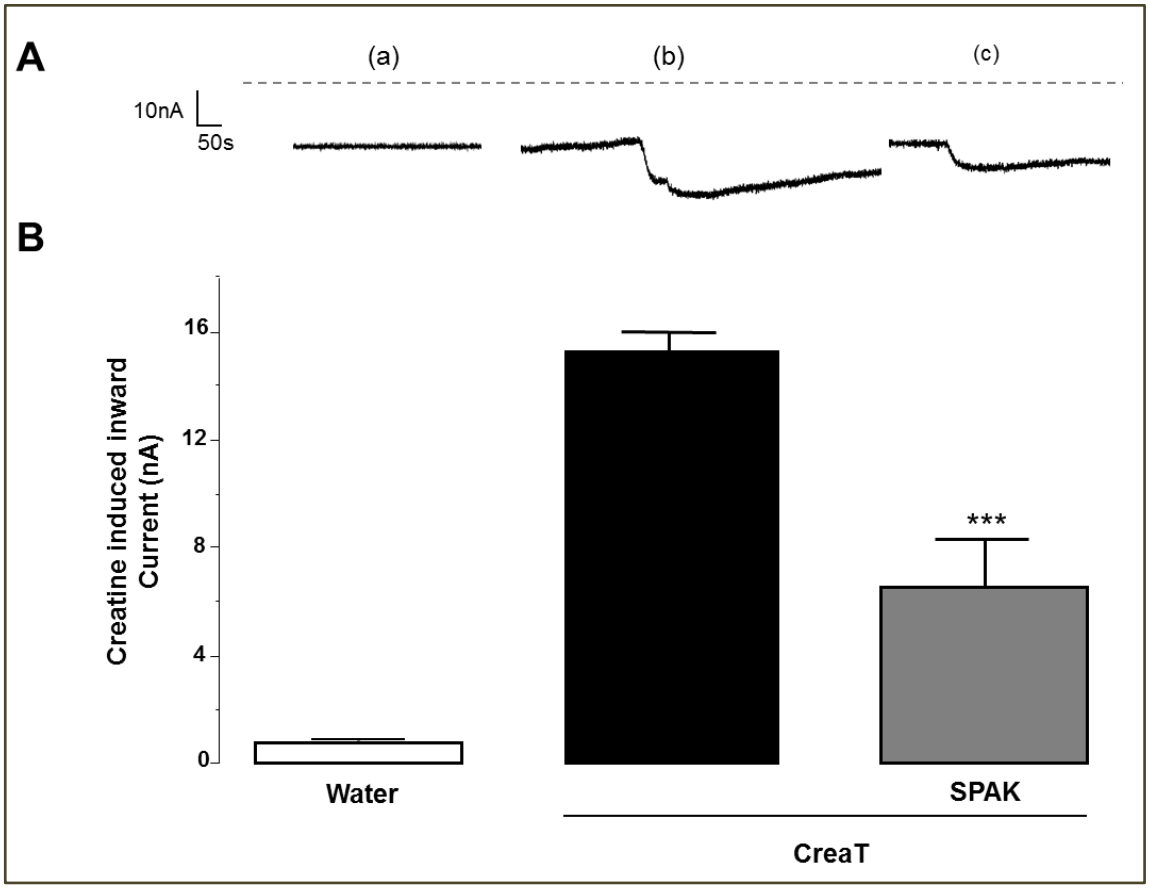

Figure 23: Creatine (1mM) transport current in CreaT (SLC6A8) decreased in presence of SPAK wild type in *Xenopus laevis* oocytes. (A): Original tracings of electrogenic creatine transport in water (a), CreaT (b) and CreaT+SPAK (c) expressing oocytes. **(B)**: Means of the maximal creatine induced current in oocytes expressing water (white bar), CreaT (black bar) and CreaT+SPAK (grey bar). (n=11-23) 4 different batches of oocytes, ***(p<0.001) shows statistical significant difference from CreaT alone (162).

3.2.1.2. SPAK decreased the maximal creatine induced current but not the affinity in CreaT expressing oocytes: Kinetic analysis

Wild type SPAK was shown to decrease Creatine induced current in CreaT co-expressing oocytes. In order to check if it affects the maximal current I_{creat} and/or the affinity of the transporter, two groups of oocytes expressing CreaT alone or CreaT+SPAK were supplemented in the ND96 superfusate with increasing concentrations of creatine (3µM – 2000µM).

The currents recorded for each single oocyte at the different concentrations (I_{creat} as function of the inward current) helped to evaluate the CreaT transporter kinetic. The same protocol of recording was used.

The analysis of kinetics demonstrated that on one hand, the maximal creatine induced inward current was significantly lower in oocytes co-expressing CreaT+SPAK with mean value (7.6 ± 1.0 nA), while in oocytes expressing CreaT only, the mean value of the maximal current was (18.4 ± 2.6 nA). On the other hand, kinetic analysis showed that the concentration needed for the half-maximal creatine induced inward current was not significantly different between the two groups of oocytes as it was highly variable: for oocytes co-expressing CreaT+SPAK (K_m = 29 ± 22 mM) and for CreaT expressing oocytes (K_m = 192 ± 102 mM).

As illustrated in the figure 24 **A**, the representative original tracings at the different concentration points, for each respective group, and in **B** the Kinetic curves of the concentration as function of the I_{creat} corresponding to each group of oocytes (162).

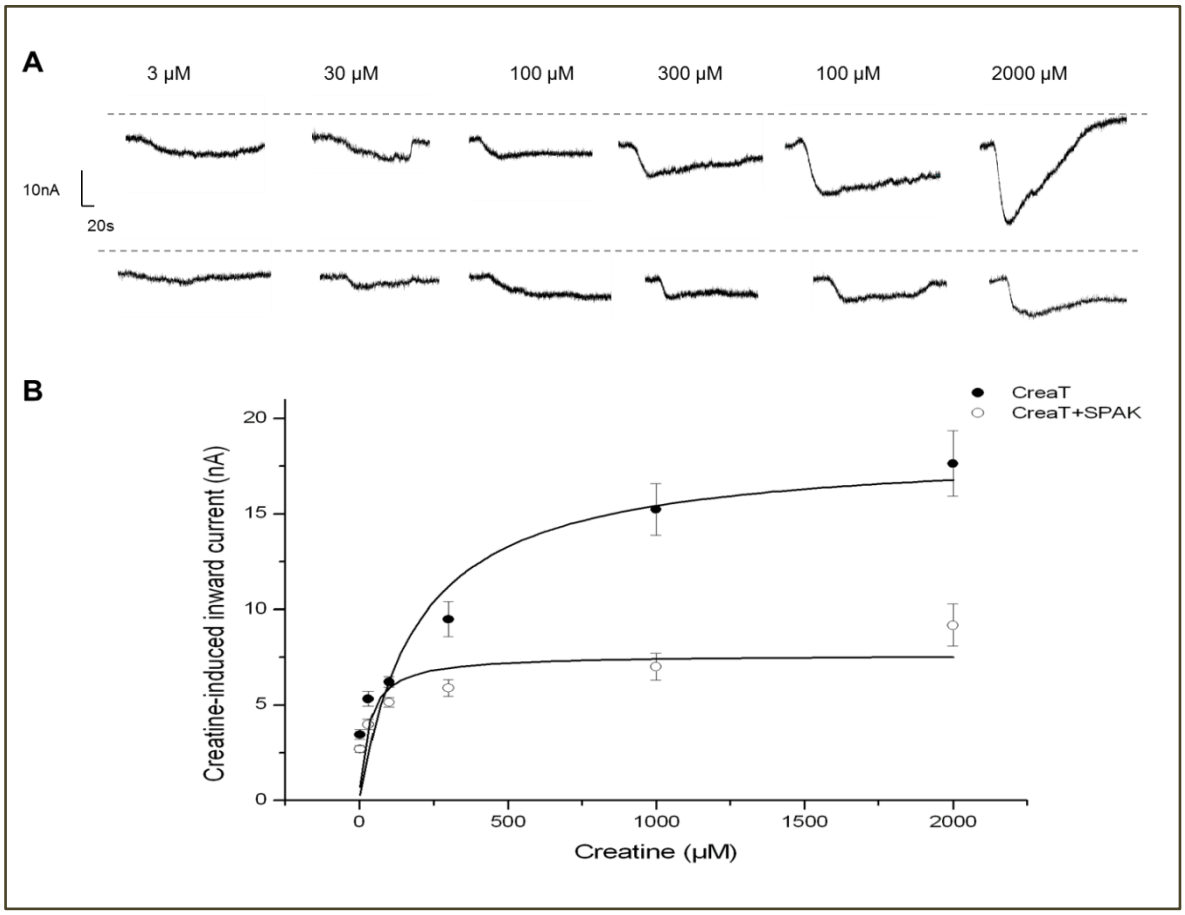

Figure 24: Maximal creatine induced current in CreaT is decreased by the co-expression of SPAK in Xenopus oocytes. **(A)**: original tracings of I_{creat} at increasing concentration of creatine (3µM-2000µM) in oocytes expressing CreaT (upper tracings) and CreaT+SPAK (lower tracings). **(B)**: arithmetic means of creatine induced current (±SEM) as function of the increasing concentration of supplemented creatine in oocytes expressing CreaT (black circles) and CreaT+SPAK (white circles). (n=6-8), 3 different batches of oocytes(162).

3.2.1.3. The creatine induced inward current decreased by constitutively active ^{T233E}SPAK but not by WNK insensitive ^{T233A}SPAK or the catalytically inactive ^{D212A}SPAK co-expression

SPAK mutants were investigated for a potential effect on the electrogenic creatine transport. *Xenopus laevis* oocytes were injected with the constitutively active ^{T233E}SPAK, the WNK insensitive ^{T233A}SPAK and the catalytically inactive ^{D212A}SPAK respectively with

the co-expression of CreaT (SLC6A8). The creatine (1mM) induced inward current was recorded by dual electrode voltage clamp. As figure 32 shows, the effect of the constitutively active ^{T233E}SPAK was similar to the wild type SPAK, since it decreased significantly the creatine current in CreaT. This effect was not observed once CreaT is co-expressed with the WNK insensitive ^{T233A}SPAK or the catalytically inactive ^{D212A}SPAK. In the figure 25, both the original representative tracings as well as the arithmetic means of the corresponding maximal inward creatine induced current illustrate the negative regulator effect of the constitutively active ^{T233E}SPAK, comparing to the absence of effect of the WNK insensitive ^{T233A}SPAK or the catalytically inactive ^{D212A}SPAK on CreaT (SLC6A8) co-expressed in *Xenopus* oocytes (162).

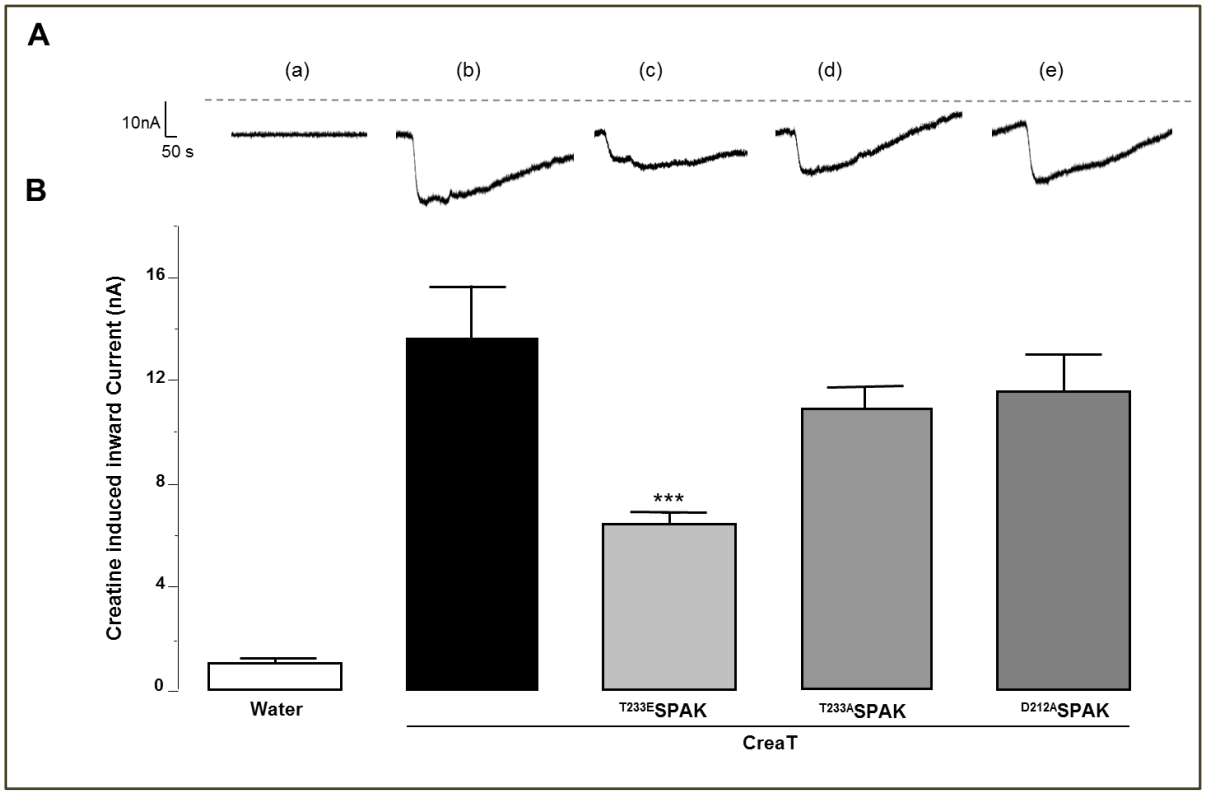

Figure 25: The constitutively active ^{T233E}SPAK decreased the creatine (1mM) induced current in CreaT co-expressing oocytes. (A): Original tracings of creatine induced current in oocytes injected with water (a), CreaT (b), CreaT+^{T233E}SPAK (c), CreaT+^{T233A}SPAK (d) and CreaT+^{D212A}SPAK (e). **(B)**: Means of the maximal inward creatine induced current (±SEM) in oocytes injected with water (white bar), CreaT (black bar), CreaT+^{T233E}SPAK (light grey bar), CreaT+^{T233A}SPAK (middle grey bar), CreaT+^{D212A}SPAK (dark grey bar). (n=12-30), 3 different

batches of oocytes. ***(p<0.001) shows statistical significant difference from oocytes injected with CreaT.(162).

3.2.2. OSR1 down-regulated CreaT (SLC6A8)

3.2.2. 1. OSR1 down-regulated the electrogenic creatine transport in CreaT

Same series of experiments were done with OSR1 to investigate the effect on the creatine transporter CreaT (SLC6A8) activity. Creatine induced-current was measured with two electrode voltage clamp. To that purpose, *Xenopus laevis* oocytes were injected with cRNA encoding for CreaT (SLC6A8) and/or OSR1 and water, using the same recording protocol.

Control oocytes did not show sizable current, which means that *Xenopus* oocytes did not express electrogenic creatine transport. Oocytes expressing SLC6A8 supplemented with 1mM creatine in the superfusate media ND96 showed an appreciable inward creatine induced current, while in oocytes co-expressing CreaT and OSR1 wild type, the current was significantly decreased. As illustrated in the figure 26 the comparative original tracings (A) displayed in histogram of the respectively maximal creatine induced currents(B) (162).

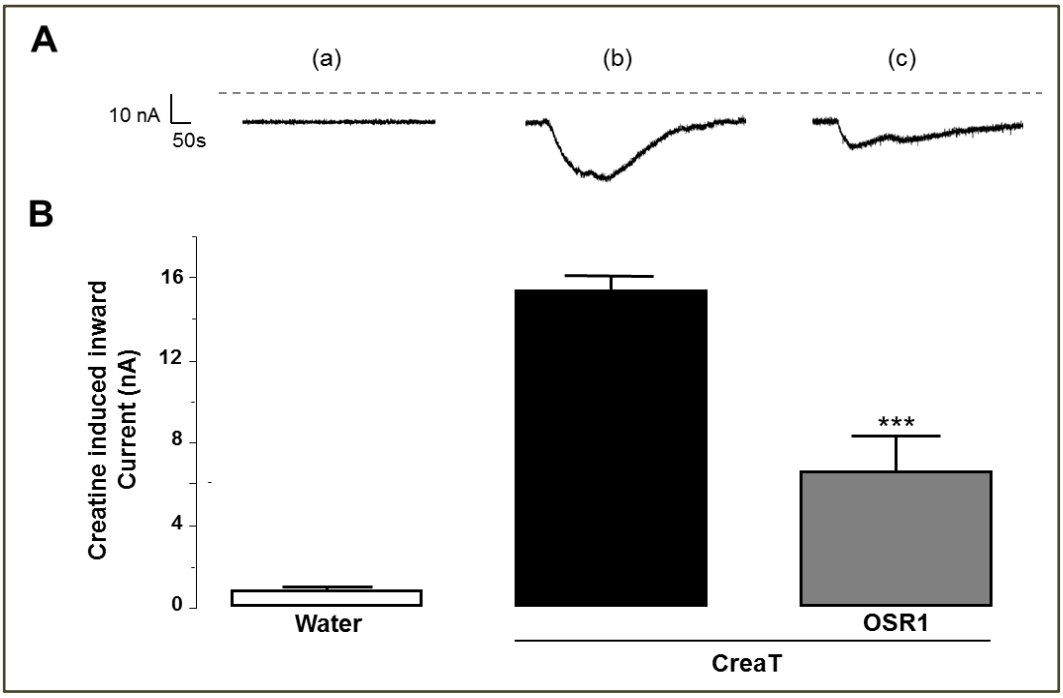

Figure 26: OSR1 decreased the I_{creat} (1mM) in *Xenopus* oocytes co-expressing CreaT. (A): Original tracings of creatine induced current in water (a), CreaT (b) and CreaT+OSR1 wild type (c)

expressing oocytes. **(B)**: Means of maximal creatine current (±SEM) in oocytes injected with water (white bar), CreaT (black bar) and CreaT+OSR1 wild type (grey bar). (n=10-30), 3 batches of oocytes. ***(p<0.001) indicates statistical significance from CreaT alone (162).

3.2.2.2. OSR1 decreased the maximal creatine induced current but not the affinity in CreaT expressing oocytes: Kinetic analysis

OSR1 wild type decreased creatine induced current in CreaT co-expressing oocytes. To check if this affects also the maximal current and/or the affinity of the carrier, *Xenopus* oocytes expressing CreaT or CreaT+OSR1 were supplemented with increasing concentrations of creatine (3µM – 2000µM) in the ND96 superfusate.

Currents were recorded for every single oocyte at different concentrations (I_{creat} as function of the inward current) to evaluate the CreaT transporter kinetic. Results analysis showed that the maximal creatine induced inward current was significantly lower in oocytes co-expressing CreaT+OSR1 wild type (8.2 ± 0.7 nA), whereas in oocytes expressing CreaT only, the mean value of the maximal current was (23.9 ± 2.1 nA).

Moreover, Kinetics analysis showed that the concentration needed for the half-maximal creatine induced inward current was significantly lower in oocytes co-expressing CreaT+OSR1 (K_m = 26 ± 14 mM) and for CreaT expressing oocytes (K_m = 152 ± 52 mM). As illustrated in the figure 27 **A**, the representative original tracings and in **B** the Kinetic curves of the creatine concentration as function of the I_{creat} corresponding to each group of oocytes (162).

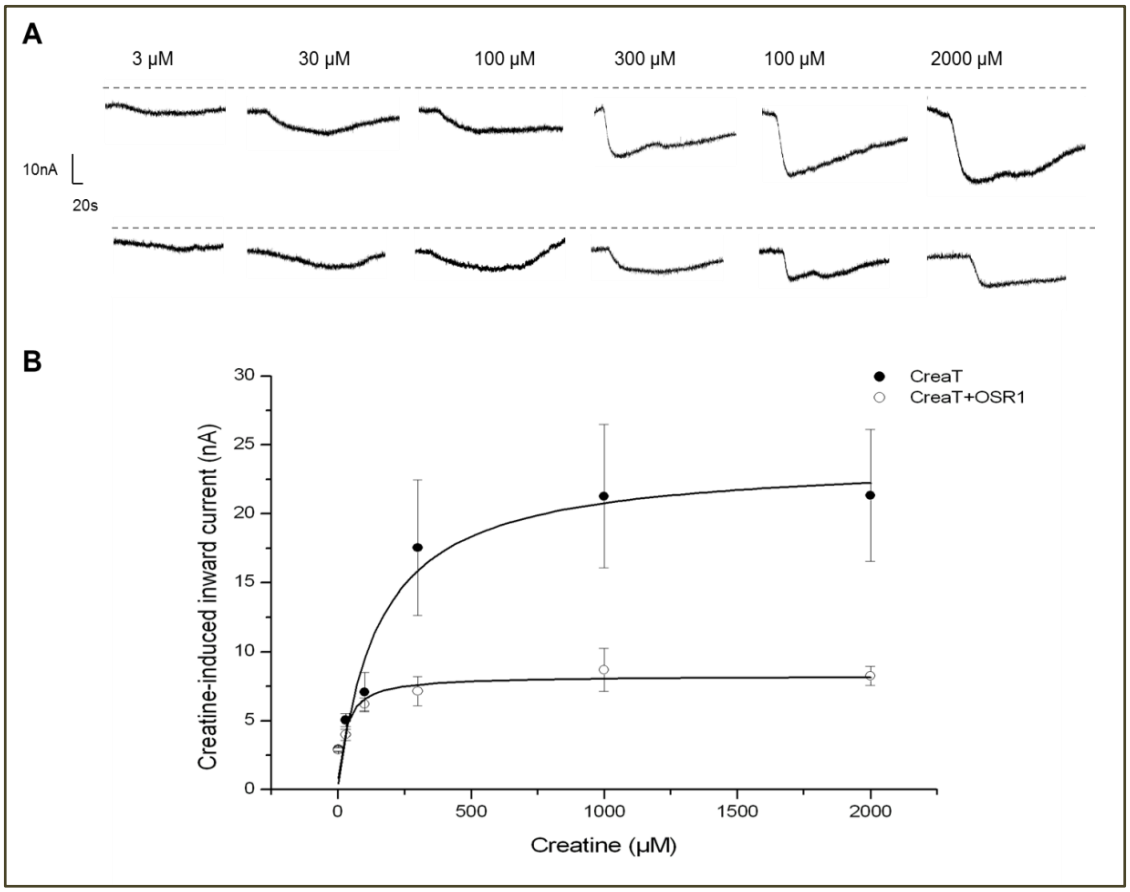

Figure 27: OSR1 decreased the maximal creatine induced current in CreaT expressing *Xenopus* oocytes. (A): Original tracings of creatine induced current at different creatine concentrations in CreaT (upper tracings) and CreaT+OSR1 wild type (lower tracings). **(B)**: Means of creatine induced current (±SEM) as a function of creatine increasing concentrations in oocytes injected with CreaT (black circles) and CreaT+OSR1 (white circles). (n=5-7), 3 batches of oocytes (162).

3.2.2.3. The creatine induced inward current decreased by constitutively active ^{T185E}OSR1 but not by WNK insensitive ^{T185A}OSR1 or the catalytically inactive ^{D164A}OSR1 co-expression

Further experiments were conducted to explore OSR1 mutants for potential effect on the creatine transporter. *Xenopus laevis* oocytes were injected with the constitutively active ^{T185E}OSR1, the WNK insensitive ^{T185A}OSR1 and the catalytically inactive ^{D164A}OSR1 with

the co-expression of CreaT. Creatine (1mM) induced current was recorded by two electrode voltage clamp. As shown in figure 35, the constitutively active ^{T185E}OSR1 decreased significantly the I_{creat} similarly to the wild type OSR1. This effect was less high with the WNK insensitive ^{T185A}OSR1 and not observed with the catalytically inactive ^{D164A}OSR1. In the figure 28, original tracings and arithmetic means of the corresponding creatine induced current illustrate the negative effect of the constitutively active ^{T185E}OSR1 and ^{T185A}OSR1 and not effect ^{D164A}OSR1 on CreaT co-expressed in *Xenopus* oocytes (162).

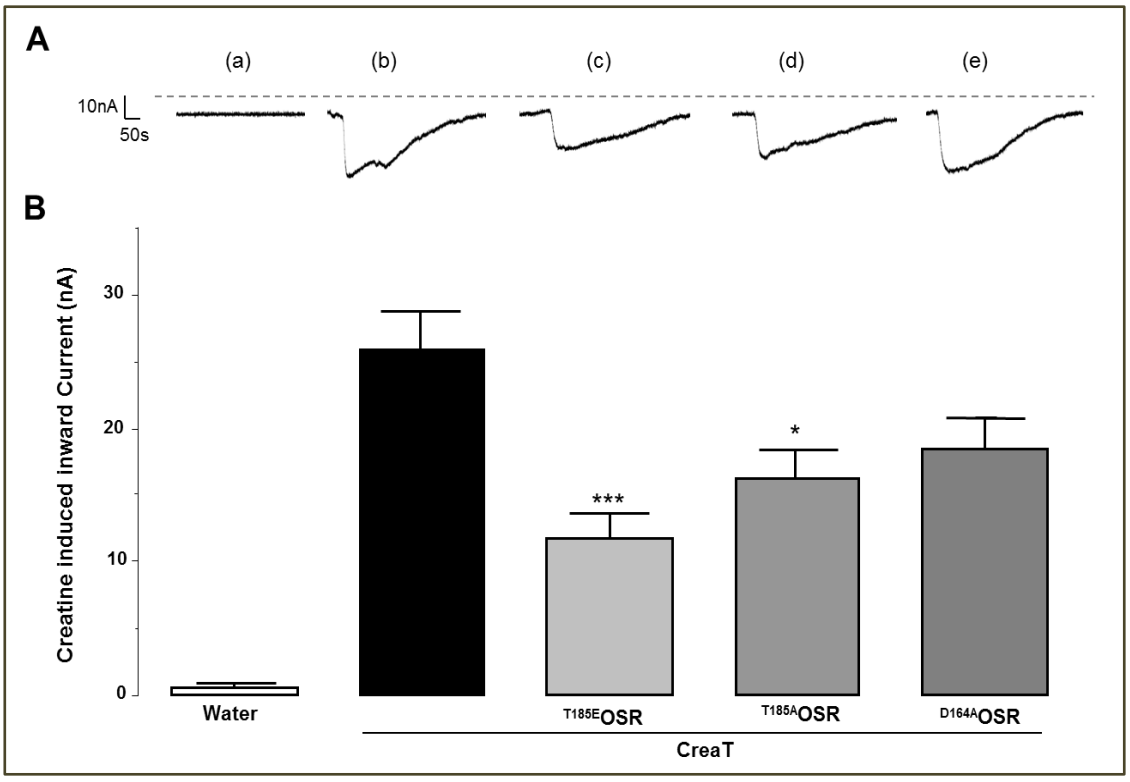

Figure 28: OSR1 mutants' effect on CreaT inward current in *Xenopus* oocytes. (A): Original tracings of water (a), CreaT (b), CreaT+ ^{T185E}OSR1 (c), CreaT+ ^{T185A}OSR1 (d) and CreaT+ ^{D164A}OSR1 (e) oocytes. **(B)**: Means (±SEM) of creatine induced current in oocytes injected with water (white bar), CreaT (black bar), CreaT+ ^{T185E}OSR1 (light grey bar), CreaT+ ^{T185A}OSR1 (middle grey bar) and CreaT+ ^{D164A}OSR1 (dark grey bar). (n=15-20), 3 batches of oocytes.*(p<0.05), ***(p<0.001) indicate statistical significant difference from CreaT expressing oocytes (162).

3.3. Phosphate transporter NaPi-IIb (SLC34A2) up-regulation by SPAK and OSR1

3.3.1. SPAK up-regulated NaPi-IIb (SLC34A2)

3.3.1. 1. SPAK up-regulated the electrogenic phosphate transport in NaPi-IIb expressed in *Xenopus* oocytes

SPAK showed an effect on the regulation of Kir2.1 and CreaT. These results lead to series of experiments exploring the effect of SPAK on the regulation of the phosphate transporter NaPi-IIb (SLC34A2). In order to study the potential effect of the kinase on the carrier, cRNA of the phosphate transporter NaPi-IIb encoded by the gene SLC34A2 was injected in oocytes in the absence and presence of SPAK wild type and compared to a control group injected with water.

Phosphate-induced currents were recorded with dual electrode voltage clamp, at a holding potential of -60mV, according to the specified NaPi-IIb protocol by addition of 1mM phosphate as substrate to the ND96 superfusate solution. The superfusate solution flow is equal to 20ml/min.

Results show that SPAK up-regulated significantly the electrogenic phosphate current in NaPi-IIb compared to the current recorded in oocytes expressing the carrier NaPi-IIb alone, while water injected oocytes showed a negligible phosphate current demonstrating that water injected oocytes did not express a sizable phosphate current. As illustrated in the figure 29 **A** shows the original tracings and in **B** histogram of the corresponding arithmetic mean of the maximal I_{Pi} at 1Mm phosphate (163).

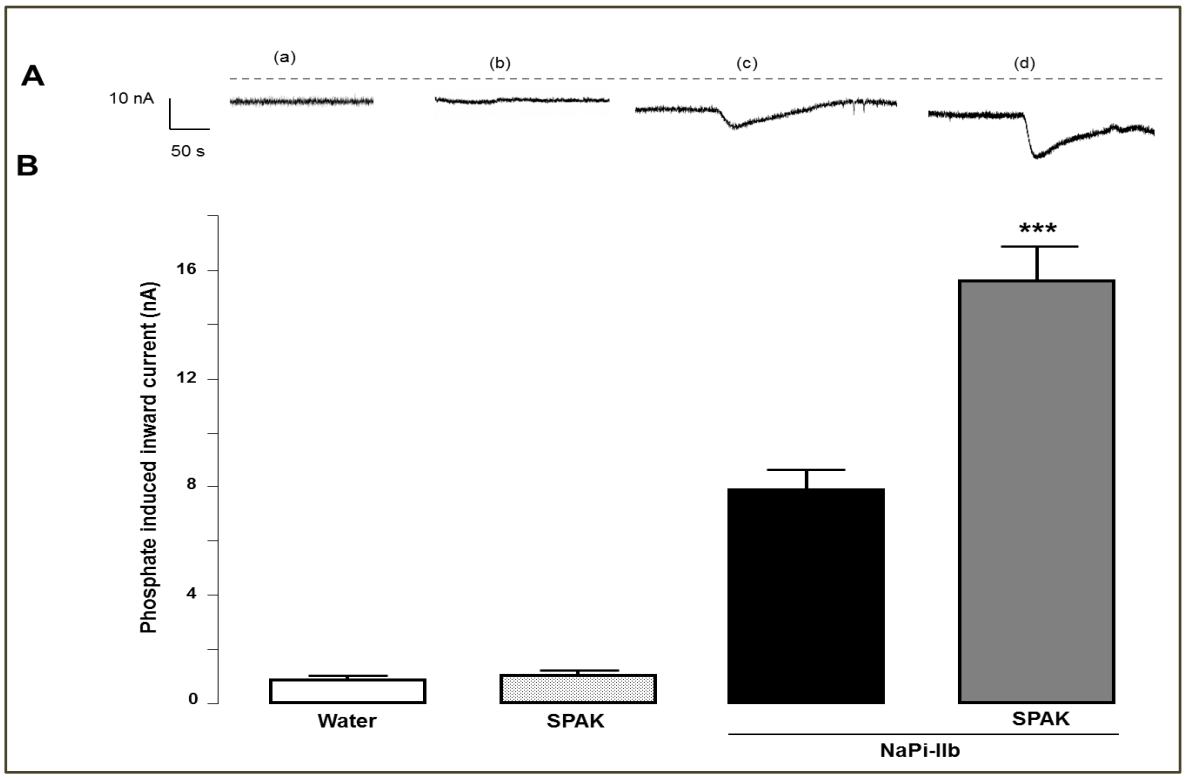

Figure 29: SPAK stimulated the phosphate transporter NaPi-IIb. (A): Original tracings of phosphate induced inward current in water (a), SPAK (b), NaPi-IIb (c) and NaPi-IIb+SPAK (d) injected oocytes at 1Mm phosphate. **(B)**: Means (±SEM) of phosphate induced inward current in *Xenopus* oocytes injected with water (white bar), SPAK (dotted bar), NaPi-IIb (black bar) and NaPi-IIb+SPAK (grey bar). (n=9-16), 3 batches of oocytes. ***(p<0.001) indicates the statistical significant difference from NaPi-IIb alone(163).

3.3.1.2. SPAK increased the maximal phosphate induced current and the affinity in NaPi-IIb expressing oocytes: Kinetic analysis

The effect of SPAK on further characteristics of the carrier, namely the maximal inward induced phosphate current and the affinity to the substrate was assessed through the analysis of kinetics. *Xenopus* oocytes were injected with NaPi-IIb alone or with additional co-injection of SPAK, and currents were recorded in the presence of increasing phosphate concentration (from 0.1mM to 4mM).

As illustrated in the figure 37, the increasing concentrations of phosphate substrate added to the ND96 superfusate solution was followed by an increasing phosphate induced inward

current in both NaPi-IIb as well as NaPi-IIb+SPAK wild type expressing oocytes. The maximal phosphate induced inward current was significantly (p<0.001) higher in oocytes expressing NaPi-IIb+SPAK showing a mean value of (20.6 ± 1.1 nA) than in those expressing NaPi-IIb alone with the mean value (8.9 ± 0.3 nA). Further analysis showed that the concentration of phosphate needed for the half maximal phosphate induced current (K_m) was significantly higher (p<0.05) in oocytes expressing NaPi-IIb+SPAK (K_m = 361 ± 66µM) than in oocytes expressing NaPi-IIb only (K_m = 193 ± 26µM). As illustrated in the figure 30 **A**, represents the original tracings at the different concentrations, for each respective group, and in **B** the Kinetic curves of the Log [P_i] in µM as function of the I_{Pi} corresponding to each group of oocytes (163).

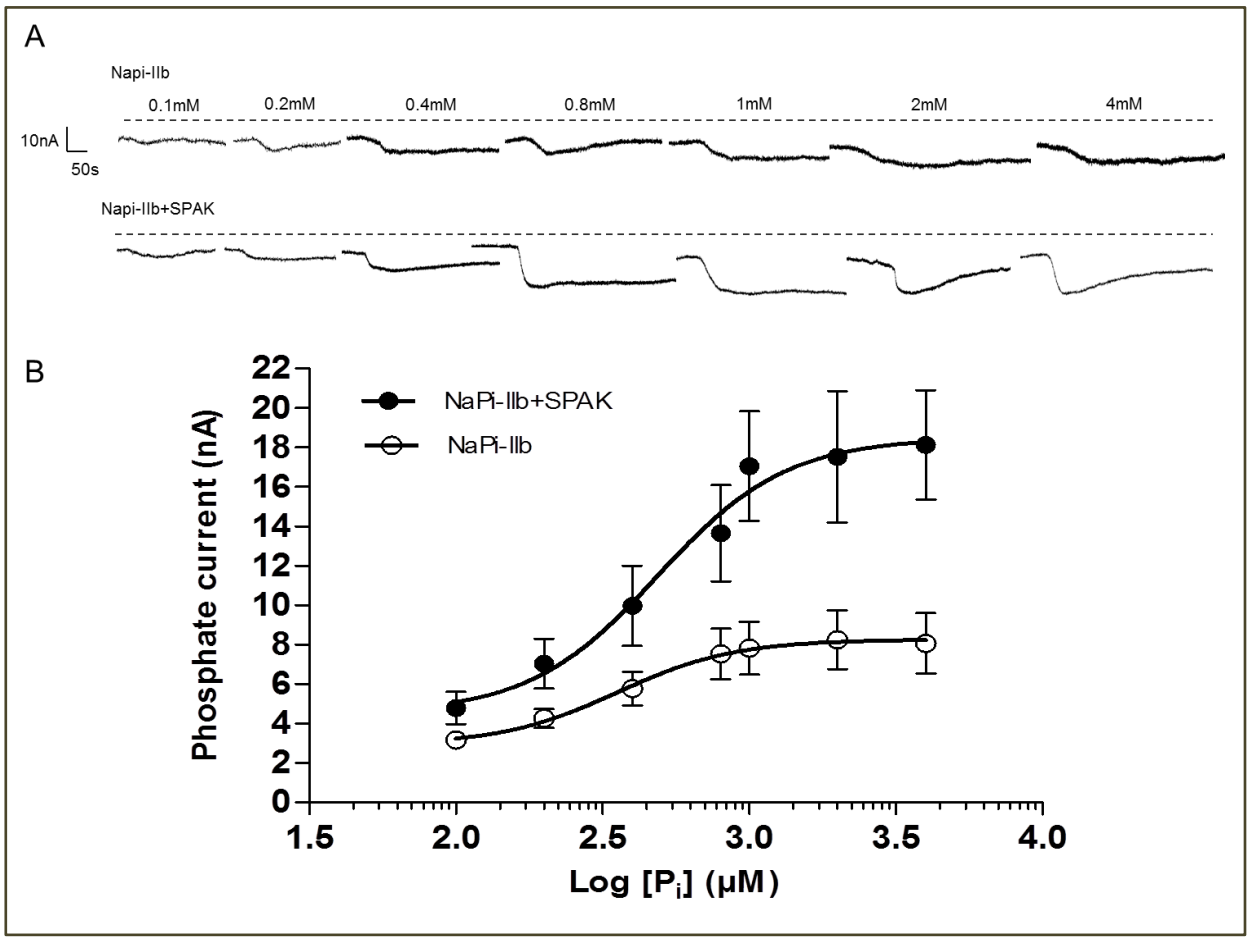

Figure 30: Additional SPAK expression increased the phosphate induced maximal current in NaPi-IIb expressing oocytes. (A): Original tracings of NaPi-IIb (upper tracings) and NaPi-

IIb+SPAK (lower tracings) at increasing concentrations of P_i. **(B)**: Means of phosphate induced currents (±SEM) as function of the logarithmic increasing phosphate concentrations in oocytes injected with NaPi-IIb alone (white circles) and NaPi-IIb+SPAK (black circles). (n=6), 3 batches of oocytes (163).

3.3.1.3. The Phosphate induced inward current increased by constitutively active ^{T233E}SPAK but not by WNK insensitive ^{T233A}SPAK or the catalytically inactive ^{D212A}SPAK co-expression

In order to check the possible effect of the different SPAK mutants, *Xenopus* oocytes were injected with the constitutively active ^{T233E}SPAK, the WNK insensitive ^{T233A}SPAK and the catalytically inactive ^{D212A}SPAK respectively with the co-expression of NaPi-IIb (SLC34A2).

The induced inward current was measured for 1mM phosphate substrate through two electrode voltage clamp at a holding potential of -60mV using the same protocol.

As figure 31 shows, the constitutively active ^{T233E}SPAK exhibited a similar effect as the wild type SPAK, since it increased significantly the phosphate current in NaPi-IIb co-expressing oocytes. This effect was not observed once NaPi-IIb is co-expressed with the WNK insensitive ^{T233A}SPAK or with the catalytically inactive ^{D212A}SPAK.

In the figure 30, both the original representative tracings as well as the arithmetic means of the corresponding maximal inward phosphate induced current showed the stimulating effect of the constitutively active ^{T233E}SPAK, comparing to the effect of the WNK insensitive ^{T233A}SPAK or the catalytically inactive ^{D212A}SPAK on NaPi-IIb co-expressed in *Xenopus* oocytes (163).

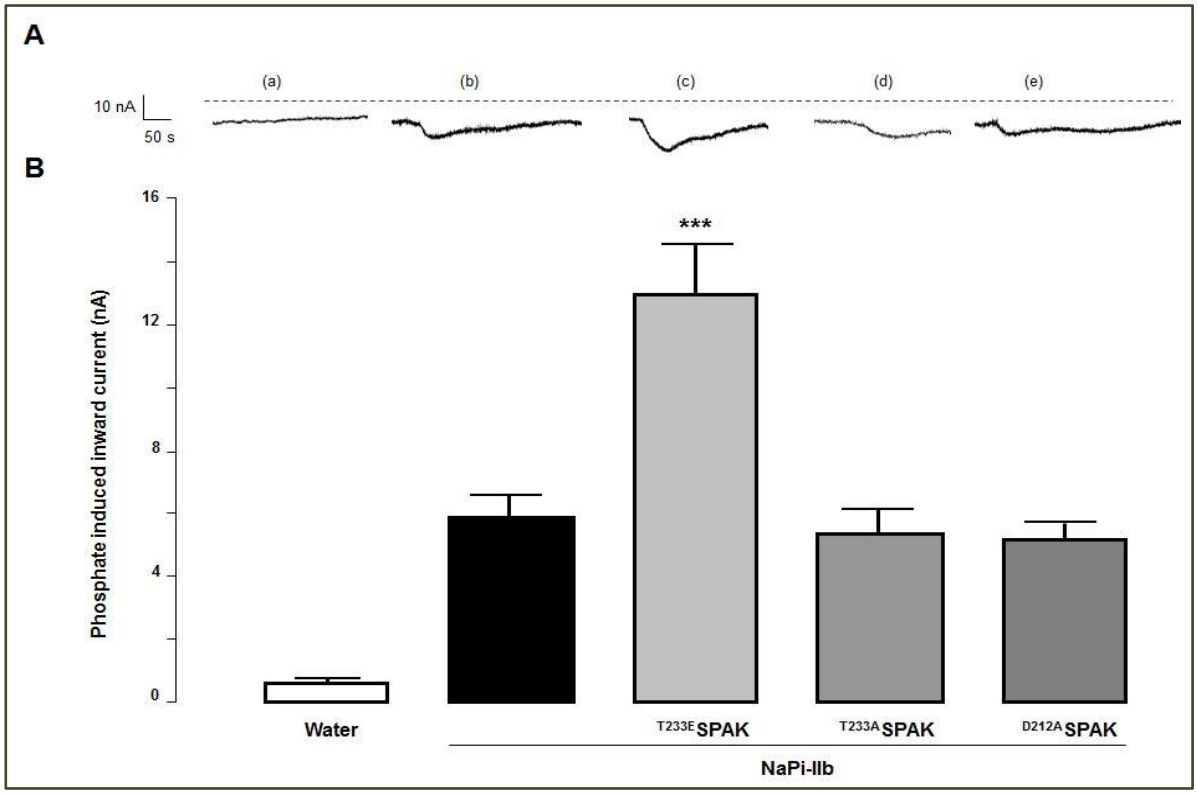

Figure 31: The constitutively active ^{T233E}SPAK increased the phosphate (1mM) induced current in NaPi-IIb co-expressing oocytes. (A): Original tracings of phosphate induced current in oocytes injected with water (a), NaPi-IIb (b), NaPi-IIb+^{T233E}SPAK (c), NaPi-IIb+^{T233A}SPAK (d) and NaPi-IIb+^{D212A}SPAK (e). **(B)**: Means of the maximal inward phosphate induced current (±SEM) in oocytes injected with water (white bar), NaPi-IIb (black bar), NaPi-IIb+^{T233E}SPAK (light grey bar), NaPi-IIb+^{T233A}SPAK (middle grey bar), NaPi-IIb+^{D212A}SPAK (dark grey bar). (n = 9-12), 3 different batches of oocytes, ***(p<0.001) indicates the statistical significant difference from NaPi-IIb alone (163).

3.3.2. OSR1 up-regulated NaPi-IIb (SLC34A2)

3.3.2.1. OSR1 up-regulated the electrogenic phosphate transport in NaPi-IIb expressed in *Xenopus* oocytes

The same series of experiments were performed with OSR1 kinase to evaluate the effect of OSR1 on NaPi-IIb (SLC34A2) phosphate transporter. Phosphate induced-currents were measured with two electrode voltage clamp. *Xenopus laevis* oocytes were injected with

cRNA encoding for SLC34A2 and/or OSR1 and water. The same recording protocol was used.

As illustrated in figure 32, oocytes injected with water did not show appreciable current, showing that *Xenopus* oocytes did not express appreciable electrogenic phosphate transport. Oocytes expressing NaPi-IIb (SLC34A2) and exposed to 1mM phosphate in the superfusate ND96 showed an appreciable inward phosphate induced current. Oocytes co-expressing NaPi-IIb and OSR1 wild type together, demonstrated a significantly increase of the phosphate current comparing to currents recorded in NaPi-IIb alone. Figure 32 shows in **A** the comparative original tracings displayed in histogram of the respectively maximal phosphate induced currents in **B** (163).

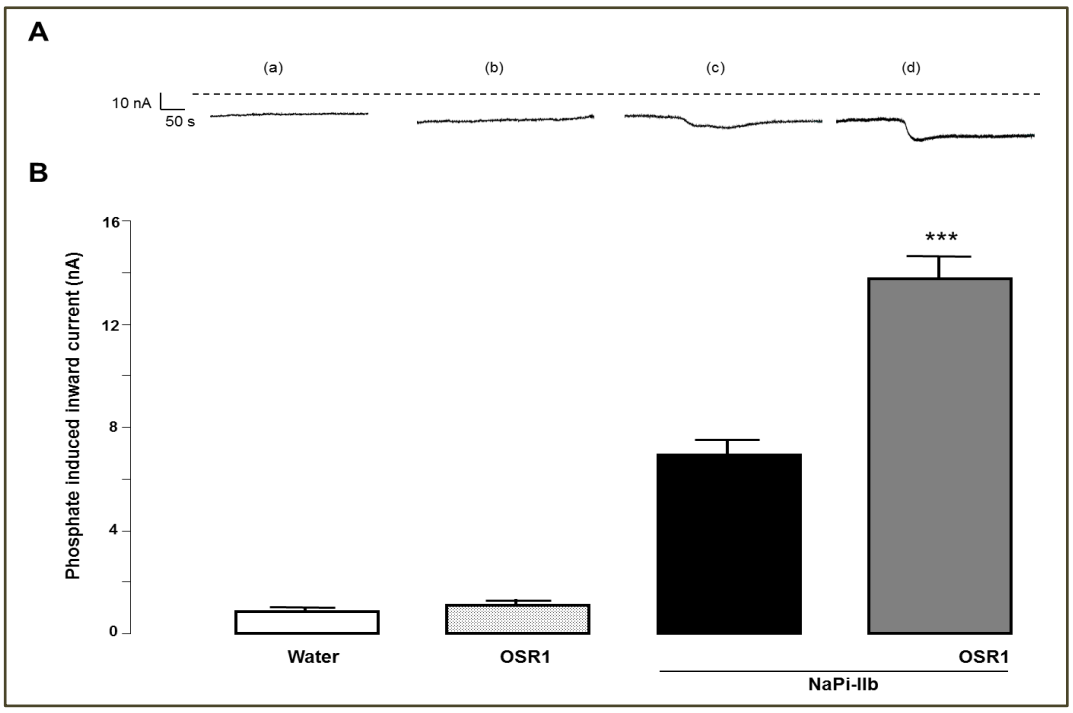

Figure 32: OSR1 up-regulated the phosphate transporter NaPi-IIb. (A): Original tracings of phosphate induced inward current in water (a), OSR1 (b), NaPi-IIb (c) and NaPi-IIb+OSR1 (d) injected oocytes at 1Mm phosphate. **(B)**: Means (±SEM) of phosphate induced current in *Xenopus* oocytes injected with water (white bar), OSR1 (dotted bar), NaPi-IIb (black bar) and NaPi-IIb+OSR1 (grey bar). (n=9-17), 3 batches of oocytes. ***(p<0.001) indicates the statistical significant difference from NaPi-IIb alone (163).

3.3.2.2. OSR1 increased the maximal phosphate induced current and the affinity of NaPi-IIb expressing oocytes: Kinetic analysis

OSR1 effect was further tested on the transporter characteristics. The maximal induced phosphate current and the affinity were analyzed from the transporter kinetics. *Xenopus laevis* oocytes were expressed with NaPi-IIb alone or with OSR1 and phosphate current was measured with increasing phosphate concentrations (from 0.1mM to 4mM). As shown in the figure 33, the increasing concentrations of phosphate substrate added to the ND96 superfusate solution showed increasing phosphate induced current in NaPi-IIb and NaPi-IIb+OSR1 wild type expressing oocytes. The maximal phosphate induced inward current was significantly (p<0.001) higher in oocytes expressing NaPi-IIb+OSR1 with the mean value (14.9 ± 1.1 nA) than in those expressing NaPi-IIb alone with the mean value (6.8 ± 0.1 nA). The analysis showed as well that the concentration of phosphate needed for the half maximal phosphate induced current (K_m) was significantly higher (p<0.05) in oocytes expressing NaPi-IIb+OSR1 (K_m = 388 ± 92µM) than in oocytes expressing NaPi-IIb only (K_m = 119 ± 11µM). Illustration in the figure 33 **A** represents the original tracings at the different concentrations, for each respective group, and in **B** the Kinetic curves of the Log [P_i] in µM as function of the I_{Pi} corresponding to each group of oocytes (163).

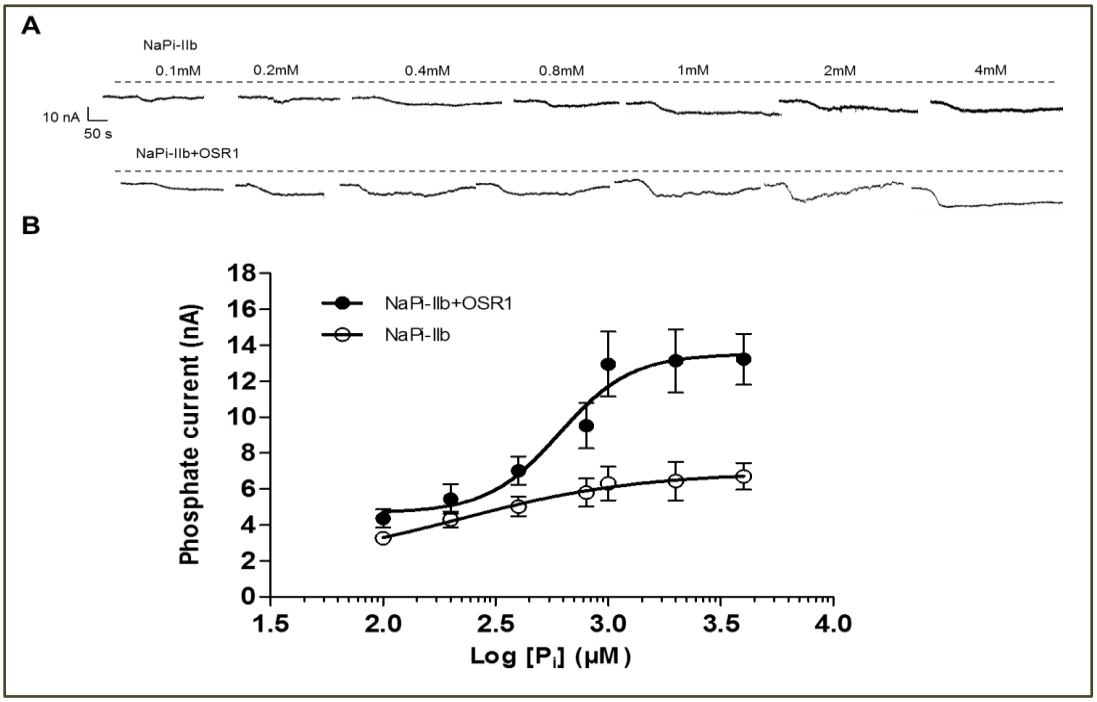

Figure 33: OSR1 additional expression increased the phosphate induced current in NaPi-IIb expressing oocytes. (A): Original tracings of NaPi-IIb (upper tracings) and NaPi-IIb+OSR1 (lower tracings) at increasing concentrations of P_i. **(B)**: Means of phosphate induced currents (±SEM) as function of the logarithmic increasing phosphate concentrations in oocytes injected with NaPi-IIb alone (white circles) and NaPi-IIb+OSR1 (black circles). (n=6), 3 batches of oocytes (163).

3.3.2.3. The phosphate induced inward current increased by constitutively active ^{T185E}OSR1 but not by WNK insensitive ^{T185A}OSR1 or the catalytically inactive ^{D164A}OSR1 co-expression

In order to explore OSR1 mutants for a potential effect on the phosphate transporter, *Xenopus laevis* oocytes were injected with the constitutively active ^{T185E}OSR1, the WNK insensitive ^{T185A}OSR1 and the catalytically inactive ^{D164A}OSR1 with the co-expression of NaPi-IIb.

Phosphate induced currents were recorded via two electrode voltage clamp with 1mM phosphate substrate, at a holding potential of -60mV, using the same protocol of NaPi-IIb.

As shown in figure 34, the constitutively active ^{T185E}OSR1 increased significantly the I_{Pi} similarly to the wild type OSR1. This effect disappeared with the WNK insensitive ^{T185A}OSR1 and the catalytically inactive ^{D164A}OSR1. In the figure 34 original tracings and arithmetic means of the corresponding phosphate induced current illustrate the stimulating effect of the constitutively active ^{T185E}OSR1 and not ^{T185A}OSR1 or ^{D164A}OSR1 effect on NaPi-IIb co-expressed in *Xenopus* oocytes (163).

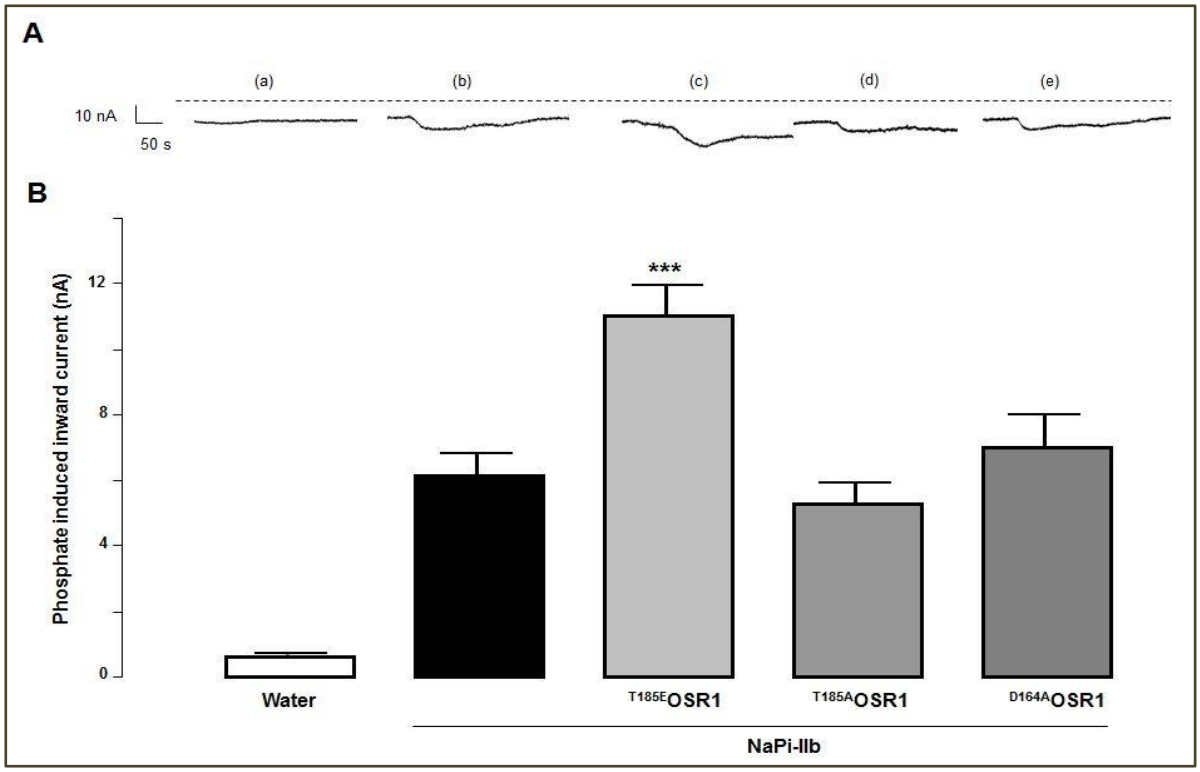

Figure 34: OSR1 mutants' effect on NaPi-IIb (SLC34A2) current in *Xenopus* oocytes. (A): Original tracings of water (a), NaPi-IIb (b), NaPi-IIb+ ^{T185E}OSR1 (c), NaPi-IIb+ ^{T185A}OSR1 (d) and NaPi-IIb+ ^{D164A}OSR1 (e) oocytes. **(B)**: Means (±SEM) of phosphate induced current in oocytes injected with water (white bar), NaPi-IIb (black bar), NaPi-IIb+ ^{T185E}OSR1 (light grey bar), NaPi-IIb+ ^{T185A}OSR1 (middle grey bar) and NaPi-IIb+ ^{D164A}OSR1 (dark grey bar). (n=9-12), 3 batches of oocytes. ***(p<0.001) indicate statistical significant difference from NaPi-IIb expressing oocytes (163).

3.3.3. Simultaneous expression of SPAK and OSR1 together with NaPi-IIb (SLC34A2) did not induce a significant synergic effect in *Xenopus* oocytes

The last series of experiments performed in *Xenopus* oocytes propose to explore the simultaneous effect of both kinases SPAK and OSR1 on the regulation of the electrogenic phosphate current in NaPi-IIb, whether it is a potential synergic, cumulative or antagonist.

For this purpose, SPAK and OSR1 were co-expressed simultaneously in NaPi-IIb-expressing oocytes. Results show in the figure 35 that the phosphate (1mM) induced currents in NaPi-IIb expressing oocytes was significantly increased in the presence of

SPAK alone, and OSR1 alone comparing to the currents recorded in NaPi-IIb expressed alone without any kinase, confirming the up-regulating effect of both kinases active separately. The oocytes co-expressing together: NaPi-IIb+SPAK+OSR1, demonstrated a significantly increased phosphate induced current comparing to oocytes expressing NaPi-IIb alone. Even though, the phosphate induced current in NaPi-IIb co-expressing both SPAK and OSR1 was a little higher comparing to the current recorded in oocytes co-expressing NaPi-IIb with either SPAK or OSR1, however the difference was not statistically significant (163).

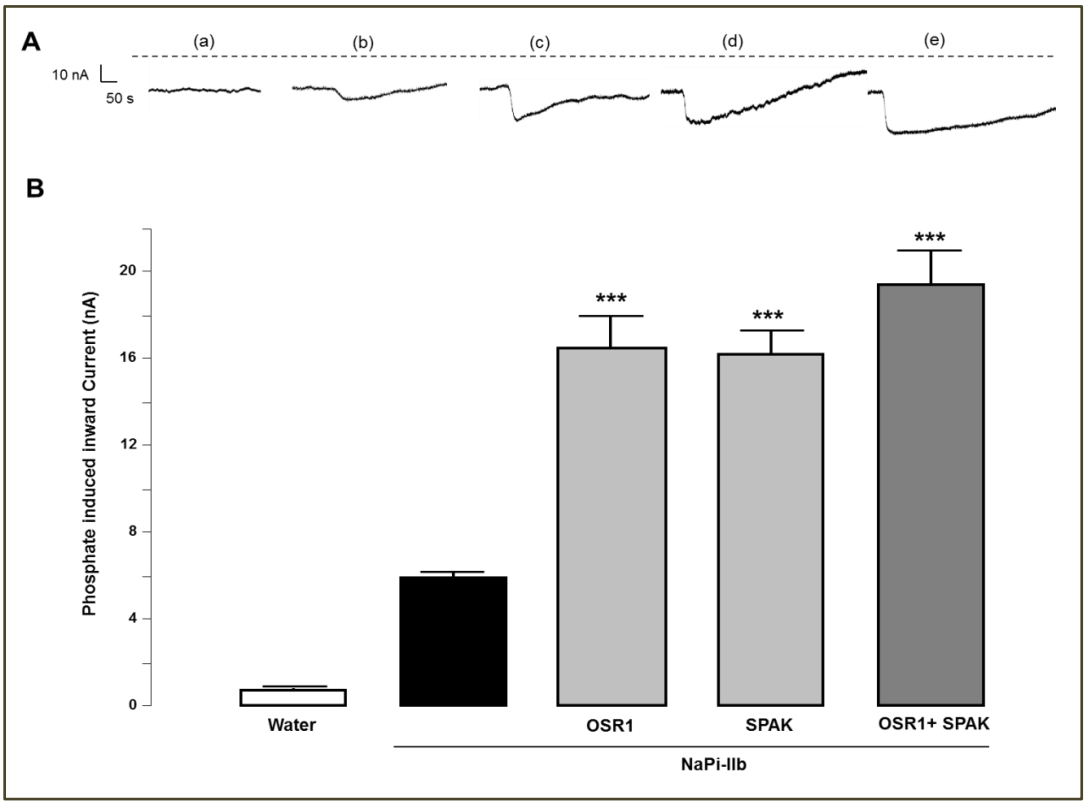

Figure 35: Simultaneous expression of SPAK and OSR1 in NaPi-IIb co-expressing oocytes. **(A)**: Original tracings of phosphate (1mM) induced current in oocytes injected with water (a), NaPi-IIb (b), NaPi-IIb+OSR1 (c), NaPi-IIb+SPAK (d) and NaPi-IIb+SPAK+OSR1 (e). **(B)**: Means of phosphate (1Mm) induced currents in oocytes injected with water (white bar), NaPi-IIb (black bar), NaPi-IIb+OSR1 (light grey bar), NaPi-IIb+SPAK (middle grey bar) and NaPi-IIb+SPAK+OSR1 (dark grey bar). (n=9-16), 3 batches of oocytes. ***(p<0.001) shows statistical significant difference from oocytes injected with NaPi-IIb only (163).

4. DISCUSSION

The WNK (with-no-K[lys]) kinases and especially their downstream kinases SPAK (SPS1-related proline/alanine-rich kinase) and OSR1 (oxidative stress-responsive kinase 1) are involved in the regulation of ion transport. Both kinases are shown to be powerful regulators for transporters and channels, with either a negative regulation as it is the case of the K^+/Cl^- co-transporter (151, 164), BK (165), EAAT3 (166), CLC-2 (167), ROMK1 (168), Kv1.5 (169); or a positive regulation such the Na^+/Cl^- (NCC), $Na^+/K^+/Cl^-$ (NKCC) co-transporters (131-133, 137, 170, 171), the Na^+-coupled phosphate transport (172) and KCNQ1/E1 (173). Nevertheless, nothing is known about the effect of SPAK and/or OSR1 on the regulation of the inwardly rectifying K^+ channel Kir2.1 (KCNJ2), the creatine transporter CreaT (SLC6A8) and the phosphate transporter NaPi-IIb (SLC34A2). This study focuses on the role of SPAK and OSR1 in the regulation of Kir2.1 channels, CreaT and NaPi-IIb transporters.

4.1. SPAK and OSR1 sensitive Kir2.1

The first part of the present study reveals the stimulating effect of SPAK and OSR1 on the inwardly rectifying K^+ channel Kir2.1. The co-expression of both SPAK and OSR1 separately was followed by an increase of the K^+ inward current in KCNJ2 expressing *Xenopus laevis* oocytes, recorded with dual electrode voltage clamp technique. The increase of the K^+ currents results, at least in part, from an increase of the channel protein abundance on the oocyte plasma membrane, as shown in chemiluminescence essays. This observed phenomenon is theoretically the result of either an enhance of channel protein migration to the cell surface, a stabilization of the protein in the plasma membrane of oocyte or a blockade and/or delay of the protein channel retrieval from the cell membrane (160). The treatment of oocytes with Brefeldin A, which inhibits the protein channel trafficking (159), abolishes the effect of both kinases respectively; demonstrating that SPAK as well as OSR1 do neither stabilize the channel protein already inserted in the plasma membrane, nor retard the protein internalization from cell membrane. These findings outlined indicate the stimulating role of the kinases SPAK and OSR1 in the

trafficking and insertion of the protein channel in the cell membrane. In addition, experiments were conducted on *Xenopus* oocytes model injected with KCNJ2 cRNA encoding for the inward rectifying K^+ channel Kir2.1, which excludes the potential effect of the kinases on the transcription (160).

Further experiments exploring the effect of the kinases mutants separately, showed that both of the constitutively active mutants ^{T233E}SPAK and ^{T185E}OSR1 exhibit a similar effect to the corresponding wild type kinases by up-regulating Kir2.1 currents whereas the WNK insensitive mutants ^{T233A}SPAK and ^{T185A}OSR1, as well as the catalytically inactive mutants ^{D212A}SPAK and ^{D164A}OSR1 do not exert any stimulating effect on the K^+ channel Kir2.1. These observations imply that SPAK and OSR1 activation involve the catalytic activity of WNK kinases. Nevertheless, the indirect role of both kinases SPAK/OSR1 in the up-regulation of Kir2.1 channel through the phosphorylation of channel regulators is not excluded (160).

Intracellular K^+ concentration plays an important role in the regulation of cell volume and maintain of resting membrane potential. K^+ loss is determinant for the cell shrinkage, a process involved among other signaling regulators in cell apoptosis. Thus, counteracting K^+ exit favors cell protection from apoptosis (152). Compelling evidence suggests the influence of SPAK and OSR1 kinases in the activation of the inwardly rectifying K^+ channel Kir2.1 through cell volume regulation, since both kinases increase the cellular K^+ uptake through not only the up-regulation of the Na^+/Cl^- co-transporter (NCC) and the $Na^+/K^+/2Cl^-$ co-transporter, but also via the down-regulation of the K^+/Cl^- co-transporter (121, 122, 131, 132, 137, 138, 143, 170, 171, 174-177). The massive K^+ entry leading to the accumulation of K^+ and Cl^- in the cell, followed by the osmotic obliged water, counteracts cell shrinkage consequently cell swelling occurs (178-180). The up-regulation of the inward rectifying K^+ channel Kir2.1 by SPAK and OSR1 may diminish K^+ and Cl^- entry and cell swelling. Nevertheless, these observations may not be conclusive regarding the significance of SPAK and OSR1 role on Kir2.1 in cell volume regulation. It was proven that Kir2.1 channel hyper-activating mutation engenders atrial fibrillation (46, 181, 182)

since Kir2.1 channels insures the inwardly rectifying K^+ current in cardiac cells (46, 181, 183).

The present study and the described phenomenon may be pertinent to neurobiology conclusions, as Kir2.1 channel is expressed in the neurons (184-187) and in the glial cells (24, 188-190) and participates as well in the spatial K^+ buffering, hence involved in the neuronal excitability (184, 189, 191). Furthermore, SPAK and OSR1 affect also neuronal excitability due to their role in the regulation of intracellular Cl^- in the neurons and the effect of the activation of Cl^- channels on the action potential through the cell membrane (151, 192, 193). Kir2.1 channels are expressed in addition in Müller cells in retina (194-198) and the disturbed kir2.1 function leads to the pathophysiology of uveitis, which is the inflammation of iris, ciliary body and choroid (194). The inwardly rectifying K^+ channel Kir2.1 is also involved in the neurovascular coupling i.e. active neurons delate arterioles via astrocytes, so that blood flow increases and supplies the needed oxygen and glucose to the neuronal process. Kir2.1 loss of function induces arterioles disability to vasodilatation leading to the neurovascular coupling impairment, which could be involved in some brain disorders (199). It is obvious that further experiments are necessary to unravel whether the kinases SPAK and OSR1 stimulation of the inwardly rectifying K^+ channel Kir2.1 is relevant for neurobiological physiology and/or pathophysiology.

In summary, the WNK activated kinases SPAK and OSR1 positively regulate the inwardly rectifying K^+ channel Kir2.1 such stimulation may be contributing to cell excitability and cell volume regulation among possible further functions (160).

4.2. SPAK and OSR1 sensitive CreaT

The second part of the study investigated the negative regulating effect of SPAK and OSR1 on the creatine transporter CreaT. The co-expression of SLC6A8 cRNA encoding for the creatine transporter with SPAK or OSR1 in *Xenopus* oocytes down-regulates the creatine induced inward current recorded by two electrodes voltage clamp. These observations are due to either a role of the kinases in the decrease of the maximal rate of creatine transport or to a decrease in the affinity of the carrier to the creatine substrate. The analysis of the

carrier kinetics, demonstrate on one hand, the significant negative regulation of both kinases SPAK and OSR1 separately on the maximal creatine induced inward current and thus the rate of creatine transport V_m, on the other hand, the K_m is not statistically significant, suggesting that the kinases do not affect the affinity of the creatine transporter to the substrate (162).

Additional experiments targeting the kinases mutants show that the same negative regulating effect of SPAK and OSR1 wild type is observed with the constitutively active mutants ^{T233E}SPAK and ^{T185E}OSR1, and thus creatine currents are decreased. Although, the presence of the WNK insensitive mutants ^{T233A}SPAK and ^{T185A}OSR1 tend to decrease the creatine induced current, only ^{T185A}OSR1 effect is significant. However the catalytically inactive mutants ^{D212A}SPAK and ^{D164A}OSR1 both do not affect the creatine transporter activity. These observations demonstrate the important role of the WNK functional kinases in the activation of SPAK and OSR1 to negatively regulate the creatine transporter CreaT, but also suggest a possible independent WNK activity of the kinases SPAK and OSR1. The phosphorylation of the creatine transporter CreaT by the kinases may not be direct, since both kinases SPAK and OSR1 may interfere indirectly by phosphorylating other regulators of the carrier (162).

The creatine transporter CreaT, is a Na^+/Cl^- co-transporter that carries creatine to cells of high energy demand such as brain, skeletal muscle, intestine, retina, heart and kidney (73) and which belongs to the superfamily of neurotransmitters (74, 75, 77) and organic osmolytes (78, 79). CreaT is determinant for brain function and neuroexitability, insuring the creatine re-uptake in synapses and regulating GABAergic as well as glutamatergic cerebral pathways (200). Since creatine synthesis requires 40% of methyl groups and the creatine transporter is regulated by AMPK, creatine is regarded as a cellular sensor of methylation (200) and maintenance of ATP for energy (73). The creatine transporter CreaT SLC6A8 is regulated by several kinases, for instance: JAK2 (201), JAK3 (202), PIKfyve (203), mTOR (204), SGK1 (205), SGK3 (205), klotho (206) and peroxisome proliferator-activated receptor-gamma co-activator-1alpha (PGC-1α) or beta (PGC-1β) (207).

Creatine deficiency following an expression disorder of the creatine transporter gene, results in mental retardation, behavioral disorders, seizure and intellectual disability (90-94, 200, 208-211). Such effects could be possibly due to a disparity of GABA and glutamate neurotransmission. In addition, these observations suggest that the effect of SPAK and OSR1 kinases on the creatine transporter SLC6A8 may modulate the methylation. Both kinases contribute as well to the modulation of neuron excitability as they are known to activate NKCC and inhibit KCC, an effect increasing the intracellular Cl^- and thus influencing the role of GABA on the membrane potential and hence the excitability of neurons (151, 164). The SPAK and OSR1 activation through WNK is consequent to low intracellular Cl^- concentration, in order to stimulate Cl^- entry (151), this could explain the Kinases disorder in arterial hypertension and the gain of function leading to epilepsy, spasticity, neuropathic pain, schizophrenia and autism (151). SPAK and OSR1 are further involved in the regulation of cell volume (121, 131-133, 136, 170, 174, 175). It is not clear whether the Creatine transporter is modulated by cell volume since other Na/Cl coupled transporters from the same SLC family are up-regulated by cell shrinkage (78, 79). This study did not elucidate the *in vivo* role of SPAK and OSR1 in the sensitivity of creatine transporter.

To summarize, both WNK downstream kinases SPAK and OSR1 down-regulate the Na^+ and Cl^- coupled creatine transporter SLC6A8, an effect presumably involved in the modulation of cell excitability (162).

4.3. SPAK and OSR1 sensitive NaPi-IIb

The third part of the investigation of the role of SPAK and OSR1 kinases reveals an up-regulation effect of both on the phosphate transporter NaPi-IIb. The co-expression of the kinases with the SLC34A2 cRNA encoding for the phosphate transporter NaPi-IIb in *Xenopus* oocytes, increases the phosphate induced inward current recorded with dual electrode voltage clamp. Such an effect is resulting from an increased maximal rate and/or increase in the affinity of the transporter to the phosphate. The NaPi-IIb kenetics analysis, show that both kinases SPAK and OSR1 not only stimulate the transport rate V_m of the

phosphate transporter NaPi-IIb by increasing significantly the maximal phosphate induced current, but also, increase the affinity K_m of NaPi-IIb transporter to the phosphate substrate. Further, the simultaneous expression of both kinases SPAK and OSR1 together with NaPi-IIb phosphate transporter in oocytes does not display an additive effect. This observation can be due to the fact that SPAK and OSR1 are expressed in different cells within the same tissue (163).

The results relative to the kinases mutants, demonstrate a mimic activity of the constitutively active mutants ^{T233E}SPAK and ^{T185E}OSR1, similar to the up-regulation observed with the corresponding wild type. The WNK insensitive mutants ^{T233A}SPAK and ^{T185A}OSR1, as well as the catalytically inactive mutants ^{D212A}SPAK and ^{D164A}OSR1 did not show any stimulating effect to the phosphate carrier. These findings imply the activation of both kinases SPAK and OSR1 by WNK phosphorylation on one hand. On the other hand, the phosphorylation of NaPi-IIb by the kinases may not be directly activated, since the effect could be due to the phosphorylation of other regulators and/or molecules involved in the signaling pathway of NaPi-IIb (163).

The Na-coupled phosphate transporter NaPi-IIb is responsible for phosphate transport in the intestines and the tumor cells as well (155). NaPi-IIb is regulated by AMPK activated kinase (212), mTOR the mammalian target of rapamycin (213), B-RAF (155) and SGK1 the serum and glucocorticoid inducible kinase (214).

Previous studies exploring SPAK and OSR1 reveal their role in the modulation of phosphate metabolism. Gene targeted mice expressing WNK-resistant SPAK (172) and OSR1 (156) demonstrate the implication of both kinases in phosphate metabolism among other regulators; moreover, OSR1 stimulates NaPi-IIa in the proximal renal tubules (156). The kinases stimulate the entry of K^+ and Cl^- by activating Na^+/Cl^- (NCC) and $Na^+/K^+/Cl^-$ (NKCC) co-transporters, on one hand, and by inhibiting the K^+/Cl^- co-transporters on the other hand (122, 133, 136, 137, 142, 170). This effect allows cell swelling to occur (178-180). Activation of Na^+-coupled phosphate transporter suggests fostering cell swelling as well, since it improves Na^+ and P_i entry, which depolarizes the cell membrane, and thus

stimulates negative- charged Cl^- up-take. Nevertheless, the cell swelling phenomenon could not be rapid giving that the extracellular concentration of phosphate is finite and the transport rate is low.

To sum up, the Na^+-coupled phosphate transporter NaPi-IIb is stimulated by the kinases SPAK and OSR1, probably this observed effect is involved in the modulation of phosphate metabolism (163).

In conclusion, this study reveals a novel role of SPAK and OSR1 kinases as powerful regulators, positively regulating the inwardly rectifying K^+ channel Kir2.1 and the Na^+-coupled phosphate transporter NaPi-IIb and negatively regulating the Na^+ and Cl^- coupled creatine co-transporter (160, 162, 163). (Figure 36).

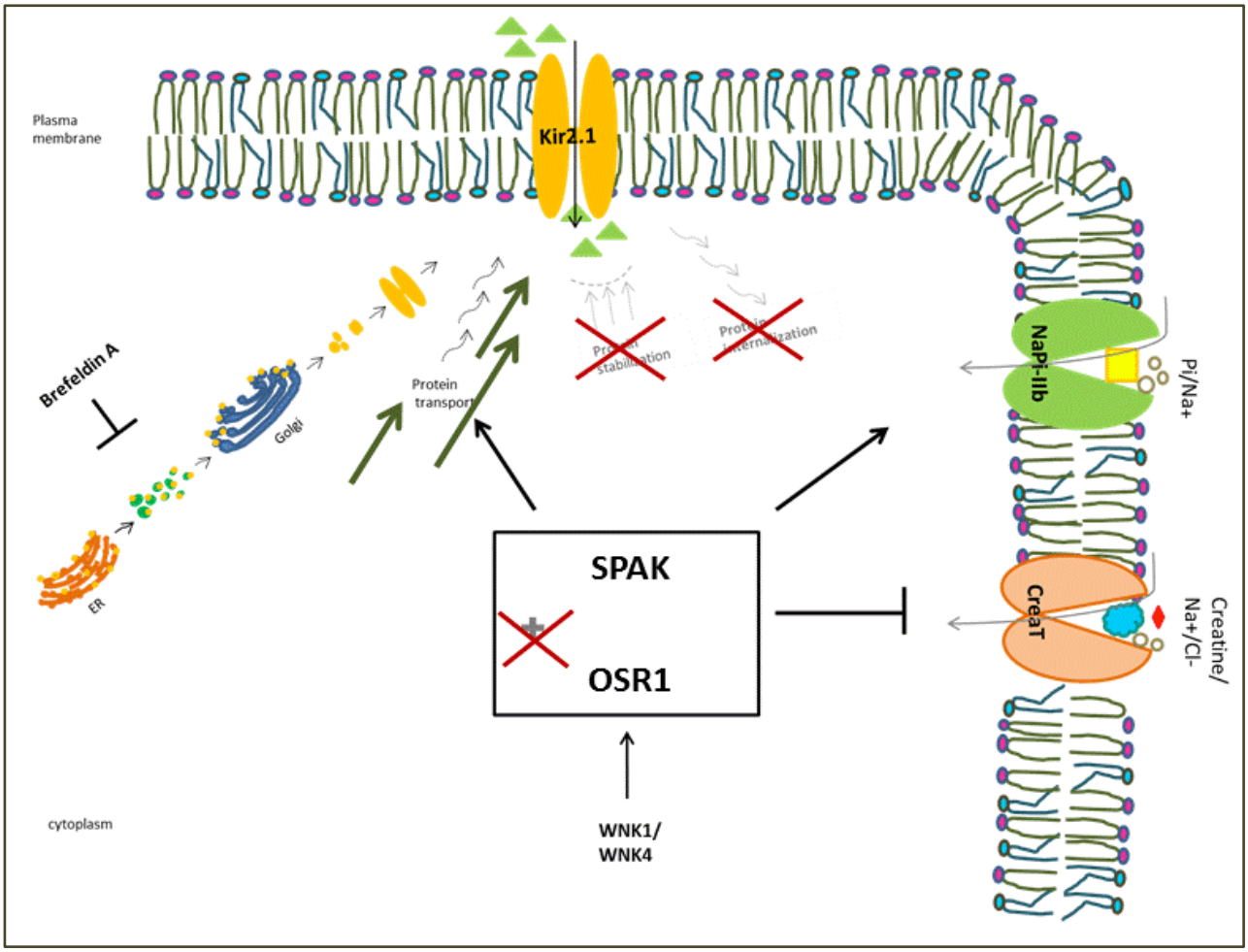

Figure 36: SPAK/OSR1 effect on Kir2.1 (KCNJ2), CreaT (SLC6A8) and NaPi-IIb (SLC34A2)

5. SUMMARY

The regulation of ion transport involves several kinases including SPAK (SPS1-related proline/alanine-rich kinase) and OSR1 (oxidative stress-responsive kinase 1), which are controlled by WNK (with-no-K[Lys]) kinases. The present study investigates whether SPAK and/or OSR1 participate in the modulation of the K^+ channel Kir2.1 (KCNJ2), the creatine transporter CreaT (SLC6A8) and the phosphate transporter NaPi-IIb (SLC34A2).
The first part of the study focuses on Kir2.1, namely: the inwardly rectifying K^+ channel, which is expressed in brain, heart and skeletal muscle. Kir2.1 maintains the resting membrane potential and is determinant for cell volume regulation, preventing cell shrinkage. In addition kir2.1 participates in the spatial K^+ buffering in neurons and contributes hence to neuro-excitability. The inwardly rectifying K^+ current in Kir2.1 co-expressing *Xenopus laevis* oocytes is significantly increased in the presence of SPAK and OSR1 respectively; as a result of the enhanced channel protein abundance on the cell surface. Moreover, treatment with Brefeldin A abolishes the stimulating effect of SPAK or OSR1 on Kir2.1 indicating that the kinases effect involves in the protein trafficking pathway towards the plasma membrane. Further investigation regarding the kinases mutations show that the constitutively active mutants ^{T233E}SPAK and ^{T185E}OSR1 mimic the effect of the corresponding wild type kinase, while neither the WNK insensitive ^{T233A}SPAK and ^{T185A}OSR1, nor the catalytically inactive ^{D212A}SPAK and ^{D164A}OSR1 enhanced kir2.1 activity.

The second part of the investigation concerns CreaT, i.e. the Na^+ and Cl^- coupled creatine transporter. CreaT carrier is expressed in cells with high energy demand such as brain, heart, intestine, retina and skeletal muscle, where it provides creatine needed for energy. The conversion of creatine to phosphocreatine by creatine kinase is important for maintaining ATP in the cells. Creatine transporter is additionally involved in mental retardation, seizure and intellectual disability. The co-expression of SPAK or OSR1 with CreaT decreases significantly the electrogenic creatine transport. Furthermore, the maximal creatine-induced inward current indicating the rate of transport is down-regulated by SPAK

or OSR1, whereas the affinity of CreaT carrier to creatine is not affected. Besides the results of wild type kinases, the respective active mutants namely the constitutively active ^{T233E}SPAK and ^{T185E}OSR1 do negatively regulate CreaT, however, the catalytically inactive mutants ^{D212A}SPAK and ^{D164A}OSR1 as well as the WNK insensitive ^{T233A}SPAK do not, while ^{T185A}OSR1 tend to reduce creatine current.

The last part of the study, explores the regulation of the Na^+ coupled phosphate transporter NaPi-IIb, which ensures phosphate up-take in the intestine and tumor cells. The carrier is stimulated by SPAK and OSR1. Both kinases increase not only the maximal phosphate inward current and thus the transport rate, but also enhance significantly the affinity of NaPi-IIb to phosphate. Moreover, the simultaneous expression of SPAK and OSR1 do not show an additive effect. Furthermore, the constitutively active mutants ^{T233E}SPAK and ^{T185E}OSR1 display same effect as the wild type kinase respectively on NaPi-IIb activity. This effect is observed neither with the inactive mutants WNK insensitive ^{T233A}SPAK and ^{T185A}OSR1 nor with the catalytically inactive ^{D212A}SPAK and ^{D164A}OSR1.

In conclusion, both kinases SPAK and OSR1 are powerful regulators of Kir2.1, NaPi-IIb and CreaT, effects may be involved in the cell volume regulation and excitability.

Zusammenfassung

An der Regulation des Ionentransports sind mehrere Kinasen, darunter SPAK (SPS1-proline/alanine-rich kinase) und OSR1 (oxidative stress-responsive kinase 1) beteiligt, die durch WNK (with-no-K[Lys]) Kinasen kontrolliert werden. Die vorliegende Studie untersucht, ob SPAK und/oder OSR1 an der Modulation des K^+ kanals Kir2.1 (KCNJ2), dem Kreatintransporter CreaT (SLC6A8) und dem Phosphattransporter NaPi-IIb (SLC34A2) eine Rolle spielen.

Der erste Teil der Arbeit konzentriert sich auf Kir2.1: den einwärts gleich-richtenden K^+ Kanal, der in Gehirn, Herz und Skelettmuskeln exprimiert wird. Kir2.1 hält das Membranruhepotential aufrecht und ist für die Regulation des Zellvolumens und das Verhindern der Zellschrumpfung. Darüber hinaus beteiligt sich Kir2.1 an der räumlichen K^+-Pufferung in Neuronen und trägt damit zur neuronalen Erregbarkeit bei. Der einwärts rektifizierende K^+ Strom in Kir2.1 exprimierenden Oozyten wird in Anwesenheit von SPAK bzw. OSR1 erhöht, als Resultat der erhöhten Vorkommen des Kir2.1 auf der Zellmembranoberfläche. Die Behandlung der Oozyten mit Brefeldin A hemmt jedoch die stimulierende Wirkung von SPAK/OSR1 auf Kir2.1, was darauf hinweist, dass SPAK und OSR1 beim Transport von Kir2.1 zur Zellmembranoberfläche involviert sind.

Eine weitere Untersuchung der Kinase-Mutationen zeigt, dass die konstitutiv aktiven Mutanten ^{T233E}SPAK und ^{T185E}OSR1 dieselbe Wirkung ausüben wie die entsprechende Wildtyp-Kinase, während weder das WNK-insensitive ^{T233A}SPAK und ^{T185A}OSR1 noch die katalytisch inaktive ^{D212A}SPAK und ^{D164A}OSR1 die kir2.1-Aktivität verstärken.

Der zweite Teil der Untersuchung betrifft CreaT, den Na^+ und Cl^--gekoppelten Kreatin-Transporter. CreaT wird in Zellen mit hohem Energiebedarf wie Gehirn, Herz, Darm, Netzhaut und Skelettmuskel exprimiert. Das transportierte Kreatin und dessen Phosphorylierung wird anschließend zur Energiegewinnung (Regeneration von ATP) benötigt. Kreatin-Transporter Defizienz oder Mutation ist ein entscheidender Faktor bei der Entstehung der geistigen Retardierung.

Die Koexpression von SPAK und/oder OSR1 mit CreaT verringert deutlich den elektrogenen Kreatintransport.

Darüber hinaus wird der maximale Kreatin-induzierte Einwärtsstrom, der die Transportrate angibt, durch SPAK und OSR1 herunterreguliert, während die Affinität von CreaT-Träger zu Kreatin nicht beeinträchtigt wird. Ähnlich wie die Wildtyp-Kinasen, beeinträchtigen die jeweiligen konstitutiv aktiven Mutanten, nämlich ^{T233E}SPAK und ^{T185E}OSR1, den CreaT, während die katalytisch inaktiven Mutanten ^{D212A}SPAK und ^{D164A}OSR1 sowie die WNK-insensitiven ^{T233A}SPAK keine Rolle spielen. Dennoch ^{T185A}OSR1 neigte dazu, den Kreatinstrom zu reduzieren.

Der letzte Teil der Studie untersucht die Regulation des Na^+-gekoppelten Phosphat-Transporters NaPi-IIb, der den Phosphat-Aufnahme in Darm- und Tumorzellen gewährleistet. Der Transporter wird durch SPAK und OSR1 stimuliert. Beide Kinasen erhöhen nicht nur den maximalen Phosphat-Einwärtsstrom und damit die Transportrate, sondern auch die Affinität von NaPi-IIb zum Phosphat deutlich. Darüber hinaus zeigt die gleichzeitige Expression von SPAK und OSR1 keinen additiven Effekt. Weiterhin zeigen die konstitutiv aktiven Mutanten ^{T233E}SPAK und ^{T185E}OSR1 dieselbe Wirkung wie die Wildtyp-Kinase. Diese hemmende Wirkung wurde weder bei den inaktiven Mutanten WNK insensitiven ^{T233A}SPAK und ^{T185A}OSR1 noch bei dem katalytisch inaktiven ^{D212A}SPAK und ^{D164A}OSR1 beobachtet.

Zusammengefasst: Die Kinasen SPAK und OSR1 als Regulatoren von Kir2.1, NaPI-IIb und CreaT könnten eine Rolle bei der Zellvolumenregulation und Erregbarkeit spielen.

6. REFERENCES

1. Hibino, H., Inanobe, A., Furutani, K., Murakami, S., Findlay, I., and Kurachi, Y. (2010) Inwardly rectifying potassium channels: their structure, function, and physiological roles. *Physiol Rev* **90**, 291-366
2. Lopatin, A. N., and Nichols, C. G. (2001) Inward rectifiers in the heart: an update on I(K1). *J Mol Cell Cardiol* **33**, 625-638
3. Jongsma, H. J., and Wilders, R. (2001) Channelopathies: Kir2.1 mutations jeopardize many cell functions. *Curr Biol* **11**, R747-750
4. Kubo, Y., Baldwin, T. J., Jan, Y. N., and Jan, L. Y. (1993) Primary structure and functional expression of a mouse inward rectifier potassium channel. *Nature* **362**, 127-133
5. Bhave, G., Lonergan, D., Chauder, B. A., and Denton, J. S. (2010) Small-molecule modulators of inward rectifier K+ channels: recent advances and future possibilities. *Future Med Chem* **2**, 757-774
6. Nichols, C. G., and Lopatin, A. N. (1997) Inward rectifier potassium channels. *Annu Rev Physiol* **59**, 171-191
7. Zaritsky, J. J., Redell, J. B., Tempel, B. L., and Schwarz, T. L. (2001) The consequences of disrupting cardiac inwardly rectifying K(+) current (I(K1)) as revealed by the targeted deletion of the murine Kir2.1 and Kir2.2 genes. *J Physiol* **533**, 697-710
8. Rodriguez-Menchaca, A. A., Navarro-Polanco, R. A., Ferrer-Villada, T., Rupp, J., Sachse, F. B., Tristani-Firouzi, M., and Sanchez-Chapula, J. A. (2008) The molecular basis of chloroquine block of the inward rectifier Kir2.1 channel. *Proc Natl Acad Sci U S A* **105**, 1364-1368
9. Matsuda, H., Saigusa, A., and Irisawa, H. (1987) Ohmic conductance through the inwardly rectifying K channel and blocking by internal Mg2+. *Nature* **325**, 156-159
10. Vandenberg, C. A. (1987) Inward rectification of a potassium channel in cardiac ventricular cells depends on internal magnesium ions. *Proc Natl Acad Sci U S A* **84**, 2560-2564
11. Lopatin, A. N., Makhina, E. N., and Nichols, C. G. (1994) Potassium channel block by cytoplasmic polyamines as the mechanism of intrinsic rectification. *Nature* **372**, 366-369
12. Kubo, Y., and Murata, Y. (2001) Control of rectification and permeation by two distinct sites after the second transmembrane region in Kir2.1 K+ channel. *J Physiol* **531**, 645-660
13. Yamada, M., and Kurachi, Y. (1995) Spermine gates inward-rectifying muscarinic but not ATP-sensitive K+ channels in rabbit atrial myocytes. Intracellular substance-mediated mechanism of inward rectification. *J Biol Chem* **270**, 9289-9294
14. Sepulveda, F. V., Pablo Cid, L., Teulon, J., and Niemeyer, M. I. (2015) Molecular aspects of structure, gating, and physiology of pH-sensitive background K2P and Kir K+-transport channels. *Physiol Rev* **95**, 179-217

15. de Boer, T. P., Houtman, M. J., Compier, M., and van der Heyden, M. A. (2010) The mammalian K(IR)2.x inward rectifier ion channel family: expression pattern and pathophysiology. *Acta Physiol (Oxf)* **199**, 243-256
16. Yang, D., Zhang, X., and Hughes, B. A. (2008) Expression of inwardly rectifying potassium channel subunits in native human retinal pigment epithelium. *Exp Eye Res* **87**, 176-183
17. Lu, Z. (2004) Mechanism of rectification in inward-rectifier K+ channels. *Annu Rev Physiol* **66**, 103-129
18. Kettenmann, H., Banati, R., and Walz, W. (1993) Electrophysiological behavior of microglia. *Glia* **7**, 93-101
19. Kettenmann, H., Hanisch, U. K., Noda, M., and Verkhratsky, A. (2011) Physiology of microglia. *Physiol Rev* **91**, 461-553
20. Eder, C. (2005) Regulation of microglial behavior by ion channel activity. *J Neurosci Res* **81**, 314-321
21. Norenberg, W., Gebicke-Haerter, P. J., and Illes, P. (1992) Inflammatory stimuli induce a new K+ outward current in cultured rat microglia. *Neurosci Lett* **147**, 171-174
22. Visentin, S., Agresti, C., Patrizio, M., and Levi, G. (1995) Ion channels in rat microglia and their different sensitivity to lipopolysaccharide and interferon-gamma. *J Neurosci Res* **42**, 439-451
23. Franchini, L., Levi, G., and Visentin, S. (2004) Inwardly rectifying K+ channels influence Ca2+ entry due to nucleotide receptor activation in microglia. *Cell Calcium* **35**, 449-459
24. Moussaud, S., Lamodiere, E., Savage, C., and Draheim, H. J. (2009) Characterisation of K+ currents in the C8-B4 microglial cell line and their regulation by microglia activating stimuli. *Cell Physiol Biochem* **24**, 141-152
25. Brockhaus, J., Ilschner, S., Banati, R. B., and Kettenmann, H. (1993) Membrane properties of ameboid microglial cells in the corpus callosum slice from early postnatal mice. *J Neurosci* **13**, 4412-4421
26. Schilling, T., and Eder, C. (2007) Ion channel expression in resting and activated microglia of hippocampal slices from juvenile mice. *Brain Res* **1186**, 21-28
27. Schilling, T., and Eder, C. (2015) Microglial K(+) channel expression in young adult and aged mice. *Glia* **63**, 664-672
28. Lam, D., and Schlichter, L. C. (2015) Expression and contributions of the Kir2.1 inward-rectifier K(+) channel to proliferation, migration and chemotaxis of microglia in unstimulated and anti-inflammatory states. *Front Cell Neurosci* **9**, 185
29. Brown, D. A., Gahwiler, B. H., Griffith, W. H., and Halliwell, J. V. (1990) Membrane currents in hippocampal neurons. *Prog Brain Res* **83**, 141-160
30. Takahashi, T. (1990) Inward rectification in neonatal rat spinal motoneurones. *J Physiol* **423**, 47-62
31. Mi, H., Deerinck, T. J., Jones, M., Ellisman, M. H., and Schwarz, T. L. (1996) Inwardly rectifying K+ channels that may participate in K+ buffering are localized in microvilli of Schwann cells. *J Neurosci* **16**, 2421-2429
32. Beeler, G. W., Jr., and Reuter, H. (1970) Voltage clamp experiments on ventricular myocarial fibres. *J Physiol* **207**, 165-190

33. Kurachi, Y. (1985) Voltage-dependent activation of the inward-rectifier potassium channel in the ventricular cell membrane of guinea-pig heart. *J Physiol* **366**, 365-385
34. McAllister, R. E., and Noble, D. (1966) The time and voltage dependence of the slow outward current in cardiac Purkinje fibres. *J Physiol* **186**, 632-662
35. Rougier, O., Vassort, G., and Stampfli, R. (1968) Voltage clamp experiments on frog atrial heart muscle fibres with the sucrose gap technique. *Pflugers Arch Gesamte Physiol Menschen Tiere* **301**, 91-108
36. Nilius, B., and Droogmans, G. (2001) Ion channels and their functional role in vascular endothelium. *Physiol Rev* **81**, 1415-1459
37. Adams, D. J., and Hill, M. A. (2004) Potassium channels and membrane potential in the modulation of intracellular calcium in vascular endothelial cells. *J Cardiovasc Electrophysiol* **15**, 598-610
38. Nilius, B., Schwarz, G., and Droogmans, G. (1993) Modulation by histamine of an inwardly rectifying potassium channel in human endothelial cells. *J Physiol* **472**, 359-371
39. Plaster, N. M., Tawil, R., Tristani-Firouzi, M., Canun, S., Bendahhou, S., Tsunoda, A., Donaldson, M. R., Iannaccone, S. T., Brunt, E., Barohn, R., Clark, J., Deymeer, F., George, A. L., Jr., Fish, F. A., Hahn, A., Nitu, A., Ozdemir, C., Serdaroglu, P., Subramony, S. H., Wolfe, G., Fu, Y. H., and Ptacek, L. J. (2001) Mutations in Kir2.1 cause the developmental and episodic electrical phenotypes of Andersen's syndrome. *Cell* **105**, 511-519
40. Fischer-Lougheed, J., Liu, J. H., Espinos, E., Mordasini, D., Bader, C. R., Belin, D., and Bernheim, L. (2001) Human myoblast fusion requires expression of functional inward rectifier Kir2.1 channels. *J Cell Biol* **153**, 677-686
41. Leichtle, A., Rauch, U., Albinus, M., Benohr, P., Kalbacher, H., Mack, A. F., Veh, R. W., Quast, U., and Russ, U. (2004) Electrophysiological and molecular characterization of the inward rectifier in juxtaglomerular cells from rat kidney. *J Physiol* **560**, 365-376
42. Lang, F., and Rehwald, W. (1992) Potassium channels in renal epithelial transport regulation. *Physiol Rev* **72**, 1-32
43. Collins, A., Wang, H., and Larson, M. K. (2005) Differential sensitivity of Kir2 inward-rectifier potassium channels to a mitochondrial uncoupler: identification of a regulatory site. *Mol Pharmacol* **67**, 1214-1220
44. Collins, A., and Larson, M. (2002) Differential sensitivity of inward rectifier K+ channels to metabolic inhibitors. *J Biol Chem* **277**, 35815-35818
45. Lodge, N. J., and Normandin, D. E. (1997) Alterations in Ito1, IKr and Ik1 density in the BIO TO-2 strain of syrian myopathic hamsters. *J Mol Cell Cardiol* **29**, 3211-3221
46. Preisig-Muller, R., Schlichthorl, G., Goerge, T., Heinen, S., Bruggemann, A., Rajan, S., Derst, C., Veh, R. W., and Daut, J. (2002) Heteromerization of Kir2.x potassium channels contributes to the phenotype of Andersen's syndrome. *Proc Natl Acad Sci U S A* **99**, 7774-7779
47. Zobel, C., Cho, H. C., Nguyen, T. T., Pekhletski, R., Diaz, R. J., Wilson, G. J., and Backx, P. H. (2003) Molecular dissection of the inward rectifier potassium current (IK1) in rabbit cardiomyocytes: evidence for heteromeric co-assembly of Kir2.1 and Kir2.2. *J Physiol* **550**, 365-372
48. Diaz, R. J., Zobel, C., Cho, H. C., Batthish, M., Hinek, A., Backx, P. H., and Wilson, G. J. (2004) Selective inhibition of inward rectifier K+ channels (Kir2.1 or Kir2.2)

abolishes protection by ischemic preconditioning in rabbit ventricular cardiomyocytes. *Circ Res* **95**, 325-332
49. Murry, C. E., Jennings, R. B., and Reimer, K. A. (1986) Preconditioning with ischemia: a delay of lethal cell injury in ischemic myocardium. *Circulation* **74**, 1124-1136
50. Weiss, J. N., and Shieh, R. C. (1994) Potassium loss during myocardial ischaemia and hypoxia: does lactate efflux play a role? *Cardiovasc Res* **28**, 1125-1132
51. Vicente, R., Coma, M., Busquets, S., Moore-Carrasco, R., Lopez-Soriano, F. J., Argiles, J. M., and Felipe, A. (2004) The systemic inflammatory response is involved in the regulation of K(+) channel expression in brain via TNF-alpha-dependent and -independent pathways. *FEBS Lett* **572**, 189-194
52. Leyland, M. L., and Dart, C. (2004) An alternatively spliced isoform of PSD-93/chapsyn 110 binds to the inwardly rectifying potassium channel, Kir2.1. *J Biol Chem* **279**, 43427-43436
53. Sampson, L. J., Leyland, M. L., and Dart, C. (2003) Direct interaction between the actin-binding protein filamin-A and the inwardly rectifying potassium channel, Kir2.1. *J Biol Chem* **278**, 41988-41997
54. Romanenko, V. G., Fang, Y., Byfield, F., Travis, A. J., Vandenberg, C. A., Rothblat, G. H., and Levitan, I. (2004) Cholesterol sensitivity and lipid raft targeting of Kir2.1 channels. *Biophys J* **87**, 3850-3861
55. Zitron, E., Kiesecker, C., Luck, S., Kathofer, S., Thomas, D., Kreye, V. A., Kiehn, J., Katus, H. A., Schoels, W., and Karle, C. A. (2004) Human cardiac inwardly rectifying current IKir2.2 is upregulated by activation of protein kinase A. *Cardiovasc Res* **63**, 520-527
56. Henry, P., Pearson, W. L., and Nichols, C. G. (1996) Protein kinase C inhibition of cloned inward rectifier (HRK1/KIR2.3) K+ channels expressed in Xenopus oocytes. *J Physiol* **495 (Pt 3)**, 681-688
57. Wischmeyer, E., Doring, F., and Karschin, A. (1998) Acute suppression of inwardly rectifying Kir2.1 channels by direct tyrosine kinase phosphorylation. *J Biol Chem* **273**, 34063-34068
58. Dart, C., and Leyland, M. L. (2001) Targeting of an A kinase-anchoring protein, AKAP79, to an inwardly rectifying potassium channel, Kir2.1. *J Biol Chem* **276**, 20499-20505
59. Leonoudakis, D., Conti, L. R., Radeke, C. M., McGuire, L. M., and Vandenberg, C. A. (2004) A multiprotein trafficking complex composed of SAP97, CASK, Veli, and Mint1 is associated with inward rectifier Kir2 potassium channels. *J Biol Chem* **279**, 19051-19063
60. Jones, S. V. (2003) Role of the small GTPase Rho in modulation of the inwardly rectifying potassium channel Kir2.1. *Mol Pharmacol* **64**, 987-993
61. Ahmed, M., Elvira, B., Almilaji, A., Bock, C. T., Kandolf, R., and Lang, F. (2015) Down-regulation of inwardly rectifying Kir2.1 K+ channels by human parvovirus B19 capsid protein VP1. *J Membr Biol* **248**, 223-229
62. Andersen, E. D., Krasilnikoff, P. A., and Overvad, H. (1971) Intermittent muscular weakness, extrasystoles, and multiple developmental anomalies. A new syndrome? *Acta Paediatr Scand* **60**, 559-564

63. Sansone, V., Griggs, R. C., Meola, G., Ptacek, L. J., Barohn, R., Iannaccone, S., Bryan, W., Baker, N., Janas, S. J., Scott, W., Ririe, D., and Tawil, R. (1997) Andersen's syndrome: a distinct periodic paralysis. *Ann Neurol* **42**, 305-312
64. Tawil, R., Ptacek, L. J., Pavlakis, S. G., DeVivo, D. C., Penn, A. S., Ozdemir, C., and Griggs, R. C. (1994) Andersen's syndrome: potassium-sensitive periodic paralysis, ventricular ectopy, and dysmorphic features. *Ann Neurol* **35**, 326-330
65. Priori, S. G., Barhanin, J., Hauer, R. N., Haverkamp, W., Jongsma, H. J., Kleber, A. G., McKenna, W. J., Roden, D. M., Rudy, Y., Schwartz, K., Schwartz, P. J., Towbin, J. A., and Wilde, A. (1999) Genetic and molecular basis of cardiac arrhythmias; impact on clinical management. Study group on molecular basis of arrhythmias of the working group on arrhythmias of the european society of cardiology. *Eur Heart J* **20**, 174-195
66. Priori, S. G., Barhanin, J., Hauer, R. N., Haverkamp, W., Jongsma, H. J., Kleber, A. G., McKenna, W. J., Roden, D. M., Rudy, Y., Schwartz, K., Schwartz, P. J., Towbin, J. A., and Wilde, A. M. (1999) Genetic and molecular basis of cardiac arrhythmias: impact on clinical management part III. *Circulation* **99**, 674-681
67. Priori, S. G., Barhanin, J., Hauer, R. N., Haverkamp, W., Jongsma, H. J., Kleber, A. G., McKenna, W. J., Roden, D. M., Rudy, Y., Schwartz, K., Schwartz, P. J., Towbin, J. A., and Wilde, A. M. (1999) Genetic and molecular basis of cardiac arrhythmias: impact on clinical management parts I and II. *Circulation* **99**, 518-528
68. Bendahhou, S., Donaldson, M. R., Plaster, N. M., Tristani-Firouzi, M., Fu, Y. H., and Ptacek, L. J. (2003) Defective potassium channel Kir2.1 trafficking underlies Andersen-Tawil syndrome. *J Biol Chem* **278**, 51779-51785
69. Lange, P. S., Er, F., Gassanov, N., and Hoppe, U. C. (2003) Andersen mutations of KCNJ2 suppress the native inward rectifier current IK1 in a dominant-negative fashion. *Cardiovasc Res* **59**, 321-327
70. Lopes, C. M., Zhang, H., Rohacs, T., Jin, T., Yang, J., and Logothetis, D. E. (2002) Alterations in conserved Kir channel-PIP2 interactions underlie channelopathies. *Neuron* **34**, 933-944
71. Schimpf, R., Wolpert, C., Gaita, F., Giustetto, C., and Borggrefe, M. (2005) Short QT syndrome. *Cardiovasc Res* **67**, 357-366
72. Bates, E. A. (2013) A potential molecular target for morphological defects of fetal alcohol syndrome: Kir2.1. *Curr Opin Genet Dev* **23**, 324-329
73. West, M., Park, D., Dodd, J. R., Kistler, J., and Christie, D. L. (2005) Purification and characterization of the creatine transporter expressed at high levels in HEK293 cells. *Protein Expr Purif* **41**, 393-401
74. Dodd, J. R., and Christie, D. L. (2001) Cysteine 144 in the third transmembrane domain of the creatine transporter is located close to a substrate-binding site. *J Biol Chem* **276**, 46983-46988
75. Sora, I., Richman, J., Santoro, G., Wei, H., Wang, Y., Vanderah, T., Horvath, R., Nguyen, M., Waite, S., Roeske, W. R., and et al. (1994) The cloning and expression of a human creatine transporter. *Biochem Biophys Res Commun* **204**, 419-427
76. Chen, N. H., Reith, M. E., and Quick, M. W. (2004) Synaptic uptake and beyond: the sodium- and chloride-dependent neurotransmitter transporter family SLC6. *Pflugers Arch* **447**, 519-531

77. Christie, D. L. (2007) Functional insights into the creatine transporter. *Subcell Biochem* **46**, 99-118
78. Takenaka, M., Bagnasco, S. M., Preston, A. S., Uchida, S., Yamauchi, A., Kwon, H. M., and Handler, J. S. (1995) The canine betaine gamma-amino-n-butyric acid transporter gene: diverse mRNA isoforms are regulated by hypertonicity and are expressed in a tissue-specific manner. *Proc Natl Acad Sci U S A* **92**, 1072-1076
79. Uchida, S., Kwon, H. M., Yamauchi, A., Preston, A. S., Marumo, F., and Handler, J. S. (1992) Molecular cloning of the cDNA for an MDCK cell Na(+)- and Cl(-)-dependent taurine transporter that is regulated by hypertonicity. *Proc Natl Acad Sci U S A* **89**, 8230-8234
80. Smith, R. N., Agharkar, A. S., and Gonzales, E. B. (2014) A review of creatine supplementation in age-related diseases: more than a supplement for athletes. *F1000Res* **3**, 222
81. Harris, R. C., Soderlund, K., and Hultman, E. (1992) Elevation of creatine in resting and exercised muscle of normal subjects by creatine supplementation. *Clin Sci (Lond)* **83**, 367-374
82. Walker, J. B. (1979) Creatine: biosynthesis, regulation, and function. *Adv Enzymol Relat Areas Mol Biol* **50**, 177-242
83. Adhihetty, P. J., Irrcher, I., Joseph, A. M., Ljubicic, V., and Hood, D. A. (2003) Plasticity of skeletal muscle mitochondria in response to contractile activity. *Exp Physiol* **88**, 99-107
84. Peral, M. J., Garcia-Delgado, M., Calonge, M. L., Duran, J. M., De La Horra, M. C., Wallimann, T., Speer, O., and Ilundain, A. (2002) Human, rat and chicken small intestinal Na+ - Cl- -creatine transporter: functional, molecular characterization and localization. *J Physiol* **545**, 133-144
85. Santacruz, L., and Jacobs, D. O. (2016) Structural correlates of the creatine transporter function regulation: the undiscovered country. *Amino Acids* **48**, 2049-2055
86. Guimbal, C., and Kilimann, M. W. (1993) A Na(+)-dependent creatine transporter in rabbit brain, muscle, heart, and kidney. cDNA cloning and functional expression. *J Biol Chem* **268**, 8418-8421
87. Braissant, O., and Henry, H. (2008) AGAT, GAMT and SLC6A8 distribution in the central nervous system, in relation to creatine deficiency syndromes: a review. *J Inherit Metab Dis* **31**, 230-239
88. Mak, C. S., Waldvogel, H. J., Dodd, J. R., Gilbert, R. T., Lowe, M. T., Birch, N. P., Faull, R. L., and Christie, D. L. (2009) Immunohistochemical localisation of the creatine transporter in the rat brain. *Neuroscience* **163**, 571-585
89. Battini, R., Chilosi, A., Mei, D., Casarano, M., Alessandri, M. G., Leuzzi, V., Ferretti, G., Tosetti, M., Bianchi, M. C., and Cioni, G. (2007) Mental retardation and verbal dyspraxia in a new patient with de novo creatine transporter (SLC6A8) mutation. *Am J Med Genet A* **143A**, 1771-1774
90. Battini, R., Chilosi, A. M., Casarano, M., Moro, F., Comparini, A., Alessandri, M. G., Leuzzi, V., Tosetti, M., and Cioni, G. (2011) Language disorder with mild intellectual disability in a child affected by a novel mutation of SLC6A8 gene. *Mol Genet Metab* **102**, 153-156

91. Braissant, O., Henry, H., Beard, E., and Uldry, J. (2011) Creatine deficiency syndromes and the importance of creatine synthesis in the brain. *Amino Acids* **40**, 1315-1324
92. Alcaide, P., Merinero, B., Ruiz-Sala, P., Richard, E., Navarrete, R., Arias, A., Ribes, A., Artuch, R., Campistol, J., Ugarte, M., and Rodriguez-Pombo, P. (2011) Defining the pathogenicity of creatine deficiency syndrome. *Hum Mutat* **32**, 282-291
93. Alcaide, P., Rodriguez-Pombo, P., Ruiz-Sala, P., Ferrer, I., Castro, P., Ruiz Martin, Y., Merinero, B., and Ugarte, M. (2010) A new case of creatine transporter deficiency associated with mild clinical phenotype and a novel mutation in the SLC6A8 gene. *Dev Med Child Neurol* **52**, 215-217
94. Ardon, O., Amat di San Filippo, C., Salomons, G. S., and Longo, N. (2010) Creatine transporter deficiency in two half-brothers. *Am J Med Genet A* **152A**, 1979-1983
95. Wagner, C. A., Hernando, N., Forster, I. C., and Biber, J. (2014) The SLC34 family of sodium-dependent phosphate transporters. *Pflugers Arch* **466**, 139-153
96. Marks, J., Debnam, E. S., and Unwin, R. J. (2010) Phosphate homeostasis and the renal-gastrointestinal axis. *Am J Physiol Renal Physiol* **299**, F285-296
97. Sabbagh, Y., O'Brien, S. P., Song, W., Boulanger, J. H., Stockmann, A., Arbeeny, C., and Schiavi, S. C. (2009) Intestinal npt2b plays a major role in phosphate absorption and homeostasis. *J Am Soc Nephrol* **20**, 2348-2358
98. Frei, P., Gao, B., Hagenbuch, B., Mate, A., Biber, J., Murer, H., Meier, P. J., and Stieger, B. (2005) Identification and localization of sodium-phosphate cotransporters in hepatocytes and cholangiocytes of rat liver. *Am J Physiol Gastrointest Liver Physiol* **288**, G771-778
99. Yin, B. W., Kiyamova, R., Chua, R., Caballero, O. L., Gout, I., Gryshkova, V., Bhaskaran, N., Souchelnytskyi, S., Hellman, U., Filonenko, V., Jungbluth, A. A., Odunsi, K., Lloyd, K. O., Old, L. J., and Ritter, G. (2008) Monoclonal antibody MX35 detects the membrane transporter NaPi2b (SLC34A2) in human carcinomas. *Cancer Immun* **8**, 3
100. Brazy, P. C., Gullans, S. R., Mandel, L. J., and Dennis, V. W. (1982) Metabolic requirement for inorganic phosphate by the rabbit proximal tubule. *J Clin Invest* **70**, 53-62
101. Brazy, P. C., Mandel, L. J., Gullans, S. R., and Soltoff, S. P. (1984) Interactions between phosphate and oxidative metabolism in proximal renal tubules. *Am J Physiol* **247**, F575-581
102. Freeman, D., Bartlett, S., Radda, G., and Ross, B. (1983) Energetics of sodium transport in the kidney. Saturation transfer 31P-NMR. *Biochim Biophys Acta* **762**, 325-336
103. Murilo Fanchiotti Cerri, L. C. D. d. R., Marcela Ferreira Paes, Ian Victor Silva, , and Leticia Batista Azevedo Rangel (2010) The Cotransporter NaPi-IIb: Characteristics, Regulation and its Role in Carcinogenesis. *Applied Cancer Research* **30**, 7
104. Hilfiker, H., Hattenhauer, O., Traebert, M., Forster, I., Murer, H., and Biber, J. (1998) Characterization of a murine type II sodium-phosphate cotransporter expressed in mammalian small intestine. *Proc Natl Acad Sci U S A* **95**, 14564-14569
105. Xu, Y., Yeung, C. H., Setiawan, I., Avram, C., Biber, J., Wagenfeld, A., Lang, F., and Cooper, T. G. (2003) Sodium-inorganic phosphate cotransporter NaPi-IIb in the epididymis and its potential role in male fertility studied in a transgenic mouse model. *Biol Reprod* **69**, 1135-1141

106. Rangel, L. B., Sherman-Baust, C. A., Wernyj, R. P., Schwartz, D. R., Cho, K. R., and Morin, P. J. (2003) Characterization of novel human ovarian cancer-specific transcripts (HOSTs) identified by serial analysis of gene expression. *Oncogene* **22**, 7225-7232
107. Jarzab, B., Wiench, M., Fujarewicz, K., Simek, K., Jarzab, M., Oczko-Wojciechowska, M., Wloch, J., Czarniecka, A., Chmielik, E., Lange, D., Pawlaczek, A., Szpak, S., Gubala, E., and Swierniak, A. (2005) Gene expression profile of papillary thyroid cancer: sources of variability and diagnostic implications. *Cancer Res* **65**, 1587-1597
108. Chen, D. R., Chien, S. Y., Kuo, S. J., Teng, Y. H., Tsai, H. T., Kuo, J. H., and Chung, J. G. (2010) SLC34A2 as a novel marker for diagnosis and targeted therapy of breast cancer. *Anticancer Res* **30**, 4135-4140
109. Amanzadeh, J., and Reilly, R. F., Jr. (2006) Hypophosphatemia: an evidence-based approach to its clinical consequences and management. *Nat Clin Pract Nephrol* **2**, 136-148
110. Arima, K., Hines, E. R., Kiela, P. R., Drees, J. B., Collins, J. F., and Ghishan, F. K. (2002) Glucocorticoid regulation and glycosylation of mouse intestinal type IIb Na-P(i) cotransporter during ontogeny. *Am J Physiol Gastrointest Liver Physiol* **283**, G426-434
111. Page, K., Bergwitz, C., Jaureguiberry, G., Harinarayan, C. V., and Insogna, K. (2008) A patient with hypophosphatemia, a femoral fracture, and recurrent kidney stones: report of a novel mutation in SLC34A3. *Endocr Pract* **14**, 869-874
112. Persy, V. P., Behets, G. J., Bervoets, A. R., De Broe, M. E., and D'Haese, P. C. (2006) Lanthanum: a safe phosphate binder. *Semin Dial* **19**, 195-199
113. Prie, D., Huart, V., Bakouh, N., Planelles, G., Dellis, O., Gerard, B., Hulin, P., Benque-Blanchet, F., Silve, C., Grandchamp, B., and Friedlander, G. (2002) Nephrolithiasis and osteoporosis associated with hypophosphatemia caused by mutations in the type 2a sodium-phosphate cotransporter. *N Engl J Med* **347**, 983-991
114. Prie, D., Urena Torres, P., and Friedlander, G. (2009) Latest findings in phosphate homeostasis. *Kidney Int* **75**, 882-889
115. Reining, S. C., Liesegang, A., Betz, H., Biber, J., Murer, H., and Hernando, N. (2010) Expression of renal and intestinal Na/Pi cotransporters in the absence of GABARAP. *Pflugers Arch* **460**, 207-217
116. Radanovic, T., Wagner, C. A., Murer, H., and Biber, J. (2005) Regulation of intestinal phosphate transport. I. Segmental expression and adaptation to low-P(i) diet of the type IIb Na(+)-P(i) cotransporter in mouse small intestine. *Am J Physiol Gastrointest Liver Physiol* **288**, G496-500
117. Indridason, O. S., and Quarles, L. D. (2002) Hyperphosphatemia in end-stage renal disease. *Adv Ren Replace Ther* **9**, 184-192
118. Locatelli, F., Cannata-Andia, J. B., Drueke, T. B., Horl, W. H., Fouque, D., Heimburger, O., and Ritz, E. (2002) Management of disturbances of calcium and phosphate metabolism in chronic renal insufficiency, with emphasis on the control of hyperphosphataemia. *Nephrol Dial Transplant* **17**, 723-731
119. Ferreira Francisco, F. A., Pereira e Silva, J. L., Hochhegger, B., Zanetti, G., and Marchiori, E. (2013) Pulmonary alveolar microlithiasis. State-of-the-art review. *Respir Med* **107**, 1-9

120. Marks, J., Debnam, E. S., and Unwin, R. J. (2013) The role of the gastrointestinal tract in phosphate homeostasis in health and chronic kidney disease. *Curr Opin Nephrol Hypertens* **22**, 481-487
121. Delpire, E., and Gagnon, K. B. (2008) SPAK and OSR1: STE20 kinases involved in the regulation of ion homoeostasis and volume control in mammalian cells. *Biochem J* **409**, 321-331
122. Gagnon, K. B., and Delpire, E. (2012) Molecular physiology of SPAK and OSR1: two Ste20-related protein kinases regulating ion transport. *Physiol Rev* **92**, 1577-1617
123. Johnston, A. M., Naselli, G., Gonez, L. J., Martin, R. M., Harrison, L. C., and DeAizpurua, H. J. (2000) SPAK, a STE20/SPS1-related kinase that activates the p38 pathway. *Oncogene* **19**, 4290-4297
124. Tamari, M., Daigo, Y., and Nakamura, Y. (1999) Isolation and characterization of a novel serine threonine kinase gene on chromosome 3p22-21.3. *J Hum Genet* **44**, 116-120
125. Hoffmann, E. K., and Pedersen, S. F. (2007) Shrinkage insensitivity of NKCC1 in myosin II-depleted cytoplasts from Ehrlich ascites tumor cells. *Am J Physiol Cell Physiol* **292**, C1854-1866
126. Ushiro, H., Tsutsumi, T., Suzuki, K., Kayahara, T., and Nakano, K. (1998) Molecular cloning and characterization of a novel Ste20-related protein kinase enriched in neurons and transporting epithelia. *Arch Biochem Biophys* **355**, 233-240
127. Miao, N., Fung, B., Sanchez, R., Lydon, J., Barker, D., and Pang, K. (2000) Isolation and expression of PASK, a serine/threonine kinase, during rat embryonic development, with special emphasis on the pancreas. *J Histochem Cytochem* **48**, 1391-1400
128. Piechotta, K., Garbarini, N., England, R., and Delpire, E. (2003) Characterization of the interaction of the stress kinase SPAK with the Na+-K+-2Cl- cotransporter in the nervous system: evidence for a scaffolding role of the kinase. *J Biol Chem* **278**, 52848-52856
129. Chen, W., Yazicioglu, M., and Cobb, M. H. (2004) Characterization of OSR1, a member of the mammalian Ste20p/germinal center kinase subfamily. *J Biol Chem* **279**, 11129-11136
130. Piechotta, K., Lu, J., and Delpire, E. (2002) Cation chloride cotransporters interact with the stress-related kinases Ste20-related proline-alanine-rich kinase (SPAK) and oxidative stress response 1 (OSR1). *J Biol Chem* **277**, 50812-50819
131. Vitari, A. C., Deak, M., Morrice, N. A., and Alessi, D. R. (2005) The WNK1 and WNK4 protein kinases that are mutated in Gordon's hypertension syndrome phosphorylate and activate SPAK and OSR1 protein kinases. *Biochem J* **391**, 17-24
132. Vitari, A. C., Thastrup, J., Rafiqi, F. H., Deak, M., Morrice, N. A., Karlsson, H. K., and Alessi, D. R. (2006) Functional interactions of the SPAK/OSR1 kinases with their upstream activator WNK1 and downstream substrate NKCC1. *Biochem J* **397**, 223-231
133. Lin, S. H., Yu, I. S., Jiang, S. T., Lin, S. W., Chu, P., Chen, A., Sytwu, H. K., Sohara, E., Uchida, S., Sasaki, S., and Yang, S. S. (2011) Impaired phosphorylation of Na(+)-K(+)-2Cl(-) cotransporter by oxidative stress-responsive kinase-1 deficiency manifests hypotension and Bartter-like syndrome. *Proc Natl Acad Sci U S A* **108**, 17538-17543

134. McCormick, J. A., Mutig, K., Nelson, J. H., Saritas, T., Hoorn, E. J., Yang, C. L., Rogers, S., Curry, J., Delpire, E., Bachmann, S., and Ellison, D. H. (2011) A SPAK isoform switch modulates renal salt transport and blood pressure. *Cell Metab* **14**, 352-364
135. Yang, S. S., Lo, Y. F., Wu, C. C., Lin, S. W., Yeh, C. J., Chu, P., Sytwu, H. K., Uchida, S., Sasaki, S., and Lin, S. H. (2010) SPAK-knockout mice manifest Gitelman syndrome and impaired vasoconstriction. *J Am Soc Nephrol* **21**, 1868-1877
136. Villa, F., Deak, M., Alessi, D. R., and van Aalten, D. M. (2008) Structure of the OSR1 kinase, a hypertension drug target. *Proteins* **73**, 1082-1087
137. Kahle, K. T., Rinehart, J., and Lifton, R. P. (2010) Phosphoregulation of the Na-K-2Cl and K-Cl cotransporters by the WNK kinases. *Biochim Biophys Acta* **1802**, 1150-1158
138. Gimenez, I. (2006) Molecular mechanisms and regulation of furosemide-sensitive Na-K-Cl cotransporters. *Curr Opin Nephrol Hypertens* **15**, 517-523
139. Rafiqi, F. H., Zuber, A. M., Glover, M., Richardson, C., Fleming, S., Jovanovic, S., Jovanovic, A., O'Shaughnessy, K. M., and Alessi, D. R. (2010) Role of the WNK-activated SPAK kinase in regulating blood pressure. *EMBO Mol Med* **2**, 63-75
140. O'Reilly, M., Marshall, E., Speirs, H. J., and Brown, R. W. (2003) WNK1, a gene within a novel blood pressure control pathway, tissue-specifically generates radically different isoforms with and without a kinase domain. *J Am Soc Nephrol* **14**, 2447-2456
141. Capasso, G., Cantone, A., Evangelista, C., Zacchia, M., Trepiccione, F., Acone, D., and Rizzo, M. (2005) Channels, carriers, and pumps in the pathogenesis of sodium-sensitive hypertension. *Semin Nephrol* **25**, 419-424
142. Achard, J. M., Disse-Nicodeme, S., Fiquet-Kempf, B., and Jeunemaitre, X. (2001) Phenotypic and genetic heterogeneity of familial hyperkalaemic hypertension (Gordon syndrome). *Clin Exp Pharmacol Physiol* **28**, 1048-1052
143. Huang, C. L., Yang, S. S., and Lin, S. H. (2008) Mechanism of regulation of renal ion transport by WNK kinases. *Curr Opin Nephrol Hypertens* **17**, 519-525
144. Xiao, F., Li, J., Singh, A. K., Riederer, B., Wang, J., Sultan, A., Park, H., Lee, M. G., Lamprecht, G., Scholte, B. J., De Jonge, H. R., and Seidler, U. (2012) Rescue of epithelial HCO3- secretion in murine intestine by apical membrane expression of the cystic fibrosis transmembrane conductance regulator mutant F508del. *J Physiol* **590**, 5317-5334
145. Yan, Y., Dalmasso, G., Nguyen, H. T., Obertone, T. S., Sitaraman, S. V., and Merlin, D. (2009) Ste20-related proline/alanine-rich kinase (SPAK) regulated transcriptionally by hyperosmolarity is involved in intestinal barrier function. *PLoS One* **4**, e5049
146. Kamat, N. V., Thabet, S. R., Xiao, L., Saleh, M. A., Kirabo, A., Madhur, M. S., Delpire, E., Harrison, D. G., and McDonough, A. A. (2015) Renal transporter activation during angiotensin-II hypertension is blunted in interferon-gamma-/- and interleukin-17A-/- mice. *Hypertension* **65**, 569-576
147. van der Lubbe, N., Zietse, R., and Hoorn, E. J. (2013) Effects of angiotensin II on kinase-mediated sodium and potassium transport in the distal nephron. *Curr Opin Nephrol Hypertens* **22**, 120-126
148. O'Shaughnessy, K. M. (2015) Gordon Syndrome: a continuing story. *Pediatr Nephrol* **30**, 1903-1908

149. Zhang, Y., Viennois, E., Xiao, B., Baker, M. T., Yang, S., Okoro, I., and Yan, Y. (2013) Knockout of Ste20-like proline/alanine-rich kinase (SPAK) attenuates intestinal inflammation in mice. *Am J Pathol* **182**, 1617-1628
150. Geng, Y., Byun, N., and Delpire, E. (2010) Behavioral analysis of Ste20 kinase SPAK knockout mice. *Behav Brain Res* **208**, 377-382
151. Alessi, D. R., Zhang, J., Khanna, A., Hochdorfer, T., Shang, Y., and Kahle, K. T. (2014) The WNK-SPAK/OSR1 pathway: master regulator of cation-chloride cotransporters. *Sci Signal* **7**, re3
152. Lang, F., and Hoffmann, E. K. (2012) Role of ion transport in control of apoptotic cell death. *Compr Physiol* **2**, 2037-2061
153. Ureche, O. N., Baltaev, R., Ureche, L., Strutz-Seebohm, N., Lang, F., and Seebohm, G. (2008) Novel insights into the structural basis of pH-sensitivity in inward rectifier K+ channels Kir2.3. *Cell Physiol Biochem* **21**, 347-356
154. Limberg, M. M., Zumhagen, S., Netter, M. F., Coffey, A. J., Grace, A., Rogers, J., Bockelmann, D., Rinne, S., Stallmeyer, B., Decher, N., and Schulze-Bahr, E. (2013) Non dominant-negative KCNJ2 gene mutations leading to Andersen-Tawil syndrome with an isolated cardiac phenotype. *Basic Res Cardiol* **108**, 353
155. Pakladok, T., Hosseinzadeh, Z., Lebedeva, A., Alesutan, I., and Lang, F. (2014) Upregulation of the Na(+)-coupled phosphate cotransporters NaPi-IIa and NaPi-IIb by B-RAF. *J Membr Biol* **247**, 137-145
156. Pathare, G., Foller, M., Daryadel, A., Mutig, K., Bogatikov, E., Fajol, A., Almilaji, A., Michael, D., Stange, G., Voelkl, J., Wagner, C. A., Bachmann, S., and Lang, F. (2012) OSR1-sensitive renal tubular phosphate reabsorption. *Kidney Blood Press Res* **36**, 149-161
157. Jackson, C. L. (2000) Brefeldin A revealing the fundamental principles governing membrane dynamics and protein transport. *Subcell Biochem* **34**, 233-272
158. Nebenfuhr, A., Ritzenthaler, C., and Robinson, D. G. (2002) Brefeldin A: deciphering an enigmatic inhibitor of secretion. *Plant Physiol* **130**, 1102-1108
159. Sciaky, N., Presley, J., Smith, C., Zaal, K. J., Cole, N., Moreira, J. E., Terasaki, M., Siggia, E., and Lippincott-Schwartz, J. (1997) Golgi tubule traffic and the effects of brefeldin A visualized in living cells. *J Cell Biol* **139**, 1137-1155
160. Fezai, M., Ahmed, M., Hosseinzadeh, Z., Elvira, B., and Lang, F. (2015) SPAK and OSR1 Sensitive Kir2.1 K+ Channels. *Neurosignals* **23**, 20-33
161. Karmazinova, M., and Lacinova, L. (2010) Measurement of cellular excitability by whole cell patch clamp technique. *Physiol Res* **59 Suppl 1**, S1-7
162. Fezai, M., Elvira, B., Borras, J., Ben-Attia, M., Hoseinzadeh, Z., and Lang, F. (2014) Negative regulation of the creatine transporter SLC6A8 by SPAK and OSR1. *Kidney Blood Press Res* **39**, 546-554
163. Fezai, M., Elvira, B., Warsi, J., Ben-Attia, M., Hosseinzadeh, Z., and Lang, F. (2015) Up-Regulation of Intestinal Phosphate Transporter NaPi-IIb (SLC34A2) by the Kinases SPAK and OSR1. *Kidney Blood Press Res* **40**, 555-564
164. Yang, L., Cai, X., Zhou, J., Chen, S., Chen, Y., Chen, Z., Wang, Q., Fang, Z., and Zhou, L. (2013) STE20/SPS1-related proline/alanine-rich kinase is involved in plasticity of GABA signaling function in a mouse model of acquired epilepsy. *PLoS One* **8**, e74614

165. Elvira, B., Singh, Y., Warsi, J., Munoz, C., and Lang, F. (2016) OSR1 and SPAK Sensitivity of Large-Conductance Ca2+ Activated K+ Channel. *Cell Physiol Biochem* **38**, 1652-1662
166. Borras, J., Salker, M. S., Elvira, B., Warsi, J., Fezai, M., Hoseinzadeh, Z., and Lang, F. (2015) SPAK and OSR1 Sensitivity of Excitatory Amino Acid Transporter EAAT3. *Nephron* **130**, 221-228
167. Warsi, J., Hosseinzadeh, Z., Elvira, B., Bissinger, R., Shumilina, E., and Lang, F. (2014) Regulation of ClC-2 activity by SPAK and OSR1. *Kidney Blood Press Res* **39**, 378-387
168. Elvira, B., Munoz, C., Borras, J., Chen, H., Warsi, J., Ajay, S. S., Shumilina, E., and Lang, F. (2014) SPAK and OSR1 dependent down-regulation of murine renal outer medullary K channel ROMK1. *Kidney Blood Press Res* **39**, 353-360
169. Elvira, B., Warsi, J., Munoz, C., and Lang, F. (2015) SPAK and OSR1 sensitivity of voltage-gated K+ channel Kv1.5. *J Membr Biol* **248**, 59-66
170. Delpire, E., and Gagnon, K. B. (2006) SPAK and OSR1, key kinases involved in the regulation of chloride transport. *Acta Physiol (Oxf)* **187**, 103-113
171. Richardson, C., and Alessi, D. R. (2008) The regulation of salt transport and blood pressure by the WNK-SPAK/OSR1 signalling pathway. *J Cell Sci* **121**, 3293-3304
172. Pathare, G., Foller, M., Michael, D., Walker, B., Hierlmeier, M., Mannheim, J. G., Pichler, B. J., and Lang, F. (2012) Enhanced FGF23 serum concentrations and phosphaturia in gene targeted mice expressing WNK-resistant SPAK. *Kidney Blood Press Res* **36**, 355-364
173. Elvira, B., Warsi, J., Fezai, M., Munoz, C., and Lang, F. (2015) SPAK and OSR1 Sensitive Cell Membrane Protein Abundance and Activity of KCNQ1/E1 K+ Channels. *Cell Physiol Biochem* **37**, 2032-2042
174. Richardson, C., Sakamoto, K., de los Heros, P., Deak, M., Campbell, D. G., Prescott, A. R., and Alessi, D. R. (2011) Regulation of the NKCC2 ion cotransporter by SPAK-OSR1-dependent and -independent pathways. *J Cell Sci* **124**, 789-800
175. Gagnon, K. B., and Delpire, E. (2010) On the substrate recognition and negative regulation of SPAK, a kinase modulating Na+-K+-2Cl- cotransport activity. *Am J Physiol Cell Physiol* **299**, C614-620
176. Glover, M., and O'Shaughnessy K, M. (2011) SPAK and WNK kinases: a new target for blood pressure treatment? *Curr Opin Nephrol Hypertens* **20**, 16-22
177. Mercier-Zuber, A., and O'Shaughnessy, K. M. (2011) Role of SPAK and OSR1 signalling in the regulation of NaCl cotransporters. *Curr Opin Nephrol Hypertens* **20**, 534-540
178. Lang, F. (2007) Mechanisms and significance of cell volume regulation. *J Am Coll Nutr* **26**, 613S-623S
179. Hoffmann, E. K., Lambert, I. H., and Pedersen, S. F. (2009) Physiology of cell volume regulation in vertebrates. *Physiol Rev* **89**, 193-277
180. Hoffmann, E. K. (2011) Ion channels involved in cell volume regulation: effects on migration, proliferation, and programmed cell death in non adherent EAT cells and adherent ELA cells. *Cell Physiol Biochem* **28**, 1061-1078
181. Tristani-Firouzi, M., and Etheridge, S. P. (2010) Kir 2.1 channelopathies: the Andersen-Tawil syndrome. *Pflugers Arch* **460**, 289-294

182. Xia, M., Jin, Q., Bendahhou, S., He, Y., Larroque, M. M., Chen, Y., Zhou, Q., Yang, Y., Liu, Y., Liu, B., Zhu, Q., Zhou, Y., Lin, J., Liang, B., Li, L., Dong, X., Pan, Z., Wang, R., Wan, H., Qiu, W., Xu, W., Eurlings, P., Barhanin, J., and Chen, Y. (2005) A Kir2.1 gain-of-function mutation underlies familial atrial fibrillation. *Biochem Biophys Res Commun* **332**, 1012-1019
183. Liu, G. X., Derst, C., Schlichthorl, G., Heinen, S., Seebohm, G., Bruggemann, A., Kummer, W., Veh, R. W., Daut, J., and Preisig-Muller, R. (2001) Comparison of cloned Kir2 channels with native inward rectifier K+ channels from guinea-pig cardiomyocytes. *J Physiol* **532**, 115-126
184. Howe, M. W., Feig, S. L., Osting, S. M., and Haberly, L. B. (2008) Cellular and subcellular localization of Kir2.1 subunits in neurons and glia in piriform cortex with implications for K+ spatial buffering. *J Comp Neurol* **506**, 877-893
185. Pruss, H., Derst, C., Lommel, R., and Veh, R. W. (2005) Differential distribution of individual subunits of strongly inwardly rectifying potassium channels (Kir2 family) in rat brain. *Brain Res Mol Brain Res* **139**, 63-79
186. Pruss, H., Wenzel, M., Eulitz, D., Thomzig, A., Karschin, A., and Veh, R. W. (2003) Kir2 potassium channels in rat striatum are strategically localized to control basal ganglia function. *Brain Res Mol Brain Res* **110**, 203-219
187. Stonehouse, A. H., Pringle, J. H., Norman, R. I., Stanfield, P. R., Conley, E. C., and Brammar, W. J. (1999) Characterisation of Kir2.0 proteins in the rat cerebellum and hippocampus by polyclonal antibodies. *Histochem Cell Biol* **112**, 457-465
188. Muessel, M. J., Harry, G. J., Armstrong, D. L., and Storey, N. M. (2013) SDF-1alpha and LPA modulate microglia potassium channels through rho gtpases to regulate cell morphology. *Glia* **61**, 1620-1628
189. Jansen, L. A., Uhlmann, E. J., Crino, P. B., Gutmann, D. H., and Wong, M. (2005) Epileptogenesis and reduced inward rectifier potassium current in tuberous sclerosis complex-1-deficient astrocytes. *Epilepsia* **46**, 1871-1880
190. Tsai, K. L., Chang, H. F., and Wu, S. N. (2013) The inhibition of inwardly rectifying K+ channels by memantine in macrophages and microglial cells. *Cell Physiol Biochem* **31**, 938-951
191. Kang, S. J., Cho, S. H., Park, K., Yi, J., Yoo, S. J., and Shin, K. S. (2008) Expression of Kir2.1 channels in astrocytes under pathophysiological conditions. *Mol Cells* **25**, 124-130
192. Kahle, K. T., and Delpire, E. (2016) Kinase-KCC2 coupling: Cl- rheostasis, disease susceptibility, therapeutic target. *J Neurophysiol* **115**, 8-18
193. Watanabe, M., and Fukuda, A. (2015) Development and regulation of chloride homeostasis in the central nervous system. *Front Cell Neurosci* **9**, 371
194. Eberhardt, C., Amann, B., Feuchtinger, A., Hauck, S. M., and Deeg, C. A. (2011) Differential expression of inwardly rectifying K+ channels and aquaporins 4 and 5 in autoimmune uveitis indicates misbalance in Muller glial cell-dependent ion and water homeostasis. *Glia* **59**, 697-707
195. Iandiev, I., Tenckhoff, S., Pannicke, T., Biedermann, B., Hollborn, M., Wiedemann, P., Reichenbach, A., and Bringmann, A. (2006) Differential regulation of Kir4.1 and Kir2.1 expression in the ischemic rat retina. *Neurosci Lett* **396**, 97-101

196. Iandiev, I., Uckermann, O., Pannicke, T., Wurm, A., Tenckhoff, S., Pietsch, U. C., Reichenbach, A., Wiedemann, P., Bringmann, A., and Uhlmann, S. (2006) Glial cell reactivity in a porcine model of retinal detachment. *Invest Ophthalmol Vis Sci* **47**, 2161-2171
197. Kofuji, P., Biedermann, B., Siddharthan, V., Raap, M., Iandiev, I., Milenkovic, I., Thomzig, A., Veh, R. W., Bringmann, A., and Reichenbach, A. (2002) Kir potassium channel subunit expression in retinal glial cells: implications for spatial potassium buffering. *Glia* **39**, 292-303
198. Raap, M., Biedermann, B., Braun, P., Milenkovic, I., Skatchkov, S. N., Bringmann, A., and Reichenbach, A. (2002) Diversity of Kir channel subunit mRNA expressed by retinal glial cells of the guinea-pig. *Neuroreport* **13**, 1037-1040
199. Longden, T. A., Dabertrand, F., Hill-Eubanks, D. C., Hammack, S. E., and Nelson, M. T. (2014) Stress-induced glucocorticoid signaling remodels neurovascular coupling through impairment of cerebrovascular inwardly rectifying K+ channel function. *Proc Natl Acad Sci U S A* **111**, 7462-7467
200. Joncquel-Chevalier Curt, M., Voicu, P. M., Fontaine, M., Dessein, A. F., Porchet, N., Mention-Mulliez, K., Dobbelaere, D., Soto-Ares, G., Cheillan, D., and Vamecq, J. (2015) Creatine biosynthesis and transport in health and disease. *Biochimie* **119**, 146-165
201. Shojaiefard, M., Hosseinzadeh, Z., Bhavsar, S. K., and Lang, F. (2012) Downregulation of the creatine transporter SLC6A8 by JAK2. *J Membr Biol* **245**, 157-163
202. Fezai, M., Warsi, J., and Lang, F. (2015) Regulation of the Na+,Cl- Coupled Creatine Transporter CreaT (SLC6A8) by the Janus Kinase JAK3. *Neurosignals* **23**, 11-19
203. Munoz, C., Almilaji, A., Setiawan, I., Foller, M., and Lang, F. (2013) Up-regulation of the inwardly rectifying K(+) channel Kir2.1 (KCNJ2) by protein kinase B (PKB/Akt) and PIKfyve. *J Membr Biol* **246**, 189-197
204. Shojaiefard, M., Christie, D. L., and Lang, F. (2006) Stimulation of the creatine transporter SLC6A8 by the protein kinase mTOR. *Biochem Biophys Res Commun* **341**, 945-949
205. Shojaiefard, M., Christie, D. L., and Lang, F. (2005) Stimulation of the creatine transporter SLC6A8 by the protein kinases SGK1 and SGK3. *Biochem Biophys Res Commun* **334**, 742-746
206. Almilaji, A., Sopjani, M., Elvira, B., Borras, J., Dermaku-Sopjani, M., Munoz, C., Warsi, J., Lang, U. E., and Lang, F. (2014) Upregulation of the creatine transporter Slc6A8 by Klotho. *Kidney Blood Press Res* **39**, 516-525
207. Brown, E. L., Snow, R. J., Wright, C. R., Cho, Y., Wallace, M. A., Kralli, A., and Russell, A. P. (2014) PGC-1alpha and PGC-1beta increase CrT expression and creatine uptake in myotubes via ERRalpha. *Biochim Biophys Acta* **1843**, 2937-2943
208. Longo, N., Ardon, O., Vanzo, R., Schwartz, E., and Pasquali, M. (2011) Disorders of creatine transport and metabolism. *Am J Med Genet C Semin Med Genet* **157C**, 72-78
209. Mancardi, M. M., Caruso, U., Schiaffino, M. C., Baglietto, M. G., Rossi, A., Battaglia, F. M., Salomons, G. S., Jakobs, C., Zara, F., Veneselli, E., and Gaggero, R. (2007) Severe epilepsy in X-linked creatine transporter defect (CRTR-D). *Epilepsia* **48**, 1211-1213

210. Puusepp, H., Kall, K., Salomons, G. S., Talvik, I., Mannamaa, M., Rein, R., Jakobs, C., and Ounap, K. (2010) The screening of SLC6A8 deficiency among Estonian families with X-linked mental retardation. *J Inherit Metab Dis* **33 Suppl 3**, S5-11
211. Salomons, G. S., van Dooren, S. J., Verhoeven, N. M., Marsden, D., Schwartz, C., Cecil, K. M., DeGrauw, T. J., and Jakobs, C. (2003) X-linked creatine transporter defect: an overview. *J Inherit Metab Dis* **26**, 309-318
212. Kirchner, S., Muduli, A., Casirola, D., Prum, K., Douard, V., and Ferraris, R. P. (2008) Luminal fructose inhibits rat intestinal sodium-phosphate cotransporter gene expression and phosphate uptake. *Am J Clin Nutr* **87**, 1028-1038
213. Shojaiefard, M., and Lang, F. (2006) Stimulation of the intestinal phosphate transporter SLC34A2 by the protein kinase mTOR. *Biochem Biophys Res Commun* **345**, 1611-1614
214. Palmada, M., Dieter, M., Speil, A., Bohmer, C., Mack, A. F., Wagner, H. J., Klingel, K., Kandolf, R., Murer, H., Biber, J., Closs, E. I., and Lang, F. (2004) Regulation of intestinal phosphate cotransporter NaPi IIb by ubiquitin ligase Nedd4-2 and by serum- and glucocorticoid-dependent kinase 1. *Am J Physiol Gastrointest Liver Physiol* **287**, G143-150

7- Declaration of contributions

I hereby declare that this dissertation is my original work and it was written by me.

Neither this work nor parts of it have been submitted elsewhere as a doctoral project, or have been accepted for the award of any other degree in my name in Germany or anywhere else in the world, either in the same or similar form. To the best of my knowledge and belief, this work contains no material previously published or written by another person, except where indicated through the proper use of citations and references.

The experimental part of this work was carried out in the Institute of Physiology I, of Eberhard Karls University of Tübingen.

This thesis contains the data of three original published papers. For all publications Professor Lang F. supervised and designed the study. I carried out all oocytes treatment, culture and injection. As well I performed all experiments with two electrode voltage clamp recording, data analyses, statistics and I designed all figures. Dr. Elvira B. carried out the molecular biology and chemiluminescence experiments and provided data for the figures 24 and 28. Dr. Hosseinzadeh Z. carried out the *Xenopus laevis* surgeries. Prof. Lang F. wrote publications drafts and I designed all the figures, completed and corrected the manuscripts. The final versions of the three publications were approved by all authors.

Here again, I declare that this thesis is my own work and effort and all the sources are duly acknowledged.

Myriam Fezai

8- Original publications

1- **Fezai M**, Ahmed M, Hosseinzadeh Z, Elvira B, Lang F. SPAK and OSR1 Sensitive Kir2.1 K^+ Channels. Neurosignals. 2015 Dec 17; 23(1):20-33.

2- **Fezai M**, Elvira B, Borras J, Ben-Attia M, Hoseinzadeh Z, Lang F. Negative regulation of the creatine transporter SLC6A8 by SPAK and OSR1. Kidney Blood Press Res. 2014 Dec 8;39(6):546-54.

3- **Fezai M**, Elvira B, Warsi J, Ben-Attia M, Hosseinzadeh Z, Lang F. Up-Regulation of Intestinal Phosphate Transporter NaPi-IIb (SLC34A2) by the Kinases SPAK and OSR1. Kidney Blood Press Res. 2015Oct 28; 40(6):555-64.

9- Acknowledgments

I hereby would like to express my recognition and satisfaction for the opportunity to realise my thesis at the institute of Physiology of Eberhard Karls University of Tübingen, Germany.

I would like to express my special appreciation and gratitude to my supervisor Professor Dr. Florian Lang for giving me the opportunity to carry out my thesis work in his department and under his supervision. I would like to thank him for encouraging my research an allowing me to grow up as a researcher.

I would like to thank Dr. Zohreh Husseinzadeh for investing her time and effort in assisting me and I'm grateful for her professional guidance.

As well, thanks to Dr. Bernat Elvira for guiding me and teaching me to the best his knowledge while being patient, I'm thankful for him for his friendly and very professional attitude.

I'm grateful to Dr. Mohamed Jemaà for his very professional assistance, guidance and nice collaboration.

I'm thankful to all the colleagues of the Physiology Institute I for their collaboration and for helping me to accomplish my work successfully especially Uwe Schüler and Dr. Mehrdad Ghashghaeinia for his precious advices and for being very collaborative. As well, I'm thankful to the technical stuff of the department especially Elfriede Faber, Lejla Subasic and Tanja Loch.